# University of Naples Federico II
Polytechnic and Basic Sciences School

Department of Chemical Sciences

Ph.D. in Chemical Sciences

Design and Production of New Hypo-caloric Protein Sweeteners Tailored for Specific Food Applications
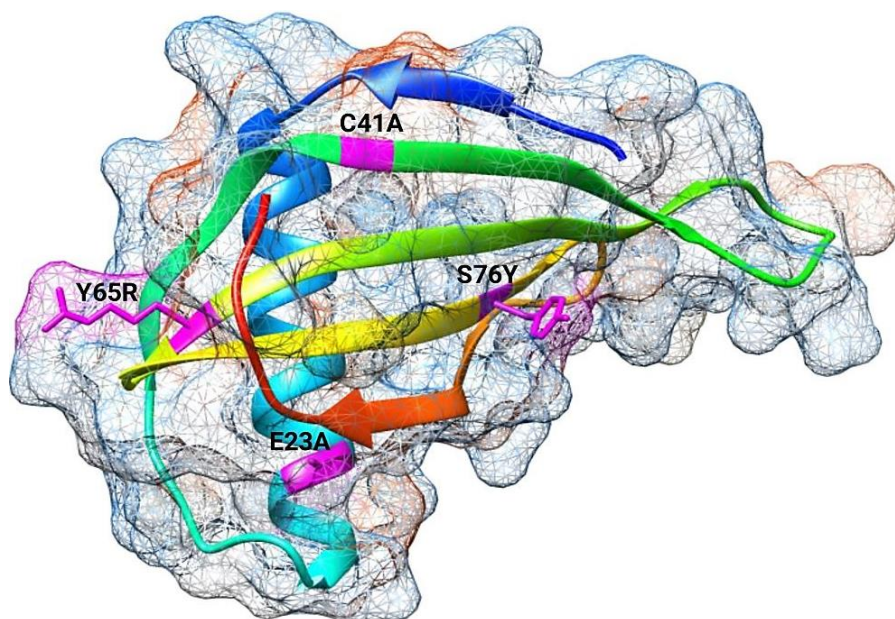
Masoud Delfi

Advisor:
professor Delia Picone

Examiner:
professor Luigi Petraccone

XXXIII Cycle 2018 – 2021
Coordinator: prof. Angela Lombardi

Table of Contents

List of Abbreviation

ATR: Attenuated Total Reflection

atm: atmosphere

CD Spectroscopy: Circular Dichroism Spectroscopy

DSC: Differential Scanning Calorimetry

Da: Dalton

EFSA: European Food Safety Authority

EMEM: Eagle's Minimum Essential Medium

E.Coli: *Escherichia coli*

FDA: Food and Drug Administration

FEMA: Flavor Extract Manufacturers Association

FLIM: Fluorescence Lifetime Imaging Microscopy

FTIR: Fourier Transform Infrared Spectroscopy

GRAS: Generally Recognized As Safe

HPLC: High Performance Liquid Chromatography

MALDI-TOF: Mixed Assisted Laser Desorption/Ionization-Time of Fly

mrw: mean residue molecular weight

mGluR1: metabotropic Glutamate Receptor 1

NMR Spectroscopy: Nuclear Magnetic Resonance Spectroscopy

PAGE: Poly-Acrylamide Gel Electrophoresis

PBS: Phosphate-Buffered Saline

PTFE beads: Poly(tetrafluoroethylene) beads

RPM: Revolutions per Minute

SDS: Sodium Dodecyl Sulfate

SGF: Simulated Gastric Fluid

SIF: Simulated Intestinal Fluid

SSF: Simulated Salivary Fluid

Stevia Reb: Stevia Rebaudioside

TDS: Temporal Dominance of Sensations

TEM: Transmission Electron Microscopy

TFA: Trifluoroacetic Acid

ThT: Thioflavin T

TIS: Time Intensity of Sweetness

TK-NAS: Tomato Ketchup-Not Added Sugar

T_m: Melting Temperature

UV-Vis Spectroscopy: Ultraviolet Visible Spectroscopy

ΔH: Enthalpy Change

Overview

In the recent years, the prevalence of some hazardous diseases, *i.e.* diabetes, obesity, hyperlipidemia and dental caries has significantly expanded due to the exponential increase in the sucrose's consumption. This hurdle increased the demand for using low-calorie sweeteners in food and beverage productions [1–3]. Artificial sweeteners such as saccharin and aspartame were introduced in the food markets as suitable low-calorie sweeteners to substitute sucrose, in particular suggested to patients suffering from diabetes and hyperlipidemia. However, some evidences revealed that such sweeteners have severe side effects and could lead to bladder cancer, heart failure and brain tumors [4,5]. Hence, the idea of seeking for natural sweeteners with no health risks found much popularity nowadays. In light of this, a large number of people still believe that sweetness can be perceived only upon consumption of table sugars or some artificial sweeteners; however it is a fact today that there are some plant-based sweet proteins that could trigger a sweet perception upon ingestion by mammalian. Indeed, some of the sweet proteins are sweeter than sucrose and most of nan-calorie sweeteners by orders of magnitude [6]. In addition to intense sweetness, these proteins do not trigger the demand for insulin [7]. To date, six sweet and sweet taste-modifying proteins were found such as Monellin [8], Thaumatin [9], Brazzein [10], Mabinlin [11], Miraculin [12] and Curculin [13], which are without glycosylation [7,14]. Miraculin and Curculin are the only sweet taste-modifying proteins with the capability to switch sour food ingredients into sweet [15–17]. Monellin and Thaumatin are the sweetest proteins among others, being up to 100,000 sweeter than sucrose on molar basis. All of sweet and sweet taste-modifying proteins have been extracted from different tropical plants; therefore, there is no structural homology between them [18]. These proteins like any other sweeteners can elicit a sweet sensation upon interaction with the sweet taste receptor, T1R2-T1R3, located on specific cells of tongue, palate, pharynx and gut [19–22]. However, the binding regions of the sweet proteins to the sweet taste

receptor are not the same with respect to low molecular weight sweeteners *i.e.* sucrose. In fact, the latter sweeteners occupy the orthosteric cavities of the Venus flytrap domains and activate the receptor, although the binding sites of these sweeteners to the receptor are diverse from one another [23–26]. On the other hand, sweet proteins are believed to have a similar mode of interaction to the sweet taste receptor, which completely differs from that of low molecular weight sweeteners. So far, one hypothesis has been proposed that best explained the interaction mode between sweet proteins and the sweet taste receptor, known as "wedge model". According to the wedge model, sweet proteins bind to the external cleft between both subunits of the receptor and activate it [24,27].

Monellin is isolated from *Dioscoreophyllum cumminsii*, found in tropical rainforest of West African countries [28]. Monellin is a small protein (~ 11 kDa) consists of 94 amino acid residues and structurally composed of two polypeptide chains. These two chains are linked together by non-covalent interactions forming a five-strand β-sheet half-wrapped around α-helix [29–31]. Although Monellin is benefited with great properties such as high sweetness intensity, however, it suffers from low thermal stability. As a matter of fact, Monellin undergoes irreversible denaturation and subsequently loss of sweetness when heated over 50 °C [32]. This hurdle was overcome by joining both subunits of Monellin through inserting a Gly-Phe dipeptide linker at the positions of 49 and 50 to produce a single-chain Monellin, called MNEI [33]. Indeed, the engineered recombinant protein, MNEI, showed an increase in the melting temperature to over 70 °C without loss of any sweetness intensity [32]. Due to the unique properties of MNEI *i.e.* intense sweetness, thermostability and cheap/easy production process, it was considered as a promising candidate to replace sucrose and other commonly consumed sweeteners in specific food applications [7,18,32,34]. In addition to its potential application in food industries, MNEI has also been accepted as a protein model for folding/unfolding and aggregation studies, because of its unique characteristics including high aggregation propensity, high thermal stability, high solubility in acidic environments

and structural versatility [35–39]. Herein, we aimed from one side to improve the stability and sweetness of MNEI via rational design of new mutants; and from the other side to run various characterization studies on MNEI such as shelf-life, enzymatic degradation, the effects of ionic compounds on the sweetness intensity of sweet proteins and aggregation studies.

Thaumatin is another sweet protein with very high sweetness intensity. It is extracted from the arils of *Thaumatococcus danielli*, found in the tropical plants of West Africa [9,40]. High sweetness intensity of Thaumatin can be explained by the capability to interact with the sweet taste receptor. The complex is stabilized by electrostatic interactions between positive charge distribution on the external surface of the protein and the complementary negative charges located on the external cleft of the receptor [41–44]. It is a single chain polypeptide and composed of 207 amino acid resides, forming 5 α-helices, 13 β-pleated sheet and bends. This macromolecule includes 16 cysteine amino acids in its primary structure, which are oxidized to form eight intermolecular disulfide bonds [45,46]. Thaumatin is also known as a thermostable protein under acidic condition, in a way that it preserves its sweetness intensity upon heating at 80 °C for several hours [47]. High thermal stability of Thaumatin is associated with the existence of eight intermolecular disulfide bridges [45]. Up to this date, Thaumatin is the only sweet protein that is Generally Recognized As Safe (GRAS) ingredient to use in different food and beverage applications [48,49]. However, there are still no reports of Thaumatin's application in food industries. In this regard, we aimed to use Thaumatin as a sweetener in two of the Kraft Heinz Company's iconic products, *i.e.* strawberry cordial and tomato ketchup, followed by performing some analytical studies such as sensory and rheology analyses.

This project started with further improvement of MNEI's stability and sweetness by designing a new mutant in a rational way. In this design, we took into account the available information extracted from some successful mutants with developed

sweetness and/or stability. For instance, each one of the following point mutations E23A [50,51], C41A [51], R65Y [52] and S76Y [53] is known to improve a specific property of MNEI. Among these point mutations, E23A, C41A and S76Y were dedicated to increase thermal and chemical stability of MNEI, whereas Y65R could improve the sweetening power of the protein. The data collected from extensive characterization studies of the new mutant (Mut9) showed a superior stability and sweetness with respect to the parent protein, MNEI. We began with the measurement of the secondary structure of Mut9 at pH 2.5, 5.1 and 6.8, followed by a comparison analysis with the obtained CD spectra of MNEI at the same pHs. The CD spectra of both proteins, Mut9 and MNEI, were characterized by two minima at 201 nm and 213 nm, indicating a high β-sheet content of these proteins, which is deduced by a strong downward shift at 213 nm. Then, Mut9 was subjected to a sensory analysis to assess the sweetness power. The sweetness threshold of Mut9 was measured by performing a triangle test and the results were compared to that of MNEI. Interestingly, the sweetness power of Mut9 has increased by a factor of about 2 folds with respect to MNEI [54,55]. The thermal stability of Mut9 and MNEI at pH 2.5, 5.1 and 6.8 was also measured by DSC. The obtained data demonstrated an astonishing improvement in the thermal stability of Mut9 compared to MNEI at all explored pHs. The striking development in the thermal stability of Mut9 was observed at pH 6.8, where the melting temperature of Mut9 was over 20 degrees °C higher than that of MNEI. The stability of Mut9 was further challenged upon extreme conditions, where samples of Mut9 and MNEI in acidic and neutral environments were boiled for maximum 10 minutes. Appealingly, the structures of both proteins at acidic conditions remained well-folded and functional with retained sweetness up to 10 minutes. Under neutral pH, Mut9 greatly preserved its secondary structure and sweetness after 10 minutes of boiling; however, MNEI was completely unfolded and lost its sweetness as short as 2 minutes of boiling [54].

In order to introduce MNEI as a sweetening agent for any commercialization trials, some characterization studies including shelf-life and physiological effects are

mandatory. Here, we performed a shelf-life study on MNEI and three of its mutants, *i.e.* Mut3, Mut4 and Mut9 to investigate their resistance and oligomerization propensity in solutions upon a prolonged incubation under various physicochemical parameters such as pH, temperature and protein concentration. According to the collected data, incubational temperature significantly affected the integrity of the proteins, where they were more stable at 4 °C. Further, the pH of incubated solutions also influenced the proteins but the effect was limited. The sweet proteins showed a better resistant in acidic environments rather than neural. On the other hand, protein concentration had a negligible influence on the resistance and integrity of the proteins in solutions. Based on the data, Mut9 and Mut3 presented a great performance in terms of resistance and oligomerization propensity, although Mut9 was even stronger than Mut3. The enzymatic digestion of MNEI was also investigated via simulating the human *in vivo* digestive system. In this experiment, three fluids *i.e.* SSF, SGF and SIF including digestive enzymes and some electrolytes were used, representing the three human digestive systems: oral, gastric and intestinal, respectively. The data collected from this study illustrated that the oral phase which contained only α-amylase did not affect the protein at all. However, MNEI was digested into many peptide fragments after the gastric phase. These results were expected due to the existence of the proteolytic enzyme pepsin, which is known to digest food proteins. After the gastric phase, the sample was subjected to the intestinal phase that included pancreatic enzymes. As a matter of fact, peptide fragments were fully degraded into very small pieces in presence of pancreatic enzymes consisting of trypsin and chymotrypsin. The identification of the peptides by mass spectrometry is in progress. Preliminary studies on peptides identification and the possible presence of toxic species formed upon enzymatic digestion have been performed *in silico*. The collected data showed that all of the digested species are nontoxic.

During preparations of home-made beverages using sweet proteins, we have encountered an inequality issue in the sweetness intensity of sweet proteins using

different types of commercial waters, which have various amounts of mineral residues and conductivities. To shed more light on this topic, we performed a systematic study to understand whether this inconvenience was resulted from protein's structural changes or disturbance in the protein-receptor interactions. In this study, we used 4 sweet proteins, *i.e.* MNEI, Mut3, Mut9 and Thaumatin as sweetening agents to prepare drinking samples in 4 commercial waters such as HPLC grade, Sant'Anna, Rocchetta and Lieve. Then, the sweetness intensity of the proteins was carefully analyzed by blind sensory analysis and the structures of the proteins by CD and NMR spectroscopies. To evaluate the effect of different types of commercial waters on the sweetness intensity of low molecular weight sweeteners, we also prepared sweet drinking samples using sucrose, sucralose and aspartame. According to the collected data, all of the explored sweet proteins followed a similar trend in terms of sensory analysis, where, the sweetness power of the proteins decreased from HPLC water (the lowest mineral residues amount) to Lieve (the highest mineral residues amount). Diversely, the structures of the proteins in all explored types of waters were preserved and the spectra (CD and NMR) of the proteins were superimposable. On the other hand, the sweetness intensity of sucrose, sucralose and aspartame in 4 types of waters remained almost identical. According to the mechanism of action of sweet taste receptor with the sweet proteins explained by wedge model, we believe that the decrease in the sweetness power of the sweet proteins is most probably linked to the presence of ionic species, which could disturb protein-receptor bindings.

In addition to high sweetness power, Monellin and its single-chain constructs were also observed to have high aggregation propensity upon incubation at specific physicochemical conditions [55–58]. These conditions, in terms of concentration, ionic strength and temperature, could resemble the ones encountered during the storage or food processing steps in industrial preparation. Many toxic species have been observed during the protein aggregation steps, thus, in order to understand the influence of physicochemical condition on the aggregation process of MNEI and to

verify if any toxic forms are formed during the incubation, we investigated the aggregation propensity of MNEI and controlled the formation and morphology of the aggregates by modifying experimental conditions. We explored the effects of temperature, intensive mechanical agitation, ionic strength, different buffering solution and protein concentration on the aggregation to analyze the kinetics or morphology of the aggregates. We observed that mechanical agitation with and without beads and addition of NaCl significantly increased the aggregation kinetics of MNEI, however, the morphologies of the formed aggregates were totally diverse, ranging from 100 nm to several μm. The Cytotoxicity of MNEI aggregates formed under different incubational conditions were assessed as well. It was found that only soluble MNEI aggregates formed after 24 hours of incubation at 65 °C and under mechanical agitation (with and without PTFE beads) were toxic and the soluble aggregates detected after 48 and 72 hours of incubations were nontoxic. Worth mentioning, mature MNEI fibrils are free of any toxicity [59]. The aggregation tendency and the associated potential toxicity seem not an issue, because only a combination of high temperature, extensive agitation, high protein concentration and high ionic strength are required to prompt the aggregation. In addition, the formation of slightly toxic forms occurs only in a very limited period of time.

These studies are encouraging in view of the possible introduction of MNEI and its derivatives in Food and beverages products, however further studies to assess their physiological effects are still needed. Therefore, as an attempt toward commercialization of sweet proteins, we collaborated with the Kraft Heinz Company to use Thaumatin as a sucrose replacer in the standard recipes of two iconic products of the Kraft Heinz Company, tomato ketchup and strawberry cordial. The reason for selecting Thaumatin among other sweet proteins for this study was the FDA approval license given to this protein. This allowed the sensory team of the Kraft Heinz Company to ingest the samples during sensory analysis. To assess the effects of Thaumatin addition in these two products, we performed a series of experiments such as sensory analysis and rheological analyses. According

to the sensory analysis data, the tomato ketchup including Thaumatin tasted more sour and bitter without sensing any sweetness. The perceived sourness and bitterness are not because of Thaumatin presence, but these attributes which are coming from other ingredients *i.e.* vinegar, were more revealed in the absence of any sweetness. The loss of Thaumatin sweetness is most likely due to the presence of other ingredients, *i.e.* salt that could disturb the protein-receptor binding. Rheological properties of tomato ketchup were also altered by sucrose removal. In fact, tomato ketchup including Thaumatin was less thick, less viscose with lower texture properties. On the other hand, strawberry cordial prepared with Thaumatin showed a different behavior. Interestingly, the cordial tasted sweet, although the sweetness perception delayed for a few seconds, which is consistent with the known sweetness profile of Thaumatin. We strongly believe that the sweetness profile of Thaumatin in strawberry cordial could be modified by combining Thaumatin with other non-calorie sweeteners such as sucralose to cover the sweetness delay of Thaumatin. In addition, the rheological properties of tomato ketchup and strawberry cordial including Thaumatin could be also adjusted by addition of some food additives *i.e.* bulky agents.

CHAPTER <u>1</u>

Mut9
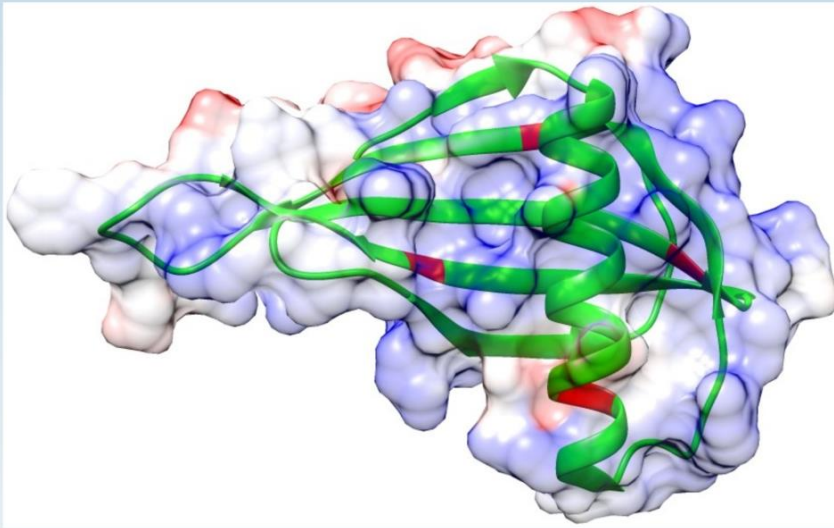
GEWEIIDIGPFTQNLGKFAVDEANKIGQYGRLTFNKVIRPAM
KKTIYENEGFREIKGYEYQLYVRASDKLFRADIYEDYKTRGR
KLLRFNGPVPPP

Rational design and production of a super stable and sweeter mutant of MNEI, single chain monellin

Abstract

MNEI, single-chain Monellin, is one of the six sweet and sweet taste-modifying proteins. It is able to elicit a sweet sensation in humans upon interaction with a heterodimeric G-protein coupled receptor, T1R2-T1R3. MNEI has also a high thermostability, but for industrial applications, it suffers from limited stability and high aggregation propensity at neutral pH. To improve MNEI's stability and/or sweetness, a new construct of MNEI was rationally designed, termed Mut9. Interestingly, Mut9 displayed an extraordinary stability from strongly acidic to mild alkaline pH, where the difference of the melting temperatures between Mut9 and MNEI reached over 20 °C at neutral pH. In Addition, Mut9 at pH 2.5 and 6.8 recovered its folding pattern and its sweetness intensity upon 10 minutes of constant boiling. Moreover, the sweetness intensity of Mut9 was increased by a factor of about 2 folds with respect to MNEI. Indeed, the sweetness threshold of Mut9 resided at 0.80 mg/L, and 1.64 mg/L is known for that of MNEI. The outcome demonstrated that Mut9 is significantly stronger and sweeter than its parent protein, MNEI. These findings strongly increase the potential of Mut9 applications in food and beverage products.

1.1 Introduction

A great number of people believe that sweetness can be perceived only upon consumption of sucrose or some non-calorie sweeteners; however, it is a fact today that there are some plant-based proteins with very high sweetness power that can be consumed instead of ordinary available sweeteners. Indeed, some of these proteins are sweeter than sucrose and most of non-calorie sweeteners by orders of magnitude [6]. Up to this date, six sweet and sweet taste-modifying proteins have been discovered including Monellin [8], Thaumatin [9], Brazzein [10], Mabinlin [11], Miraculin [12] and Curculin [13]. In this list, Miraculin and Curculin are known as sweet taste-modifying proteins, since they can switch the sour substances into sweet [15–17]. All of the sweet and sweet taste-modifying proteins have been isolated and purified from unrelated tropical plants. Except their plant origin, they share neither sequence nor structural homology among themselves [18]. In the recent years, the prevalence of some hazardous sugar-related diseases such as obesity, diabetes, hyperlipidemia and carries inspired food and beverage customers and manufacturers to seek for healthier replacements for ordinary sweeteners. This is why natural sweeteners *i.e.* sweet proteins, attracted much attention after unsuccessful experience of using artificial sweeteners; this is proved by many evidences demonstrating the consequences *i.e.* lethal diseases of consuming artificial sweeteners [3].

Monellin is extracted and purified from *Dioscoreophyllum cumminsii*, found in tropical rainforest of West African countries [28]. Monellin has an extraordinary sweetness intensity reaching to 100,000 times sweeter than sucrose, on molar basis [18]. Thanks to its sweetness power, Monellin in principle could be an ideal candidate to substitute the commonly used sweeteners in different industrial applications [7]. Morphologically, Monellin is a small globular protein (~ 11 kDa), which is structurally composed of two polypeptide chains, A and B containing 45 and 50 amino acid residues, respectively. The two polypeptide chains of Monellin

are linked together by non-covalent interactions forming a five-strand β-sheet half-wrapped around an α-helix [29–31]. This potent natural sweetener, however, undergoes irreversible denaturation and subsequently loss of sweetness when heated over 50 °C [32]. To resolve this inconvenience, single-chain Monellin, MNEI, was designed by joining both subunits of Monellin through a Gly-Phe dipeptide linker inserted in the amino acid sequence positions of 51-52 (**Fig. 1**) [33]. Indeed, this led to an increase in the melting temperature of the new recombinant protein to over 70 °C without loss of sweetness intensity [32].
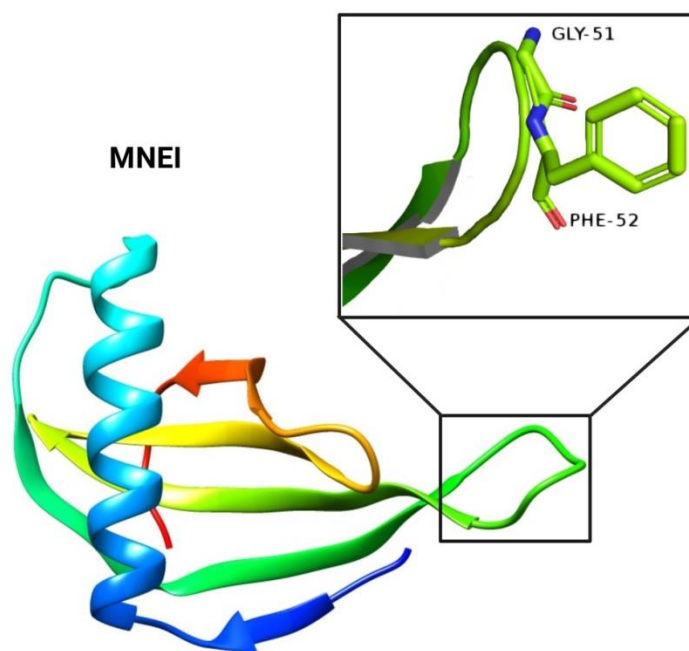
Figure 1. Carton mode presentation of MNEI designed from Monellin. A dipeptide linker, Gly-Phe at the positions of 51-52 is shown in the inset.

All types of sweeteners including sweet and sweet taste-modifying proteins elicit a sweet sensation upon interaction with the sweet taste receptor, a heterodimeric G-protein coupled receptor which is composed of two subunits, T1R2-T1R3. This receptor is located on specialized cells of tongue, palate, pharynx and gut [19–22]. In addition to the seven helix transmembrane domain that is commonly observed in

class C G protein coupled receptors, the sweet taste receptor includes an extra membrane domain, named Venus flytrap domain. These two domains are connected together by a cysteine-rich domain. The Venus flytrap domain named after the carnivorous plant, since it resembles this plant in two ways: 1) both contain an active site for orthosteric ligands and, 2) analogous change of shape upon ligand binding [19]. It is worth mentioning that the sequences of the sweet taste receptor's subunits are highly homologous but not identical [23,60].

Sucrose and other low molecular weight sweeteners occupy the orthosteric cavities of the Venus flytrap domains and activate the sweet taste receptor. However, the binding regions of low molecular weight sweeteners, including sucrose, to the receptor are not the same [23–26]. On the other hand, sweet proteins with considerably larger dimensions are believed to have similar mode of interaction to the receptor, which is completely different from that of low molecular weight sweeteners. So far, one hypothesis has been proposed that best explains the interaction mode between sweet proteins and the sweet taste receptor, known as "wedge model". According to the wedge model, sweet proteins bind to the external cleft between both subunits of the receptor and activate it [24,27,61]. To create the wedge model, metabotropic glutamate receptor 1 (mGluR1) with high structural homology to the sweet taste receptor was used. The reason of using mGluR1 is that when the taste receptors were discovered, mGluR1 was the only class C G proteins with the solved structure. In this model, the sweet taste receptor is under equilibrium conditions between two conformations, inactive and active form. According to the wedge model, sweet proteins stabilize the active conformation of the sweet taste receptor upon binding to a wide cleft between both subunits of the receptor, T1R2-T1R3 [62].

In biotechnology, the most practical technique to improve the properties of proteins is site-directed mutagenesis [63]. Deep structural studies of receptor-protein complex in parallel with protein engineering technique are the key of building new

mutants with improved properties. In order to design new mutants of sweet proteins, it is vital to preserve the three dimensional shape of the protein to keep its functionality. Moreover, surface charge can be a very decisive factor on the sweetness potency of the protein. It is known that the surface of sweet taste receptor, T1R2-T1R3, is covered by many acidic amino acid residues [24,27]. This is why, mutations increasing the acidic amino acids on the outer surface of single and double chain Monellin [52,64–66], Thaumatin [43,67–69] and Brazzein [70–72] led to decrease or cancelation of sweetness. On the other hand, random increase of basic amino acids on the external surface of the sweet proteins might abate the sweetness intensity as well. For instance, some mutants of single-chain Monellin such as M42R, Y63R, Y65R and D68R were designed by introducing surface basic amino acids and the obtained data demonstrated that only the sweetness intensity of mutant MNEI-Y65R was increased, while other point mutations reduced the sweetness [52]. The reason is that the acidic amino acids distribution on the surface of sweet taste receptor is non-homogeneous. Therefore, to design new sweet proteins with improved sweetness and/or thermal stability, positive charges should be located on specific positions on the surface [24,27].

Considering the promising industrial applications of sweet proteins, some attempts have already been performed to improve the properties of MNEI based on the surface interactions with the sweet taste receptor predicted by the wedge model. The sweetness and stability of MNEI were developed via designing new mutants such as Mut3, Mut2 [73], Y65R-MNEI [52] and E23Q-MNEI [50]. In this study, we aimed to further improve the stability and sweetness intensity of single-chain Monellin, MNEI, by designing 5 mutants. Only one mutant, dubbed Mut9, was successfully produced and characterized by different biophysical techniques, with a particular attention to assess its thermal/chemical stability and sweetness potency. The results achieved from the evaluation of stability and sweetness intensity of Mut9 confirmed the possibility to further improve MNEI properties in response to the markets

demands for replacing ordinary sweetening substances in food and beverage products.

1.2 Materials and Methods

1.2.1 Cloning, Expression and Purification of the Mutant

The synthetic full-length genes encoding for the sequences of Mut5, Mut6, Mut7, Mut8 and Mut9 were purchased from Eurofins Genomic Company. The genes were cloned into the expression vector of pET22b(+) (Novagen) between the *NdeI* and *BamHI* restriction sites. The recombinant proteins were expressed in *Escherichia coli* BL21(DE3) and purified from the cell lysate by ion-exchange chromatography followed by size-exclusion chromatography for salt removal as previously described [34]. The identity and purity of the proteins were confirmed by SDS-PAGE electrophoresis and circular dichroism spectroscopy. Protein concentration was measured using UV-Vis spectrophotometer (Thermo GENESYS™ 10UV, USA).

1.2.2 Circular Dichroism Spectroscopy (CD)

CD measurements were performed on a Jasco J-715 spectropolarimeter (Jasco, Essex, UK), equipped with a Peltier temperature control system (PTC-348WI, Jasco, Essex, UK), using a 0.1 cm quartz cell. The CD curves of Mut9 and MNEI were obtained in 0.020 M sodium phosphate buffer at pH 2.5, 3.5, 4.5, 5.5, 6.8 and 8.0. To assess the effect of temperature, spectra of Mut9 and MNEI in 0.020 M sodium phosphate buffer at pH 2.5 and 6.8 were measured at 10 °C intervals in the range of 25 - 95 °C and back to 25 °C. In another experiment, CD spectra were acquired upon boiling Mut9 and MNEI dissolved in the same buffers for 2, 5 and 10 minutes, and cooling back the protein solutions to room temperature. The spectra measured in the far UV-range (195-250 nm) with a scan speed of 50 nm/min and each experiment was performed with 3 accumulations. Thermal denaturation profiles

were also recorded following the signal at 215 nm while varying the temperature from 25 to 95 °C at a rate of 1 °C/min. Molar ellipticity per mean residue [θ] was calculated according to the formula:

$$[\theta] = [\theta]_{obs}\, mrw \,/\, (10 \times l \times C), \quad deg\, cm^2\, dmol^{-1}$$

where $[\theta]_{obs}$ is the raw ellipticity values measured in degrees, mrw is the mean residue molecular weight of each protein (Da), C is the protein concentration in g/ml and l is the optical path length of the quartz cell in cm. In all experiments, the concentration of Mut9 and MNEI was 0.2 mg/mL, measured by UV absorbance at 280 nm using a calculated value of the absorbance at 0.1 % of 1.41. In order to have a quantitative estimation of the secondary structure content, the CD spectra were deconvoluted using the BestSel online tool [74].

1.2.3 Sensory Analysis

Sweetness intensity was evaluated by triangle test [52]. A team of 5 panelists participated in the sensory analysis. MNEI solutions and mineral water were used as positive and negative controls, respectively. Three paper cups, one containing 5 mL of protein sample and two cups containing 5 mL of mineral water were provided for the panelists to taste the samples and record their evaluation from 0 (no taste) to 2. A value of 1 indicated the perception of an unidentified taste and 2 meant the taste was recognized as sweet. The sample solutions were provided from the lowest (35 nM) to the highest (220 nM) concentration. Sweetness threshold was the concentration at which the protein scored 2 on average.

To assess taste performance upon thermal treatment, a blind sensory analysis was performed on 20 mg/L Mut9 and MNEI sample solutions before and after boiling for 2, 5 and 10 minutes. The boiled samples were tasted and the assessments were made on a table with three tasting rates: same sweetness, decreased sweetness and loss of sweetness. In both experiments, the subjects tested the sample solutions

without any time constraints, then spat it out and rinsed their mouth thoroughly with mineral water within 1 minute.

1.2.4 Differential Scanning Calorimetry (DSC)

Calorimetric measurements were performed using a Nano-DSC 6300 (TA Instruments, USA). Protein samples were prepared in 0.020 M sodium phosphate buffer with a concentration of 1 mg/mL and ran with a scanning speed of 1 °C/min and in a temperature range of 20–110 °C for Mut9 and 20-100 °C for MNEI. During the temperature scans, a total pressure of 3.0 atm was applied to both cells using nitrogen gas. Buffer scans were recorded separately under the same conditions and subtracted from sample scans to obtain the excess molar heat capacity function [75]. A second run heating of the protein samples under identical conditions, after cooling down from the first run heating was also performed to verify the reversibility of the process. The reversibility percentage is calculated by dividing ΔH_{cal} of the second scan to ΔH_{cal} of the first scan $\times$ 100.

The denaturation temperature, T_d and enthalpy $\Delta_d H$ were obtained by the maximum of the DSC peak and the integrated area under the peak, respectively. All DSC data analyses were performed using the Nano-Analyze software supplied with the instrument.

1.3 Results and Discussion

1.3.1 Protein design and production

In this study, we aimed to design new mutants of MNEI with a particular focus on the thermochemical stability improvement. As a result, we rationally designed 5 new mutants *i.e.* Mut5, Mut6, Mut7, Mut8 and Mut9 using molecular dynamics and literature data. The collected data indicated that upon high temperature (over T_m of

MNEI), the α-helix of the protein dissociates from the β-sheet resulting in protein denaturation. To avoid this from happening, we introduced 2 cysteine residues for each of the proteins: Mut5, Mut6, Mut7 and Mut8, one on the α-helix and another one on the β-sheet with a close distance in order to form disulfide bonds and make the protein resistant against any structural dissociation. The sequences of the proteins including Mut5, Mut6, Mut7 and Mut8 are presented in **Table 1**. The genes of the proteins were cloned into the expression vector for production. Among these proteins, only Mut7 was isolated as a folded protein whereas the other ones precipitated during purification procedure. The results of characterization studies on Mut7 showed that the protein has low solubility, no sweetness functionality and low stability with respect to its parent protein, MNEI. On the other hand, Mut9 was successfully produced and characterized.

Table 1. The amino acid sequences of MNEI and its designed mutants *i.e.* Mut5, Mut6, Mut7 and Mut8.

Mutant	Sequence
MNEI	1 11 21 31 GEWEIIDIGP FTQNLGKFAV DEENKIGQYG RLTFNKVIRP 41 51 61 71 CMKKTIYENE GFREIKGYEY QLYVYASDKL FRADISEDYK 81 91 TRGRKLLRFN GPVPPP
Mut5	1 11 21 31 GEWEIIDIGP FTCNLGKFAV DEQNKIGQYG RLTFNKCIRP 41 51 61 71 SMKKTIYENE GFREIKGYEY QLYVYASDKL FRADISEDYK 81 91 TRGRKLLRFN GPVPPP
Mut6	1 11 21 31 GEWEIIDIGP FTQNLGCFAV DEQNKIGQYG RLTCNKVIRP 41 51 61 71 SMKKTIYENE GFREIKGYEY QLYVYASDKL FRADISEDYK 81 91 TRGRKLLRFN GPVPPP
Mut7	1 11 21 31 GEWEIIDIGP FTCNLGKFAV DEQNKIGKYG RLTFNKCIRP 41 51 61 71 SMKKTIYENE GFREIKGYEY QLYVRASDKL FRADISEDYK 81 91 TRGRKLLRFN GPVPPP
Mut8	1 11 21 31 GEWEIIDIGP FTQNLGCFAV DEQNKIGKYG RLTCNKVIRP 41 51 61 71 SMKKTIYENE GFREIKGYEY QLYVRASDKL FRADISEDYK 81 91 TRGRKLLRFN GPVPPP

To design Mut9, we took advantage of some successful mutants such as E23A-MNEI, C41A-MNEI [51], Y65R-MNEI [52] and S76Y-MNEI [53] (**Fig. 2**). Each one of these point mutations is reported to develop a specific property. For instance, E23A, C41A and S76Y could enhance the thermal and chemical stability of MNEI [51,53]. In more detail, the mutation E23A increased the pH stability of MNEI from strongly acidic to mild alkaline pH. This gain in the chemical stability is due to the peculiar position of this residue that is buried inside the C-terminal region of the α-

helix [50,51]. In addition to E23A, the point mutation C41A also increased the pH stability of MNEI by removing the possibility of MNEI to dimerize through an inter-chain disulfide bonds [51]. The last point mutation dedicated to improve the thermal stability of MNEI is S76Y. In fact, this mutation alone could elevate the melting temperature of the protein by 10 °C through increasing the van der Waals interactions with the surrounding amino acid residues [53]. On the other hand, Y65R mutation is known to increase the sweetness intensity of the protein by lowering the sweetness threshold of MNEI from 1.64 to 0.66 mg/L [55]. Mut9 was expressed in *E.Coli* using standard recombinant expression protocols and purified by the same procedure already reported for the parent protein, MNEI [34,55]. The only mentionable variation in the purification process is that Mut9 eluted by higher salt concentration solution (200 mM NaCl), compared to MNEI which elutes by 100 - 150 mM NaCl solution.

MNEI **Mut9**
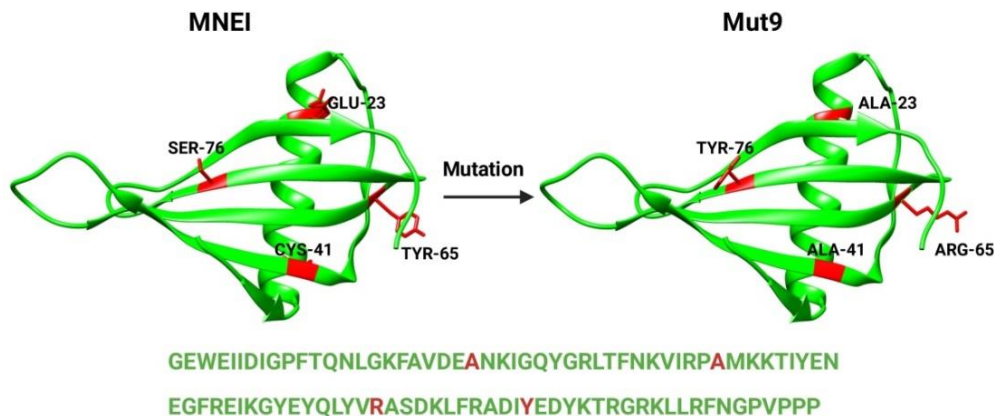
Figure 2. Carton mode representation of MNEI (left) and Mut9 (right). The positions of the single point mutations before and after mutations are highlighted by red color.

1.3.2 Secondary structure of Mut9 and MNEI

The folding pattern and the secondary structure contents of Mut9 and MNEI at different pHs (2.5, 5.1 and 6.8) were evaluated by circular dichroism spectroscopy (CD) and deconvolution of CD spectra using the BestSel online tool [74],

respectively. The collected data showed that the CD spectra of both proteins remained mostly unchanged from strong acidic to neutral pH (**Fig. 3**). At all explored pHs, the spectra of Mut9 were characterized by two minima at 201 and 213 nm similar to those of the parent protein, which is also analogous to the total folding pattern of cystatin C protein [76,77]. The observed strong minimum at 213 nm in the secondary structures of MNEI and Mut9 indicated a high β-sheet content of these proteins [78]. The strong minimum in the CD spectra of Mut9 at ~ 201 nm could be explained by higher α-helix content of Mut9 with respect to MNEI.
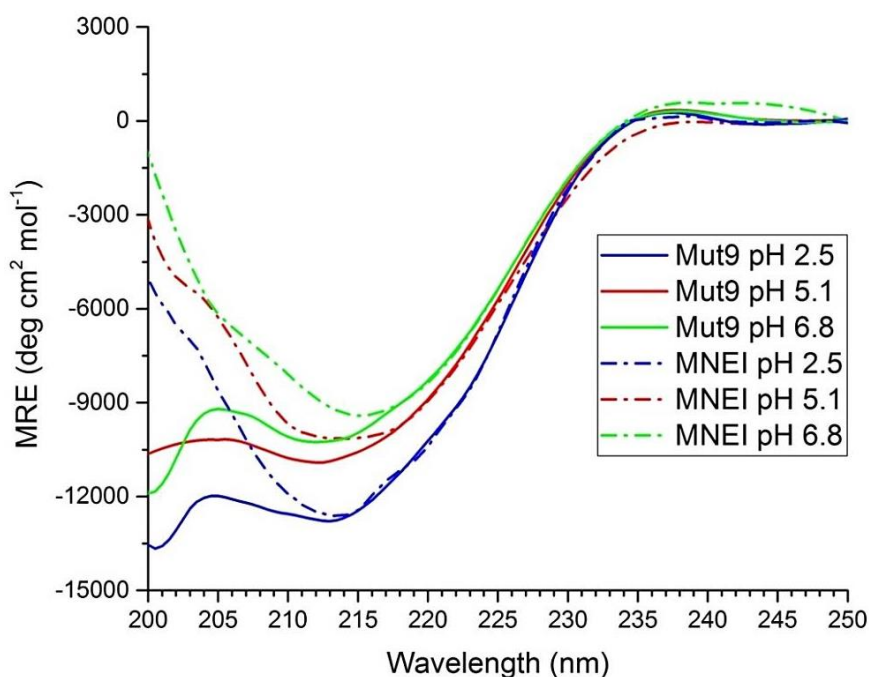
Figure 3. CD spectra of 0.2 mg/mL MNEI and Mut9 in 0.020 M sodium phosphate buffer at pH 2.5, 5.1 and 6.8. The spectra were taken at 25 °C. The spectrum of each measured pH is presented by a defined color code in the insets. This figure is adapted from [54].

The secondary structure contents of Mut9 and MNEI at pH 2.5, 5.1 and 6.8 were quantitatively estimated by deconvolution of their spectra using the BestSel online tool [74]. The β-sheet and α-helix contents of Mut9 and MNEI were highly

preserved over the examined pH range, confirming the high stability of the folding pattern of both proteins from strongly acidic to neutral pH (**Table 2**).

Table 2. Quantitative estimations of the secondary structure contents of Mut9 and MNEI by spectra deconvolution (bestsel). Errors on the secondary structure content values are within ± 2% [74]. This table is adapted from [54].

SS (%)	Mut9			MNEI		
	pH 2.5	pH 5.1	pH 6.8	pH 2.5	pH 5.1	pH 6.8
α-helix	19.8	13.7	17.3	13.7	14.7	8.4
β-sheet (antiparallel)	42.2	38.3	38.8	43.8	47.0	45.3
β-sheet (parallel)	1.8	0	0	0	4.7	0
Turn	4.0	8.3	4.7	9.9	4.1	10.5
Random coil	32.2	39.7	39.2	32.6	29.6	35.7

1.3.3 Sensory analysis of Mut9

In order to determine the influence of point mutations on the sweetness power of Mut9, triangle test technique was performed on this protein to assess the sweetness threshold. The outcome showed that the sweetness threshold of Mut9 was resulted in 0.80 mg/L (71 nM) by 80 % of the panel. To confirm the accuracy of the panel, the same tasters also performed triangle test on MNEI as a positive control, and the sweetness threshold was 1.48 mg/L (132 nM), which is in a good agreement with the already known data [55]. The data clearly indicated that the point mutation raised the sweetness intensity of Mut9 by a factor of about 2 folds with respect to its parent protein, and consistent to the sweetness intensity of Y65R-MNEI [55]. The presented column graph (**Fig. 4**) is showing the sweetness threshold of both proteins.
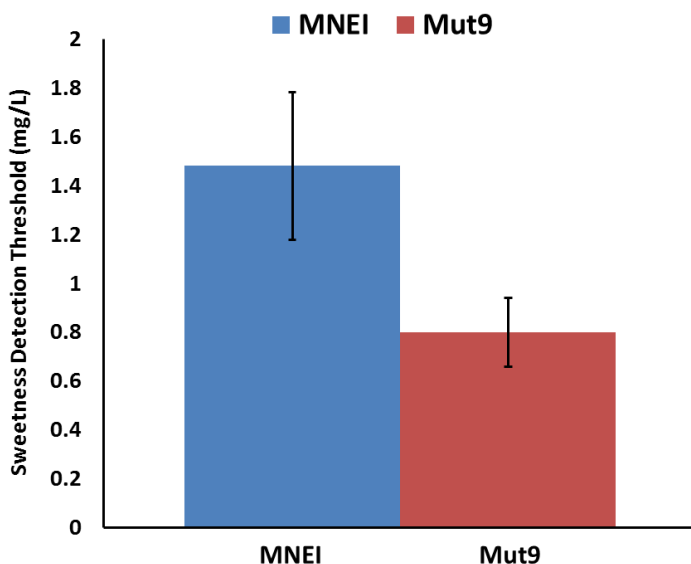
Figure 4. Bar chart presenting the sweetness threshold of Mut9 and MNEI. This figure is reprinted from [54].

1.3.4 Stability of Mut9

Thermal denaturation profiles of Mut9 were measured from strongly acidic to slightly alkaline pH (2.5 to 8.0) to monitor the thermal and chemical stability of Mut9 using CD spectroscopy. In addition, the CD spectra of Mut9 before and after measuring the T_m for each pH were taken to assess the reversibility status of the protein. Interestingly, the collected results from CD spectroscopy indicated that Mut9 at all examined pHs is more stable than its parent protein, MNEI (**Fig. 5A**-5**F**) [32,58]. Indeed, Mut9 presented a marked stability from pH 4.5 to 8.0, where the thermal denaturation profile did not complete even at the maximum temperature limit (95 °C) of CD spectroscopy instrument (**Fig. 5C**-**5F**). The melting temperatures of Mut9 at pH 2.5 and 3.5 were recorded to be ~ 79 °C and 90 °C, respectively. According to these data, the obtained T_m values of Mut9 at strongly acidic environment is higher than that of MNEI by 10 °C (**Fig. 5A** and **5B**) [58]. Furthermore, the CD curves of Mut9 at pH 2.5 and 3.5 measured after recording the melting temperature profiles revealed that the spectral line-shape of the protein was

totally preserved, confirming the reversibility of Mut9 in acidic environment (**Fig. 5A** and **5B**). Since the CD spectroscopy could not measure the melting temperature of Mut9 from mild acidic to mild alkaline pH due to a very high thermal stability of the protein, therefore, Differential Scanning Calorimetry (DSC) was used to determine the T_m of Mut9 at this pH range; and compared them to MNEI's results at the same pHs.
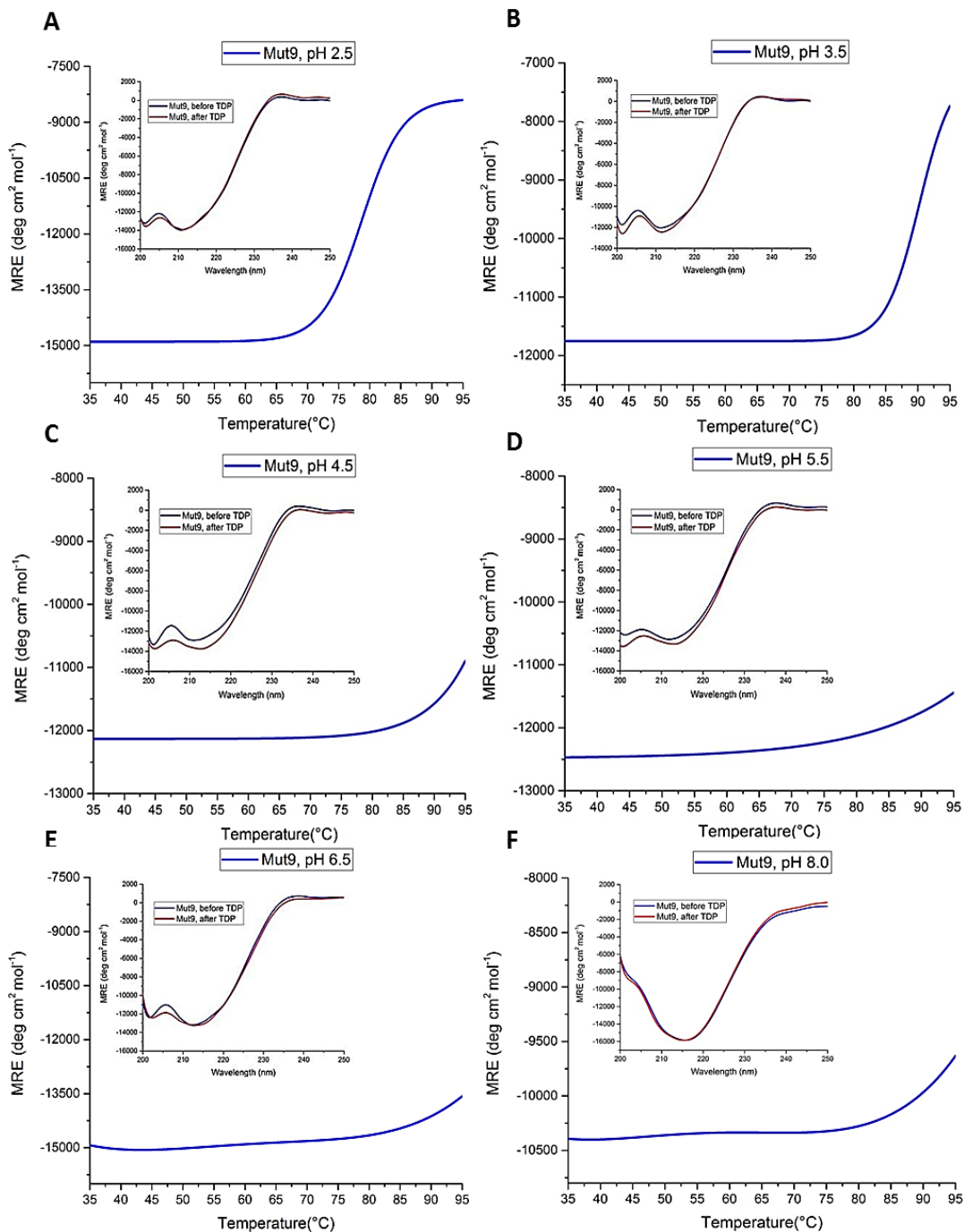
Figure 5. Thermal denaturation profiles and CD spectra of 0.2 mg/mL Mut9 in 0.020 M sodium phosphate buffer at pH: A) 2.5, B) 3.5, C) 4.5, D) 5.5, E) 6.5 and F) 8.0. The thermal denaturation profiles were obtained at 215 nm with a heating rate of 1.0 °C/min. CD spectra measured at 25 °C before (blue) and after (red) thermal denaturation are reported in the inset of each panel.

The calorimetric studies were carried out in collaboration with Professor Luigi Petraccone's research group, Chemical Sciences Department of the University Naples Federico II, Naples, Italy. DSC measurements were performed on Mut9 and MNEI at the pH values of 2.5, 5.1 and 6.8. The results of this experiment confirmed the CD spectroscopy data, indicating that Mut9 is more thermostable than MNEI at all tested pHs (**Fig. 6**). The measured melting temperatures of Mut9 at pH 5.1 and 6.8 recorded a significant improvement reaching to over 20 °C with respect to MNEI at the same pHs (**Fig. 6**). Both proteins, Mut9 and MNEI, exhibited an increase in the thermal stability from pH 2.5 to pH 6.8, with the obtained maximum values of T_m and ΔH at pH 5.1. These observations indicated that both proteins favor slightly acidic environment over strongly acidic and neutral pH.
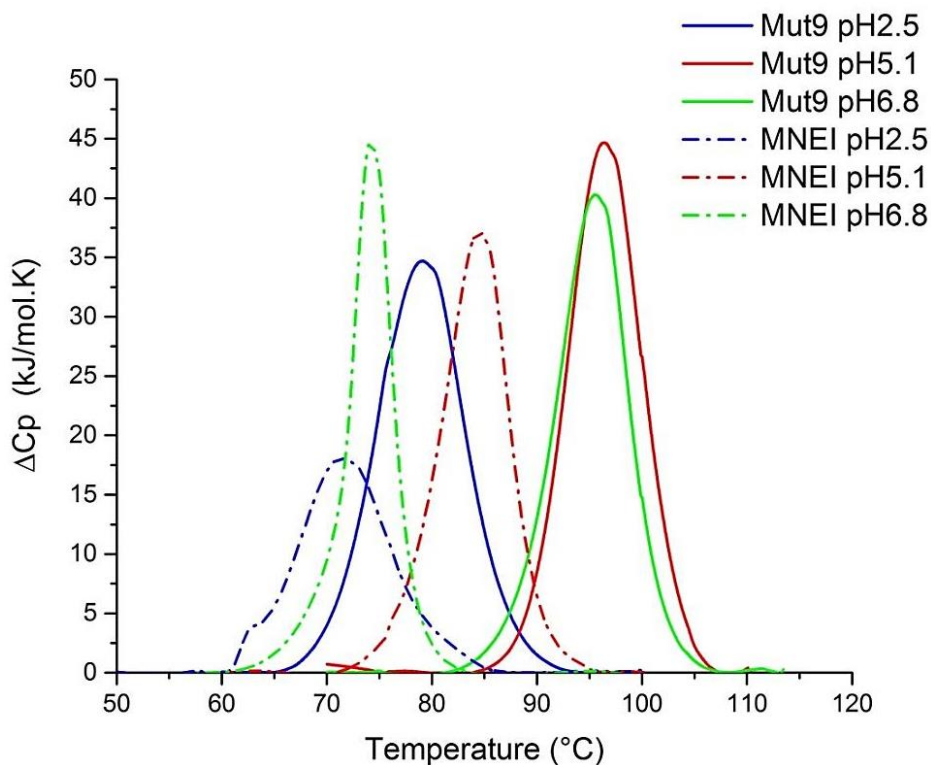
Figure 6. DCS thermograms of 1 mg/mL Mut9 and MNEI solution in 0.020 M sodium phosphate buffer recorded at different pH values. The thermogram of Mut9 and MNEI for each measured pH is presented by a defined color code in the insets. This figure is reprinted from [54].

Furthermore, DSC provided us the possibility to measure the reversibility of the thermal denaturation process of Mut9 and MNEI by performing second heating run of the same samples right after cooling down the samples from the first heating process. Indeed, Mut9 displayed an extraordinary reversibility capability at strong and mild acidic pH, while the denaturation was irreversible at the neutral pH (**Table 3**). Noteworthy, MNEI at pH 2. 5 also presented great denaturation reversibility characteristic, whereas it was irreversible at mild acidic and neutral conditions (**Table 3**).

Table 3. Thermodynamic parameters extracted from the DSC measurements. Errors on enthalpy and transition temperature are within ± 5 % and ± 0.2 °C, respectively. This table is adapted from [54].

Properties	Mut9			MNEI		
	pH 2.5	pH 5.1	pH 6.8	pH 2.5	pH 5.1	pH 6.8
T_m (°C)	79	96.2	95.8	71.4	84.4	74.2
ΔH_{cal} (KJ/mol)	327	384	336	241	253	246.5
Reversibility (%)	81	67	No	92	No	No

Further investigations on the stability and reversibility of Mut9 and MNEI were carried out using CD spectroscopy. In this experiment, a series of CD curves of Mut9 and MNEI were taken at pH 2.5 and 6.8, with temperature increasing interval of 10 °C per each measurement starting from 25 °C to 95 °C and cooling back to 25 °C. The obtained data demonstrated that both proteins under acidic conditions maintained their folding patterns upon very high temperature (**Fig. 7A** and 7**C**). Indeed, the spectral line-shape of Mut9 was preserved up to 75 °C, but at higher heating temperature *i.e.* 85 °C, the protein lost its folding pattern (**Fig. 7A**). In a similar way, MNEI at the same pH maintained its folding pattern up to 65 °C, however, the secondary structure of MNEI was completely disturbed at 75 °C (**Fig. 7C**). Interestingly, both proteins, Mut9 and MNEI, at acidic pH showed great denaturation reversibility through refolding back to their initial line-shape and spectrum intensity after cooling back from 95 °C to 25 °C (**Fig. 7A** and **7C**). At neutral pH, Mut9 displayed a fantastic stability, where the protein remained folded even at 95 °C, although a slight reduction in the spectral intensity could be observed at this temperature (**Fig. 7B**). Worth mentioning, the spectra measured before and after heating were superimposable, indicating that the structure of Mut9 was totally recovered after cooling down from 95 °C to 25 °C. Unlike Mut9, the secondary

structure of MNEI at pH 6.8 began to unfold when heated above 75 °C (**Fig. 7D**), and the spectral line-shape of the protein did not retain after cooling back from 95 °C to 25 °C. Therefore, it can be concluded that the denaturation process of MNEI is irreversible in neutral environment (**Fig. 7D**).
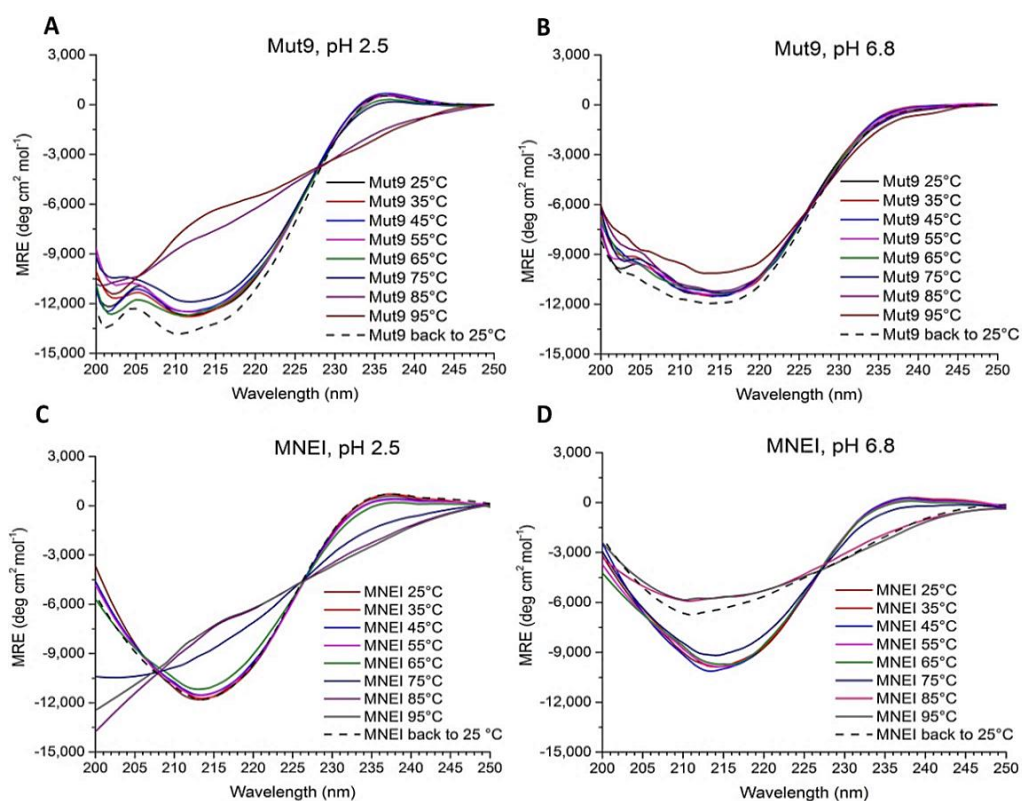
Figure 7. CD curves of Mut9 and MNEI were obtained with a protein concentration of 0.20 mg/mL in 0.020 M sodium phosphate buffer. The presented data are: A) Mut9 at pH 2.5, B) Mut9 at pH 6.8, C) MNEI at pH 2.5 and D) MNEI at pH 6.8. The spectra were taken from 25 °C with 10 °C increasing interval to 95 °C and cooling back to 25 °C. The spectrum of each measured temperature is presented by a defined color code in the insets. This figure is reprinted from [54].

To shed more light on the chemical and thermal resistance and folding stability of Mut9 and MNEI, we designed a new experiment in which the proteins were subjected to extreme conditions *i.e.* boiling at acidic and neutral conditions for different time periods, followed by evaluating the secondary structure and functionality of the proteins using CD spectroscopy and sensory analysis, respectively. The concentration of both proteins was adjusted on 0.20 mg/mL and the samples were heated at 100 °C for 2, 5 and 10 minutes. The goal of this experiment was to simulate the possible industrial treatments on the proteins for any preparation procedures of food and beverage products. Intriguing results were observed for both proteins at pH 2.5. In fact, the CD spectra of Mut9 and MNEI at pH 2.5 were highly overlapping upon boiling up to 10 minutes (**Fig. 8A** and **8C**). On the other hand, Mut9 under neutral conditions showed an incredible thermal resistance. Indeed, the secondary structure of Mut9 remained mostly unchanged even after boiling for 10 minutes, although a little reduction in the spectrum intensity could be detected (**Fig. 8B**). In contrast, at neutral pH the line-shape of MNEI was totally disturbed after as short as 2 minutes of boiling, which can be explained by high aggregation propensity of MNEI (**Fig. 8D)** [58,79]. In addition, we assessed the functionality of the proteins by running a sensory analysis on the samples boiled for 2, 5 and 10 minutes. This evaluation was performed on the 20 mg/L proteins, a lower concentration than that used for CD studies (0.20 mg/mL), but it is comparable with the concentration of a potential drink. The data evidenced that the increase in the thermal resistance of Mut9 was also paralleled by the sweetness resistance of this protein with respect to MNEI. In fact, both proteins retained their sweetness at acidic pH after 10 minutes of constant boiling, whereas at neutral pH, MNEI completely lost its sweetness after only 2 minutes of boiling, while Mut9 preserved its sweetness intensity even after 10 minutes boiling (**Table 4**). These results are in a great agreement with the collected data from CD experiment.
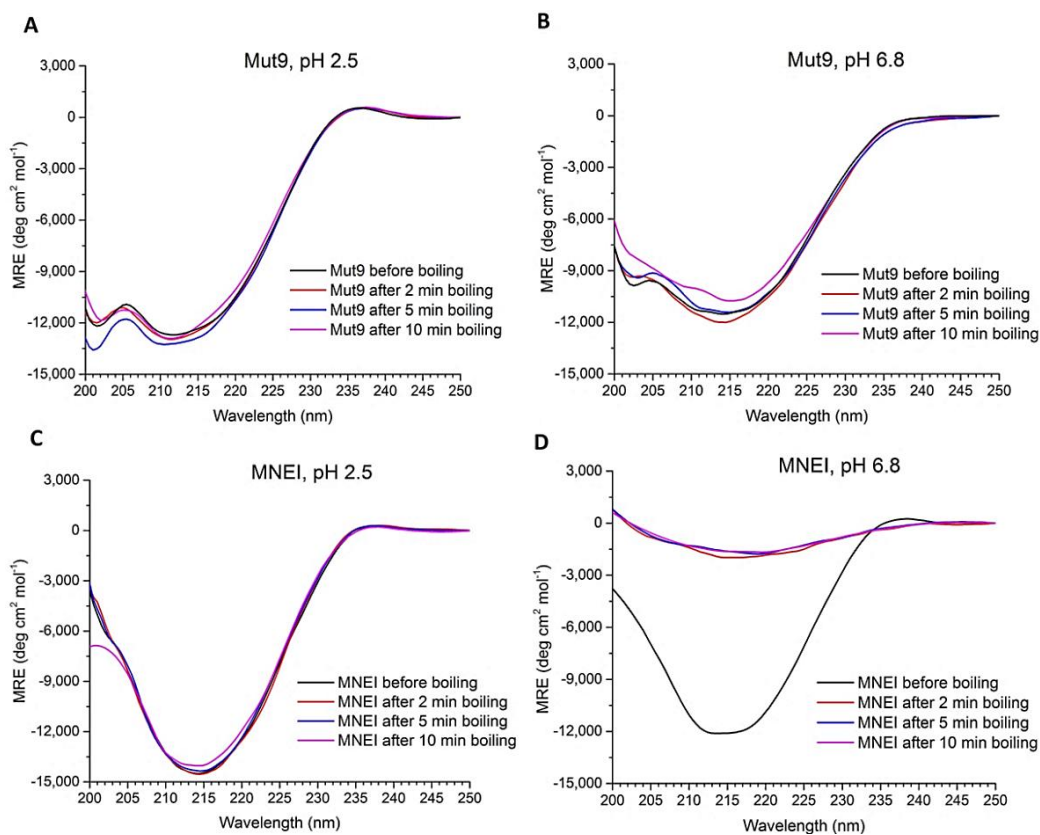
Figure 8. CD curves of Mut9 and MNEI with a concentration of 0.20 mg/mL in 0.020 M sodium phosphate buffer. The presented spectra are A) Mut9 at pH 2.5, B) Mut9 at pH 6.8, C) MNEI at pH 2.5 and D) MNEI at pH 6.8. This experiment performed under boiling conditions for 2, 5, and 10 minutes as reported in the inset of each spectrum. All the spectra were taken at 25 °C. This figure is reprinted from [54].

Table 4. The sweetness assessment of Mut9 and MNEI at pH 2.5 and 6.8 upon boiling for 2, 5 and 10 minutes.

Protein	Boiling Time (min)	pH 2.5			pH 6.8		
		Same sweetness	Decrease sweetness	Loss sweetness	Same sweetness	Decrease sweetness	Loss sweetness
MNEI	0	✓			✓		
	2	✓					✓
	5	✓					✓
	10	✓					✓
Mut9	0	✓			✓		
	2	✓			✓		
	5	✓			✓		
	10	✓			✓		

1.4 Conclusions

The prevalence of some sucrose-related hazardous diseases *i.e.* obesity, hyperlipidemia, caries, type 2 diabetes and etc., has turned into a health dilemma in all societies around the globe, more severely in the developed countries [3]. In some food and beverage products, sucrose has been replaced by non-nutritive sweeteners. However, these substances have recently been linked to severe health consequences [4]. Therefore, seeking for natural-based and healthier sweeteners to replace sucrose in foods and beverages is of the utmost importance today [3]. Among natural sweeteners, sweet proteins presented a great potential to substitute sucrose in beverage and food products, mostly due to their intense sweetness and plant origin. Monellin is one of the sweetest proteins [6,7]. However, native Monellin suffered from low thermal stability which limits its possible applications as food sweetener. This inconvenience was partially improved via designing a single-chain Monellin, MNEI, which has increased the thermal stability by 20 °C [32,33]. MNEI is a well-characterized globular protein which combines an extraordinary sweetness with suitable thermostability [18,32,33]. From industrial point of view, MNEI's

application is still challenging due to limited stability and high aggregation propensity at neutral pH. In the recent years, many efforts have been made to improve MNEI's sweetness and/or stability using biotechnology techniques, in particular site-directed mutagenesis. As a result, some mutants of MNEI including Mut3, Mut2 [73], Y65R-MNEI [52], E23Q-MNEI [50] and others more were designed with improved sweetness and/or stability. In this work, we aimed at improving the stability and sweetness of MNEI by taking advantage of already available literature data. Indeed, we could rationally design a new mutant of MNEI with a fantastic combination of stability and sweetness.

The new protein was characterized starting with structural analysis. The secondary structures of Mut9 and MNEI were identified by two minima at 201 nm and 213 nm that indicate a high β-sheet content of these two proteins, which could be deduced by a strong downward shift at 213 nm (**Fig. 3**). The sweetness threshold of Mut9 was measured by triangle test technique and compared to that of MNEI. Interestingly, the sweetness potency of Mut9 increased by a factor of about 2 folds with respect to its parent protein, MNEI, where the sweetness threshold of Mut9 resulted in 0.80 mg/L and for that of MNEI is known to be 1.64 mg/L [55]. Furthermore, a remarkable gain in the thermal stability of Mut9 was obtained from acidic to neutral conditions compared to MNEI. The stability of Mut9 and MNEI was further examined upon boiling the protein samples at pH 2.5 and 6.8 for maximum 10 minutes. The secondary structures of Mut9 and MNEI at acidic pH were preserved for 10 minutes of boiling (**Fig. 8**). But under neutral conditions, MNEI lost its folding pattern and precipitated as short as 2 minutes of boiling, while the structure of Mut9 remained fully folded even after 10 minutes of boiling (**Fig. 8**). These data were confirmed by monitoring the functionality of the proteins via running a series of tasting sessions on the boiled samples at the same pHs (**Table 4**). To summarize, the new mutant of MNEI, Mut9, presented a fantastic thermal and chemical stability. In addition to incredible stability, Mut9 was also endowed by a great rise in the sweetness potency. These properties made Mut9 even a better

candidate for food and beverage applications with respect to its parent protein, MNEI.

CHAPTER 2
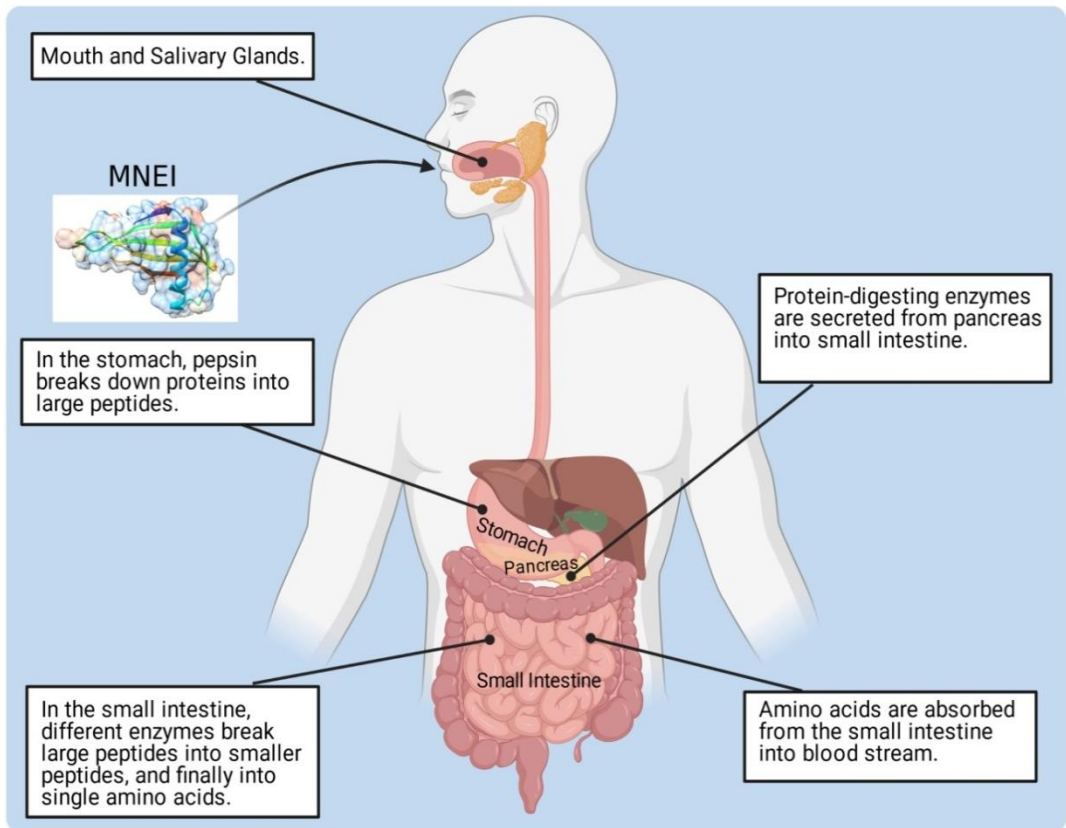
Shelf-life and enzymatic digestion studies of MNEI and its mutants

Abstract

MNEI, single-chain Monellin, is a very promising sweet protein to replace Sucrose and other artificial sweeteners in food and beverage industries. However, there is a lack of data in some aspects *i.e.* shelf-life and enzymatic degradation in view of a possible application of this protein as a sweetener. To overcome this inconvenience, we performed a long-term shelf-life study on MNEI and three of its mutants including Mut3, Mut4 and Mut9. The sweet proteins in acidic and neutral environments were incubated at 4 °C and 37 °C to simulate fridge storage and accelerated shelf-life conditions, respectively. Based on the data collected from UV measurement and SDS-PAGE, MNEI at acidic conditions presented a higher stability at 4 °C, where 50 % of the protein remained unaltered after 6 months of incubation. Instead, the oligomerization trend of the protein incubated at 4 °C was higher compared to the incubation at 37 °C. On the other hand, Mut3 was very stable at 4 °C, where only 25 % of the protein was lost upon 6 months incubation. High integrity of Mut3 was also reflected on the oligomerization tendency of the protein. In fact, no oligomers in the Mut3 samples could be detected under all explored physicochemical conditions. The shelf-life data of Mut4 showed almost a similar resistant with respect to its parent protein, MNEI. However, the oligomerization propensity of Mut4 was higher than MNEI. Among the examined sweet proteins, Mut9 was the most resistant protein under all experimental conditions. The enzymatic digestion of MNEI was also studied by simulating human *in vivo* digestive systems *i.e.* oral phase, gastric phase and intestinal. The protein remained fully intact by running the oral phase, while after the gastric phase, the protein was digested into many peptide fragments. These peptides were completely degraded into very small pieces upon using pancreatic enzymes in the intestinal

phase. The data obtained from running *in silico* studies indicated that the peptide fragments formed after performing the enzymatic digestion experiment on MNEI were free of any toxicity.

2.1 Introduction

MNEI, single-chain Monellin, possesses great properties such as high sweetness potency [18], high thermal stability [32], low structural complexities [29–31], feasible production procedure [34] and reversibility at acidic conditions. All these advantages increased the potential of MNEI for food and beverage industrial applications. However, some data are still missing to introduce MNEI as a sweetening agent to food markets. First of all, the functional stability and shelf-life studies of MNEI upon prolonged incubation are mandatory data for any trial in large scale industrial productions. In addition, it is also necessary to ascertain if the protein is fully degraded upon enzymatic digestion and, possibly, if any potentially toxic or allergenic products are formed by simulating the human *in vivo* digestive systems.

Precipitation, aggregation or degradation of proteinaceous food products is a common phenomenon that is highly undesirable in food and pharmaceutical industries [80–82]. Thinking positively, the formed precipitates and aggregates are impurities that must be totally removed from the products, and in the best case scenario, the process leading to participation and/or aggregation could be controlled [83–85]. Here, precipitates and aggregates refer to any self-associated state of a protein that is permanently irreversible under the formed conditions [86–89]. Worth to mention, MNEI is also known for its aggregation propensity, however this process requires conditions far from the ones usually adopted for food processing and storage (see chapter 5_aggregation study of MNEI). In order to assess the functional and shelf-life stability of MNEI and some of its well-characterized mutants such as Mut3 [73], Mut4 [50] and Mut9 [54], we performed a prolonged incubation (up to six months) of these proteins under various physicochemical conditions, *i.e.* two different temperatures, to simulate fridge storage and accelerated shelf-life conditions, two protein concentrations and different pHs. The analysis of

functional stability and shelf-life study were performed by UV-Vis spectroscopy and polyacrylamide gel electrophoresis.

Among the known MNEI constructs, Mut3 is the sweetest mutant known up to this date [73]. Indeed, the sweetness threshold of Mut3 has been measured to be 0.28 mg/L [73], where it is 1.64 mg/L for the parent protein [55]. Mut3 is also benefited with a little higher thermal stability under neutral condition with respect to MNEI, where the melting temperatures of Mut3 and MNEI at pH 6.8 are 77.8 °C and 75 °C, respectively [58,73]. Mut3 bears 4 point mutations in total, 3 of them *i.e.* E23Q, Q28K and C41S, introduced to improve the protein's stability, and Y65R, is dedicated to increase the sweetness power of MNEI [73]. Mut4 is another construct of MNEI that has a greater stability than its parent protein under neutral and mild alkaline pH. In fact, the thermal stability of Mut4 in the range of 6.8 – 8.0 is higher than that of MNEI by over 10 °C. The pH-related instability of MNEI was associated to E23 residue, which is buried in a hydrophobic pocket at the C-terminal of the α-helix. Exposure the protein to water can make an abrupt jump in pKa (and protonation state), leading to protein destabilization in neutral and alkaline environments [50,51,58]. This is why, it is important to protonate E23 residue in order to decrease the flexibility of *Lα2* loop. For the design of Mut4, the glutamic acid at the position 23 was mutated into glutamine amino acid to prevent deprotonation of E23 at neutral pH, that could reduce the possibility of the water molecules to penetrate in the hydrophobic cavity [50]. Mut9 is one of the most stable and resistant mutant of MNEI, which has also a double sweetness power with respect to its parent protein (see Chapter 1) [54].

Besides the structural and functional integrity of the protein over time, the aim of this study was also to assess the capability of physiological enzyme to fully digest MNEI into small and nontoxic fragments. Simulation of digestive systems using *in vitro* approaches is a widely used strategy to investigate the gastro-intestinal behavior of food products. Some privileges such as quick performance, cheap, less

labor intensive, no ethical restrictions, reproducibility and high capability to control the experimental conditions make the *in vitro* methods one of the best options to analyze the behavior of the oral, gastric, small intestinal and sometimes large intestinal systems upon ingestion of food and beverage products. In fact, *In vitro* models imitate the *in vivo* digestive systems with the actual physiological conditions *i.e.* presence of digestive enzymes with respecting their correct concentrations, pH, digestion time periods, salt concentrations and some other factors [90]. These models were used to study the digestibility and bioaccessibility status of proteins as well [91,92]. To assess the *in vitro* digestibility of MNEI, we simulated the human *in vivo* digestive systems including oral, gastric and intestinal. The decomposition of MNEI was followed during the entire digestive process: oral phase, oral + gastric phase and oral + gastric + intestinal phase and gastric + intestinal phase, using HPLC and MALDI-TOF MS techniques. The peptide fragments of MNEI and their toxicity were tested through *in silico* study using Expasy and ToxicPred softwares, respectively.

2.2 Materials and Methods

2.2.1 Protein expression and purification

The recombinant proteins, *i.e.* MNEI, Mut3, Mut4 and Mut9 were produced using the same procedure described in the Materials and Methods section of Chapter 1.

2.2.2 UV-Vis spectroscopy

The variation of solution concentration of MNEI, Mut3, Mut4 and Mut9 was evaluated upon extended storage: samples of MNEI, Mut3, Mut4 and Mut9 at the concentrations of 0.5 mg/mL and 5.0 mg/mL were prepared at pH 2.5, 5.1 and 6.8 in 0.020 M phosphate buffers. The samples were stored for 6 months at 4 °C to simulate fridge storage or at 37 °C for an accelerated shelf-life assessment. The

protein concentration of the samples was measured using a UV-Vis spectrophotometer (Thermo GENESYS^{TM} 10UV, USA). Prior to each measurement, the samples with higher protein concentration (5.0 mg/mL) were diluted 10 times by deionized water and the protein concentration was calculated using the UV absorbance at 280 nm. Protein content (%) = (measured protein concentration/Initial protein concentration) × 100.

2.2.3 SDS-PAGE

The integrity of MNEI, Mut3, Mut4 and Mut9 was evaluated using SDS polyacrylamide gel electrophoresis (PAGE) following the protocol already reported [93]. Samples of MNEI, Mut3, Mut4 and Mut9 with the concentrations of 0.5 mg/mL and 5.0 mg/mL were prepared at pH 2.5, 5.1 and 6.8 in 0.020 M phosphate buffers. The samples were incubated for 6 months at 4 °C to simulate fridge storage temperature and 37 °C for accelerated shelf-life. At different incubation time points, 10 µg aliquot of each protein was withdrawn and loaded on 12% SDS-PAGE. Gels were stained with Coomassie Brilliant Blue R-250.

2.2.4 Enzymatic Digestion

Enzymatic digestion experiment was performed on MNEI using a standardized static *in vitro* method reported in [90]. In this experiment, 4 samples solutions including oral phase, oral + gastric phase and oral + gastric + intestinal phase and gastric + intestinal phase were prepared with respect to their physiological conditions such as presence of digestive enzymes and their concentrations, pH, digestion time periods and salt concentrations. For enzymatic digestion of MNEI, three fluids *i.e.* simulated salivary fluid (SSF), simulated gastric fluid (SGF) and simulated intestinal fluid (SIF) were used to simulate oral, gastric and intestinal physiological conditions, respectively. The constituents of the three fluids and their corresponding concentrations according to the actual human *in vivo* data are shown in **Table 1**.

Simulated oral, gastric and intestinal fluids contain α-amylase, pepsin and pancreatic enzymes, respectively. For oral phase, MNEI was incubated for 2 minutes in SSF at pH 7.0, which contains 75 U/mL α-amylase and some electrolytes with their respected concentrations (**Table 1**). For gastric phase, the protein was incubated in SGF at pH 2.0 and physiological temperature (37 °C). After two hours of incubation (an estimated incubation time of foods in the human gastric organ), the reaction was stopped by increasing the pH up to 7.0 by adding 1 M NaOH. The SGF contained pepsin enzyme with a final concentration of 3380 U/mL and some electrolytes reported in **Table 1**. For Intestinal phase, MNEI was incubated in the presence of SIF at pH 7.0 for 2 hours. Simulated intestinal fluid (SIF) contained pancreatic enzymes (trypsin and chymotrypsin) with the final concentration of 2000 U/mL and some electrolytes reported at **Table 1**. After 2 hours of incubation, the reaction was interrupted by using a protease inhibitor pefabloc with the final concentration of 5 mM. In the case of performing a sequence of digestion systems, the protein was incubated with the simulated fluids in order with considering the incubation time. MNEI with the concentration of 1 mg/mL in each phase was included and incubated for the specified time periods. After incubation, the samples were lyophilized for the analytical experiments.

Table 1. Electrolytes and their concentrations in Simulated Salivary Fluid (SSF), Simulated Gastric Fluid (SGF) and Simulated Intestinal Fluid (SIF), based on human *in vivo* obtained data.

Constituent	SSF	SGF	SIF
	Mmol L^{-1}	Mmol L^{-1}	Mmol L^{-1}
K$^+$	18.8	7.8	7.6
Na$^+$	13.6	72.2	123.4
Cl$^-$	19.5	70.2	55.5
H$_2$PO$_4^-$	3.7	0.9	0.8
HCO$_3^-$,CO$_3^{2-}$	13.7	25.5	85
Mg^{2+}	0.15	0.1	0.33
NH$_4^+$	0.12	1.0	–
Ca^{2+}	1.5	0.15	0.6

2.2.5 High-Performance Liquid Chromatography (HPLC)

High performance liquid chromatography (HPLC) analysis of MNEI digested by three digestive systems was performed by an LC-20AD XR HPLC instrument (SHIMADZU) with a SPD-M20A set. All the samples obtained from oral phase, oral + gastric phase and oral + gastric + intestinal phase and gastric + intestinal phase were monitored at the wavelength of 210 nm using photodiode array detector. For MNEI analysis, a 250 × 4.6 mm C18 column (Pursuit XRs 5 -VARIAN) was used. Acetonitrile–water solutions consisting of 0.1 % TFA with the gradient presented at **Table 2** were used as the mobile phase. All HPLC trials were run with a flow rate of 1 mL/min at room temperature. The injection volume was 20 µL of 2.5 mg/mL for all the samples. The running method was designed after performing trial and error experiments to find a suitable method presented at **Table 2**.

Table 2. Description of HPLC running method and the gradient used for mobile phase.

Time (min)	Acetonitrile (%)
0 - 10	5%
10 - 40	5% to 60%
40 - 50	60% to 95%
50 - 60	95%

2.2.6 Peptide Fragments and Toxicity Predictions

The peptide fragments of MNEI after gastric and intestinal digestive systems were predicted via Expasy (https://web.expasy.org/peptide_mass/) software described at [94]. The software's settings were adjusted to digest the protein with pepsin for gastric phase and pancreatic enzymes for intestinal phase. Then, the peptide fragments obtained were analyzed by ToxicPred (https://webs.iiitd.edu.in/raghava/toxinpred/index.html) to predict their toxicity through *in silico* study [95]. The dataset used in this analysis is SwissProt (NOT KW800 NOT KW20, the keywords 800 and 20 stand for toxin and allergen as molecular functions)

2.3 Results and Discussion

2.3.1 Shelf-life assessment

The long-term stability and resistance of MNEI, Mut3, Mut4 and Mut9 was assessed by performing prolonged incubation (up to six months) of the proteins under various physicochemical conditions. The samples were analyzed by determination of the total protein loss and the oligomerization tendency using UV-Vis spectroscopy and SDS-PAGE experiments, respectively. Each protein was incubated at two different temperatures, 4 °C in order to simulate fridge storage temperature and 37 °C to simulate accelerated shelf-life conditions. Furthermore, the proteins were incubated

at different pH values (2.5, 5.1 and 6.8) and protein concentrations (0.5 and 5.0 mg/mL) to evaluate the chemical stability and crowding effect of the proteins upon long-term incubations, respectively. The results of these experiments are presented for each single protein.

2.3.1.1 MNEI

According to MNEI results, it is clear that there were no noticeable differences in terms of protein loss detected by UV-Vis spectroscopy between incubated proteins at 0.5 mg/mL and 5.0 mg/mL (**Fig. 1**). However, the data indicated that incubational temperature had a big impact on the protein stability. On the other hand, the incubational pH had a limited influence on the stability of MNEI. In fact, MNEI at 4 °C was more resistant under strong acidic conditions rather than mild acidic or neutral pH, but at 37 °C, it was the least stable at pH 2.5 (**Fig. 1**). The results presented in **Figure 1** showed that after 2 months of incubation, MNEI at pH 2.5 lost about 15 % of its initial content at 4 °C, while at 37 °C with the same pH, the amount of protein loss reached 25 %. Upon longer incubation time (6 months), MNEI lost approximately 60 % percent of its initial amount at accelerated shelf-life conditions (37 °C), where only 40 % of MNEI was lost when the protein was incubated at storage temperature (4 °C) (**Fig. 1**).
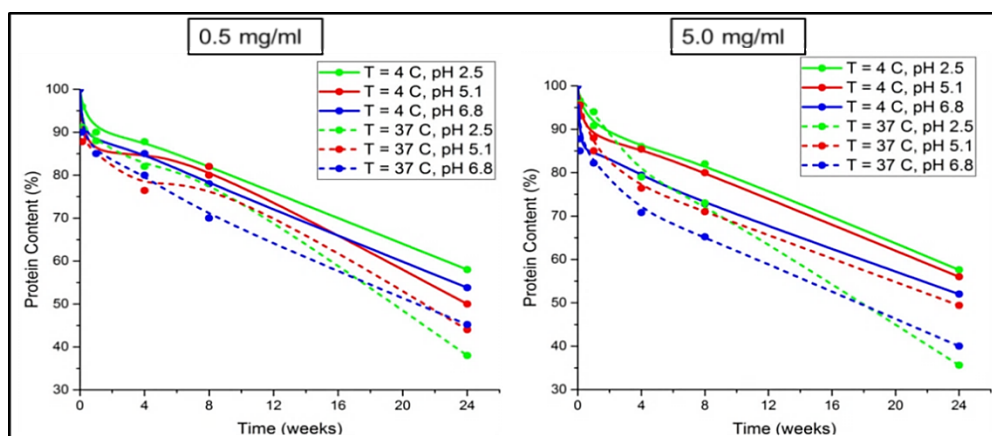
Figure 1. Amount of MNEI remaining in solution upon incubation at different physicochemical parameters for 6 months. The protein content was calculated from the UV absorbance at 280 nm. The left graph is MNEI incubated at 0.5 mg/mL protein concentration and the right one is 5.0 mg/mL protein concentration. The lines and dash-lines are presented by a color code defined in the insets.

The outcome of SDS-PAGE experiments demonstrated that both integrity and oligomerization tendency of MNEI at two applied protein concentration (0.5 mg/mL and 5.0 mg/mL) were quite similar (**Fig. 2**). According to the SDS-PAGE gels, MNEI is more resistant at fridge storage temperature (4 °C) rather than accelerated shelf-life. In fact, MNEI at pH 2.5 incubated at 4 °C lost about 40 % of its initial content after 6 months incubation, whilst at accelerated shelf-life temperature (37 °C), the protein loss was 60 - 70 % (**Fig. 2**). Further, MNEI incubated at pH 5.1 and 37 °C formed ~ 5 % of oligomers after 2 and 6 months of incubation (**Fig. 2**). It is worth mentioning that the results obtained from UV measurements (**Fig. 1**) are highly consistent with the SDS-PAGE data (**Fig. 2**) in terms of protein resistance in solution.
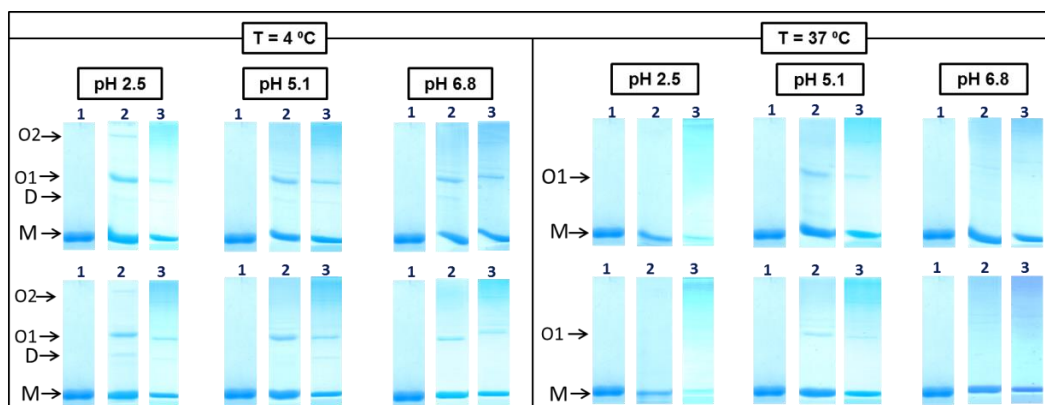

Figure 2. SDS gels showing the integrity and oligomerization tendency of MNEI upon 6 months incubation under different physicochemical conditions. The top gels: MNEI at 0.5 mg/mL; bottom gels: MNEI at 5.0 mg/mL. The running numbers on the lanes of each gel are: 1) reference (MNEI_No incubation), 2) 2 months and 3) 6 months incubation. Each

presented gel categories are defined in the insets. The arrows indicate the position of the monomers (M), dimers (D), oligomer 1 (O1) and oligomer 2 (O2).

2.3.1.2 Mut3

A prolonged shelf-life experiment was performed on Mut3 as well. The data of UV measurements showed that protein concentration had a negligible influence on Mut3 resistance in solution (**Fig. 3**). Mut3 remained mostly soluble with a monomeric form upon prolonged incubation under all tested conditions. On the other hand, incubational temperature significantly influenced the integrity of Mut3, since the protein incubated at 37 °C lost about 20 % more of its content with respect to the protein incubated at fridge storage temperature (4 °C). In detail, Mut3 at pH 2.5 and incubational temperature of 4 °C lost about 20 % of its content after 6 months incubation, while this number increased to 35 % for the protein at the same pH incubated at 37 °C (**Fig. 3**). Interesting to mention, Mut3 at the pH range of 2.5 to 6.8 incubated at 4 °C showed a great resistance from 2 to 6 months, where only a few percentages of the protein's content was lost. Also, the pH had an impact on the stability of the protein, indicating that Mut3 is more stable in acidic environment rather than in neutral (**Fig. 3**). As a matter of fact, the protein showed a better resistance at all explored physicochemical conditions with respect to MNEI. As expected, the introduced point mutations to Mut3 including E23Q, Q28K and C41S could increase the stability and the resistance of the protein from acidic to neutral pH.
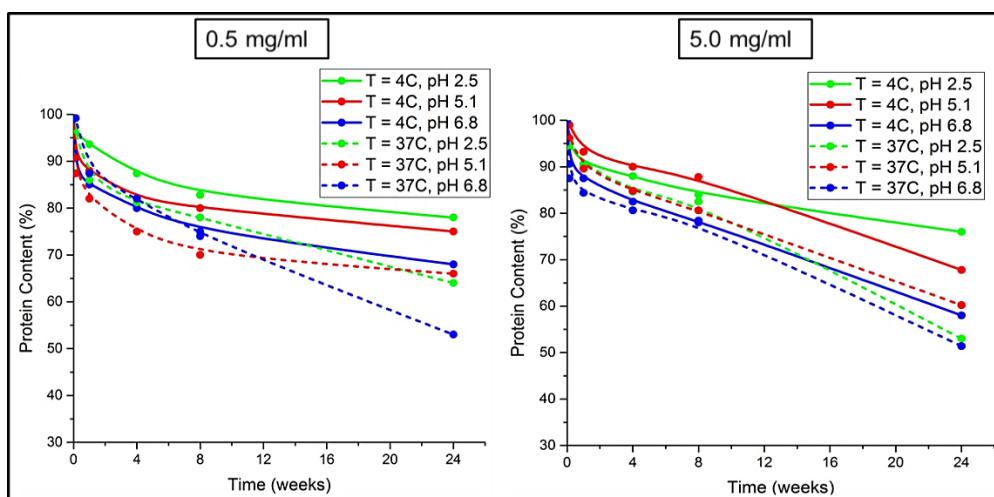
Figure 3. Amount of Mut3 remaining in solution upon incubation at different physicochemical parameters for 6 months. The protein content was calculated from the UV absorbance at 280 nm. The left graph is Mut3 incubated at 0.5 mg/mL protein concentration and the right one is 5.0 mg/mL protein concentration. The lines and dash-lines are presented by a color code defined in the insets.

Appealingly, Mut3 demonstrated a great integrity upon long-term incubation (6 months) under all explored physicochemical conditions. Indeed, no aggregates of any size could be noticed after 2 and 6 months of incubation (**Fig. 4**), only 1-2 % of oligomers could be observed for the sample incubated at pH 2.5 and 4 °C after 2 months incubation, however, the oligomers completely disappeared after 6 months of incubation (**Fig. 4**). Notably, Mut3 did not form covalent dimers due to the mutation of the only cysteine residue in the MNEI's sequence (Cys41) into Serine [73]. According to the data, the only challenging condition for Mut3 was at pH 6.8 and 37 °C after 6 months of incubation, in which the protein lost about 45 % of its initial content. Worth mentioning, Mut3 displayed high resistance capability under strong and mild acidic conditions at incubational temperatures of 4 and 37 °C (**Fig. 4**). Like MNEI, protein concentration had no influence on the resistance property of Mut3.
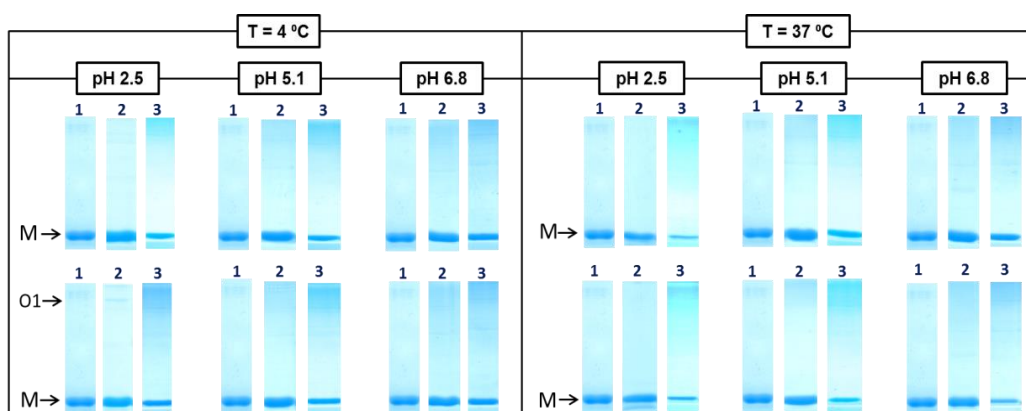
Figure 4. SDS gels showing the integrity and oligomerization tendency of Mut3 upon 6 months incubation under different physicochemical conditions. The top gels: Mut3 at 0.5 mg/mL; bottom gels: Mut3 at 5.0 mg/mL. The running numbers on the lanes of each gel are: 1) reference (Mut3_No incubation), 2) 2 months and 3) 6 months incubation. Each presented gel categories are defined in the insets. The arrows indicate the position of the monomers (M) and oligomer 1 (O1).

2.3.1.3 Mut4

The shelf-life data of Mut4 illustrated that the least parameter influenced the resistant of Mut4 was protein concentration, whereas pH and temperature considerably affected the protein stability (**Fig. 5**). The results of total protein loss presented in **Figure 5** demonstrated that Mut4 is more stable in slightly acidic environments at both temperatures (4 and 37 °C), where the protein preserved about 80 % of its initial content after 2 months of incubation, while this number decreased to 70 % for neutral pH (**Fig. 5**). Upon longer incubation time, the protein loss continued to reach 60 - 70 % of its initial protein content under neutral condition at 37 °C (**Fig. 5**). Mut4 was less resistant than Mut3 at all explored experimental conditions.
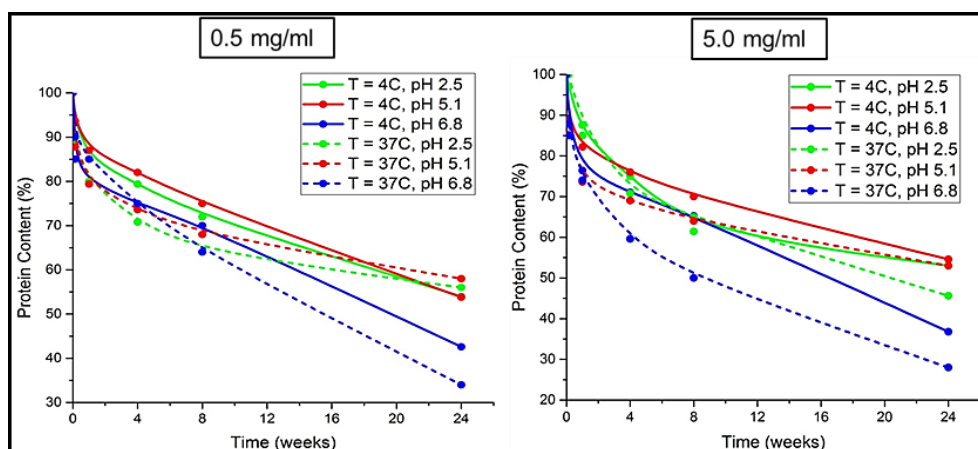
Figure 5. Amount of Mut4 remaining in solution upon incubation at different physicochemical parameters for 6 months. The protein content was calculated from the UV absorbance at 280 nm. The left graph is Mut4 incubated at 0.5 mg/mL protein concentration and the right one is 5.0 mg/mL protein concentration. The lines and dash-lines are presented by a color code defined in the insets.

The data collected from the UV measurements were confirmed by SDS gels (**Fig. 6**). Indeed, there were no mentionable differences in terms of resistance or oligomerization trend between the tested protein concentrations (0.5 mg/mL and 5.0 mg/mL). On the other hand, the incubational temperature had a large impact on the resistance and the oligomerization tendency of Mut4. In fact, the accelerated shelf-life temperature (37 °C) led to the maximum protein loss at pH 2.5 and 6.8, reaching to over 70 % (**Fig. 6**). Moreover, the protein incubated at 4 °C formed multi-sized soluble SDS resistant oligomers after 2 and 6 months of incubation (**Fig. 6**). Worth mentioning, the oligomerization tendency of Mut3 was mostly suppressed due to the point mutation of C41S, which prevented covalent dimerization (**Fig. 4**), whereas, the oligomerization propensity of Mut4 was very high due to the presence of cysteine residue at the position of 41.
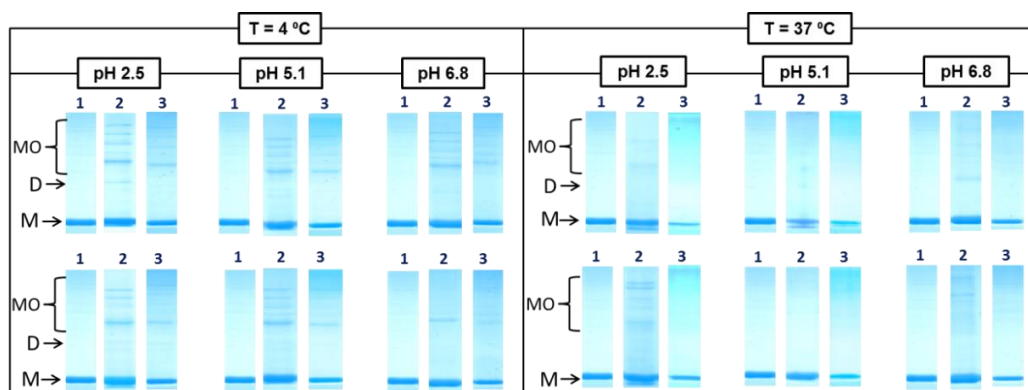
Figure 6. SDS gels showing the integrity and oligomerization tendency of Mut4 upon 6 months incubation under different physicochemical conditions. The top gels: Mut4 at 0.5 mg/mL; bottom gels: Mut4 at 5.0 mg/mL. The running numbers on the lanes of each gel are: 1) reference (Mut4_No incubation), 2) 2 months and 3) 6 months incubation. Each presented gel categories are defined in the insets. The arrows indicate the position of the monomers (M), dimers (D) and Multi Oligomers (MO).

2.3.1.4 Mut9

The long-term resistant of Mut9 was also monitored by running a prolonged incubation (up to six months). Mut9 displayed a wonderful stability in all tested physicochemical conditions. In fact, the results demonstrated that Mut9 is the most resistant protein among the tested sweet proteins. Based on the UV data, about 80 % of the protein at strong and slightly acidic conditions was maintained over 6 months of incubation at both incubational temperatures (4 °C and 37 °C) (**Fig. 7**). Only 30 % of Mut9 content was lost at neutral pH after incubation for 24 weeks at 4 °C and 37 °C. Interestingly, this protein under almost all experimental conditions did not lose any mentionable amount of protein from 2 to 6 months incubation, except at pH 6.8 that led to 10 % more protein loss. It is worth mentioning that protein concentration had a minor influence on the stability of Mut9 (**Fig. 7**).
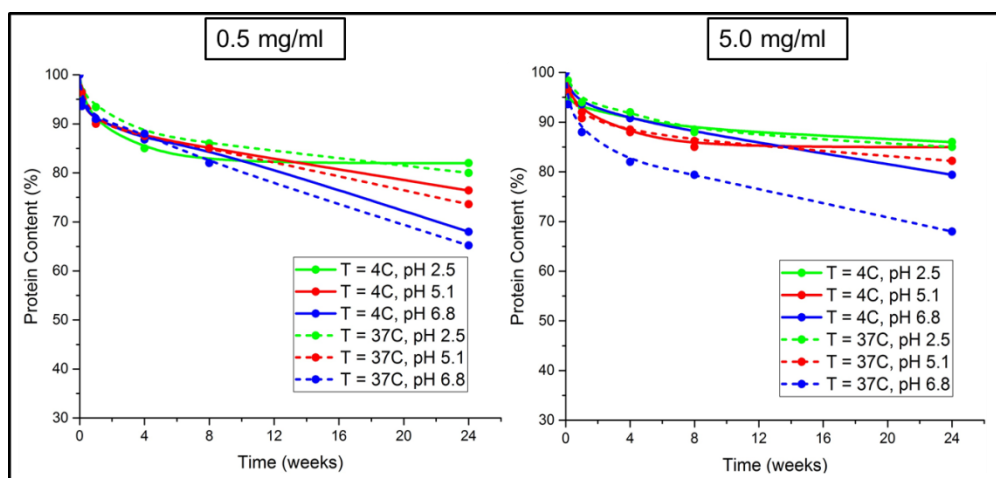
Figure 7. Amount of Mut9 remaining in solution upon incubation at different physicochemical parameters for 6 months. The protein content was calculated from the UV absorbance at 280 nm. The left graph is Mut9 incubated at 0.5 mg/mL protein concentration and the right one is 5.0 mg/mL protein concentration. The lines and dash-lines are presented by a color code defined in the insets.

SDS-PAGE was also applied to screen the integrity and oligomerization propensity of Mut9 (**Fig. 8**). Consistent with the UV results, protein concentration had negligible effect on the protein integrity or oligomerization process of Mut9. The data clearly indicated that upon prolonged incubation, Mut9 was very resistant at all explored physicochemical conditions. These results were expected because Mut9 was designed to elevate the stability of MNEI, in particular the chemical stability (**Fig. 8**). The protein remained soluble with a monomeric form within 6 months incubation under all experimental conditions. Mut9 incubated at fridge storage temperature (4 °C) prompted 2-3 % Mut9 oligomeric forms at acidic and neutral pH after 2 months incubation, but the oligomers disappeared after that (**Fig. 8**). Worth to mention, Mut9 showed very low dimerization tendency, diversely from MNEI that is prone to dimerize through disulfide bonds of cysteine amino acid residues [58]. In the case of Mut9, the cysteine residue in MNEI's sequence position 41 was mutated into alanine. Surprisingly, a faint band of dimer could be noticed with the sample incubated at pH 6.8 and 37 °C for 6 months,

however, it is not cysteine-correlated dimers; instead, they might be dimers formed from other oligomerization processes.
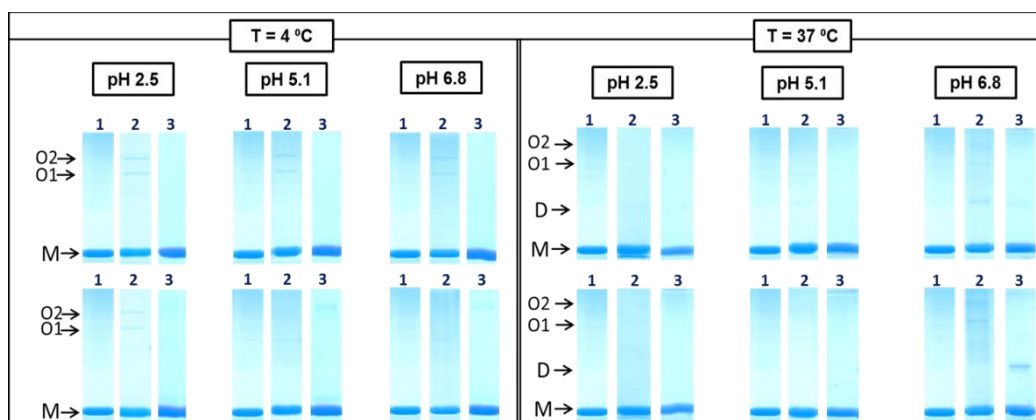
Figure 8. SDS gels showing the integrity and oligomerization tendency of Mut9 upon 6 months incubation under different physicochemical conditions. The top gels: Mut9 at 0.5 mg/mL; bottom gels: Mut9 at 5.0 mg/mL. The running numbers on the lanes of each gel are: 1) reference (Mut9_No incubation), 2) 2 months and 3) 6 months incubation. Each presented gel categories are defined in the insets. The arrows indicate the position of the monomers (M), dimers (D), oligomer 1 (O1) and oligomer 2 (O2).

2.3.2 Enzymatic Digestion of MNEI

Enzymatic degradation of MNEI was performed using *in vitro* standard protocol reported in [90]. In this experiment, we simulated the *in vivo* digestive systems using three fluids: simulated salivary fluid (SSF), simulated gastric fluid (SGF) and simulated intestinal fluid (SIF), containing digestive enzymes and salt compositions with their corresponding concentrations, pH and respecting the approximate digestion time. Enzymatic digestion of MNEI was carried out by running different digestive systems, *i.e.* oral, oral + gastric, oral + gastric + intestinal and gastric + intestinal phase. Then, the samples were analyzed by HPLC to understand the digestibility of MNEI after running digestion systems. The HPLC chromatograms are shown by a spectrum at 210 nm presenting the absorption of dipeptide bonds.

First of all, we obtained a protein reference chromatogram by loading freshly dissolved and pretreated MNEI on the C18 column. In this experiment, 20 µL of 2.5 mg/mL MNEI (50 µg) was injected to clearly detect the retention time of the reference protein. The data obtained from HPLC chromatogram showed that MNEI eluted at a retention time of 32.56 minutes, which is at about 41.3 % of acetonitrile + 0.1 % of TFA (**Fig. 9**).
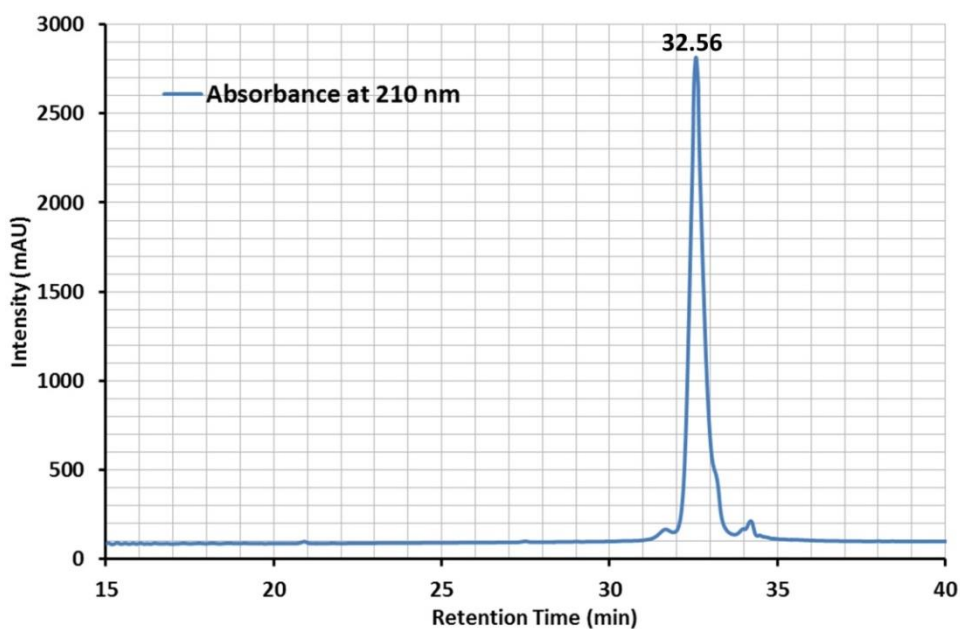
Figure 9. HPLC chromatogram of 50 µg MNEI in 5 mM HCl. The loaded protein volume was 20 µL of 2.5 mg/mL MNEI on C18 column. The chromatogram includes a spectrum at 210 nm showing the absorption of dipeptide bonds. The HPLC spectra were taken at 25 °C.

The enzymatic degradation study of MNEI began with the oral phase, which is the first digestive system in foods and beverages digestion processes. The HPLC data collected after running the oral phase on MNEI clearly evidenced that the protein remained fully intact. This result was totally expected since the SSF included only α-amylase, which serves to digest carbohydrate species not proteins. In this chromatogram (**Fig. 10**), the buffer spectrum (SSF without addition of the protein)

was also presented in red line for control purposes. A peak at a retention time of 33.6 minutes corresponds to α-amylase (**Fig. 10**_red line).
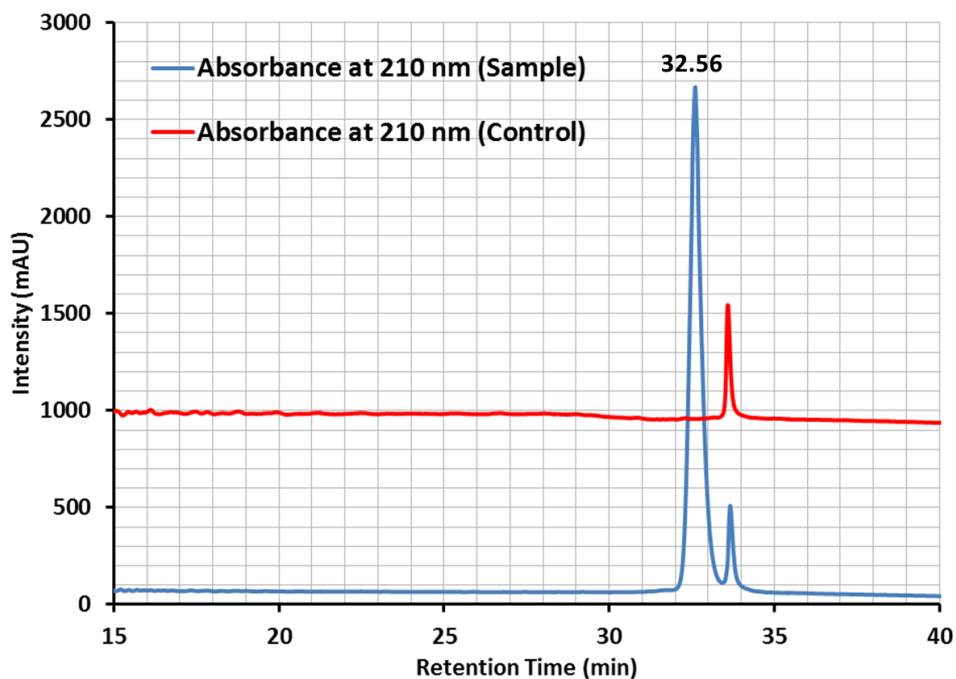
Figure 10. HPLC chromatogram of MNEI after running the oral phase. A volume of 20 µL was loaded on C18 column. The chromatogram showing the spectra of protein sample (blue line) and the control (red line) at 210 nm. The HPLC spectra were taken at 25 °C.

We carried on the enzymatic degradation study by simulating oral and gastric phase in a sequence to monitor digestion procedure of MNEI. The HPLC chromatogram indicated that MNEI after oral and gastric phase was completely digested into many peptide fragments (**Fig. 11**). The identification study of the peptide fragments by MALDI-TOF MS is in progress.
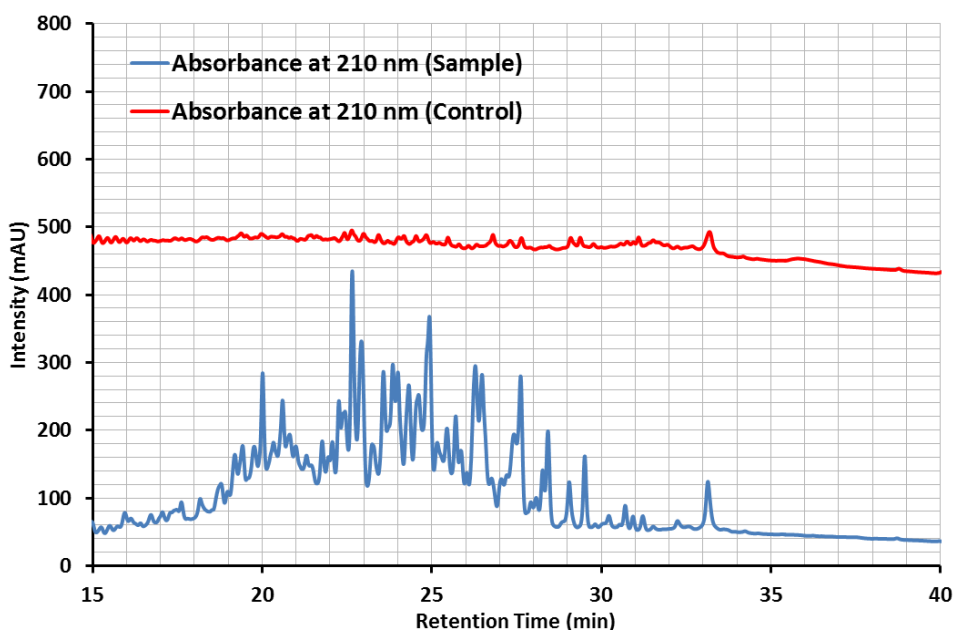
Figure 11. HPLC chromatogram of MNEI after running oral and gastric phase. A volume of 20 µL was loaded on C18 column. The chromatogram showing the spectra of protein sample (blue line) and the control (red line) at 210 nm. The HPLC spectra were taken at 25 °C.

The identification analysis of peptide fragments obtained from MNEI after oral and gastric phase was performed via running *in silico* study using Expasy software. After the gastric phase, in which the protein was digested by pepsin, a group of peptide fragments with the size ranging from 2 to 18 amino acid residues were predicted (**Table 3**). To examine the potential toxicity of these peptides, another *in silico* analysis was carried out via ToxinPred software using SwissProt dataset (toxin and allergen). The results showed that all of the obtained peptide fragments after MNEI digestion by pepsin were non-toxic (**Table 3**). In the **Table 3**, other information such as hydrophobicity, hydrophilicity, charge, pI and average mass of the peptide fragments are included as well.

Table 3. Peptide fragments of MNEI after running oral and gastric systems and their *in silico* toxicity tests. More data of the peptide fragments: hydrophobicity, hydrophilicity, charge, pH and average mass are presented.

Peptide Sequence	Prediction	Hydrophobicity	Hydrophilicity	Charge	pI	Mass
NKVIRPCMKKTIYENEGF	Non-Toxin	-0.26	0.32	2.00	9.17	2170.84
RADISEDYKTRGRKL	Non-Toxin	-0.55	1.17	2.00	9.71	1808.23
AVDEENKIGQYGRL	Non-Toxin	-0.27	0.54	-1.00	4.68	1591.95
REIKGYEYQL	Non-Toxin	-0.33	0.40	0.00	6.49	1298.61
GEWEIIDIGPF	Non-Toxin	0.13	-0.21	-3.00	3.58	1275.59
YVYASDKL	Non-Toxin	-0.09	-0.26	0.00	6.18	958.18
NGPVPPP	Non-Toxin	-0.03	-0.19	0.00	5.88	676.86
TQNL	Non-Toxin	-0.24	-0.45	0.00	5.88	474.57
GKF	Non-Toxin	-0.11	0.17	1.00	9.11	350.45
RF	Non-Toxin	-0.57	0.25	1.00	10.11	321.39
TF	Non-Toxin	0.21	-1.45	0.00	5.88	266.31

Enzymatic digestion study was completed by simulating the entire human *in vivo* digestion procedure using a sequence of digestive systems including oral phase, gastric phase and intestinal phase. The outcome of HPLC analysis clearly indicated that the protein was totally degraded after running oral, gastric and intestinal phase (**Fig.12**). Obviously, pancreatic enzymes (trypsin and chymotrypsin) are responsible for cutting the peptide fragments into very small pieces.
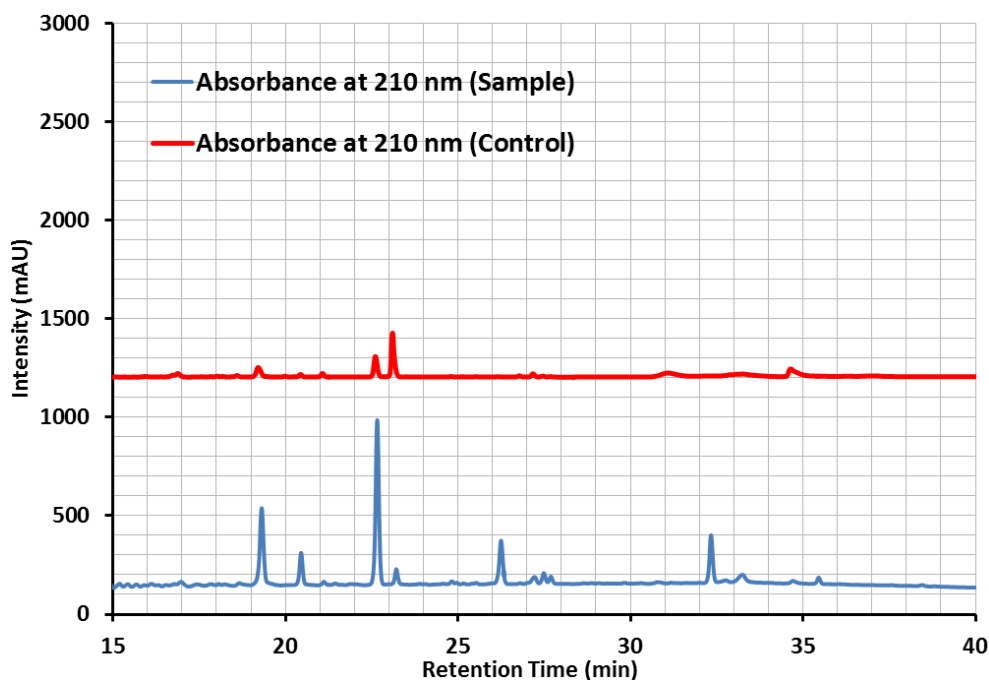
Figure 12. HPLC chromatogram of MNEI after performing the entire digestive system: oral. gastric phase and intestinal phase. A volume of 20 μL was loaded on C18 column. The chromatogram showing the spectra of protein sample (blue line) and the control (red line) at 210 nm. The HPLC spectra were taken at 25 °C.

After performing the entire enzymatic degradation process on MNEI, we predicted the formed peptide fragments through running *in silico* study via Expasy software. After incubating the protein with pepsin and pancreatic enzymes, many peptide pieces with the size starting from 2 to 13 were predicted (**Table 4**). Again, the toxicity of these peptides were assessed by ToxinPred software using SwissProt data set (toxin and allergen), and the results demonstrated that all of the formed peptides were free of toxicity (**Table 4**). Other information of the formed peptides such as hydrophobicity, hydrophilicity and etc. are included in **Table 4**.

Table 4. Peptide fragments of MNEI after running oral, gastric and intestinal systems and their *in silico* toxicity tests. More data of the peptide fragments: hydrophobicity, hydrophilicity, charge, pH and average mass are presented.

Peptide Sequence	Prediction	Hydrophobicity	Hydrophilicity	Charge	pI	Mass
AVDEENKIGQYGR	Non-Toxin	-0.33	0.72	-1.00	4.68	1478.77
AVDEENKIGQY	Non-Toxin	-0.24	0.57	-2.00	4.14	1265.50
AVDEENKIGQY	Non-Toxin	-0.24	0.57	-2.00	4.14	1265.50
GEWEIIDIGPF	Non-Toxin	0.13	-0.21	-3.00	3.58	1275.59
VIRPCMKKTIY	Non-Toxin	-0.17	-0.10	3.00	9.80	1351.89
NKVIRPCMKK	Non-Toxin	-0.42	0.66	4.00	10.33	1216.71
ADISEDYKTR	Non-Toxin	-0.44	1.03	-1.00	4.56	1197.39
KTIYENEGF	Non-Toxin	-0.18	0.24	-1.00	4.54	1100.32
NKVIRPCMK	Non-Toxin	-0.34	0.40	3.00	10.07	1088.52
RADISEDYK	Non-Toxin	-0.46	1.19	-1.00	4.56	1096.27
VIRPCMKK	Non-Toxin	-0.31	0.43	3.00	10.07	974.40
TIYENEGF	Non-Toxin	-0.07	-0.10	-2.00	3.80	972.13
VIRPCMK	Non-Toxin	-0.19	0.06	2.00	9.55	846.21
RADISEDY	Non-Toxin	-0.38	0.96	-2.00	4.03	968.08
ADISEDYK	Non-Toxin	-0.30	0.96	-2.00	4.03	940.07
EIIDIGPF	Non-Toxin	0.19	-0.24	-2.00	3.67	903.16
IGQYGRL	Non-Toxin	-0.12	-0.39	1.00	9.10	806.04
AVDEENK	Non-Toxin	-0.42	1.46	-2.00	4.14	803.91
ADISEDY	Non-Toxin	-0.19	0.67	-3.00	3.50	811.88
EIKGYEY	Non-Toxin	-0.20	0.37	-1.00	4.54	901.08
YVYASDK	Non-Toxin	-0.18	-0.04	0.00	6.18	845.00
VYASDKL	Non-Toxin	-0.11	0.03	0.00	6.18	794.99
NGPVPPP	Non-Toxin	-0.03	-0.19	0.00	5.88	676.86
IGQYGR	Non-Toxin	-0.23	-0.15	1.00	9.10	692.86
VYASDK	Non-Toxin	-0.21	0.33	0.00	6.18	681.81
GYEYQL	Non-Toxin	-0.10	-0.53	-1.00	4.00	771.91
REIKGY	Non-Toxin	-0.43	0.82	1.00	8.93	764.96
KTRGR	Non-Toxin	-0.93	1.72	3.00	12.01	616.78
TRGRK	Non-Toxin	-0.93	1.72	3.00	12.01	616.78
ENEGF	Non-Toxin	-0.22	0.74	-2.00	3.80	594.64
EIKGY	Non-Toxin	-0.16	0.38	0.00	6.35	608.76
ASDKL	Non-Toxin	-0.26	0.80	0.00	6.19	532.65
TRGR	Non-Toxin	-0.89	1.40	2.00	12.01	488.59
GRKL	Non-Toxin	-0.54	1.05	2.00	11.01	472.64
KTIY	Non-Toxin	-0.13	-0.37	1.00	8.94	523.68
EYQL	Non-Toxin	-0.19	-0.22	-1.00	4.00	551.65
REIK	Non-Toxin	-0.69	1.80	1.00	9.10	544.70
GYEY	Non-Toxin	-0.10	-0.40	-1.00	4.00	530.58
IGQY	Non-Toxin	0.06	-0.97	0.00	5.88	479.59
ASDK	Non-Toxin	-0.46	1.45	0.00	6.19	419.47
TQNL	Non-Toxin	-0.24	-0.45	0.00	5.88	474.57
KTR	Non-Toxin	-1.01	1.87	2.00	11.01	403.51
GRK	Non-Toxin	-0.90	2.00	2.00	11.01	359.46
TIY	Non-Toxin	0.19	-1.50	0.00	5.88	395.49
GEW	Non-Toxin	-0.03	-0.13	-1.00	4.00	390.43
GRL	Non-Toxin	-0.36	0.40	1.00	10.11	344.45
EIK	Non-Toxin	-0.33	1.40	0.00	6.35	388.50
YVY	Non-Toxin	0.19	-2.03	0.00	5.87	443.53
GKF	Non-Toxin	-0.11	0.17	1.00	9.11	350.45
RF	Non-Toxin	-0.57	0.25	1.00	10.11	321.39
TF	Non-Toxin	0.21	-1.45	0.00	5.88	266.31

In another trial, we performed an enzymatic digestion experiment on MNEI through running gastric and intestinal systems, i.e. without the oral phase, as in drinks this can be really fast. After analyzing the sample by HPLC, the results indicated that the whole protein was completely degraded into very small pieces (**Fig. 13**), very similar to the chromatogram obtained after running the whole human digestive systems including the oral phase (**Fig. 12**). Thus as shown in **Figure 10** and **13**, oral phase had no influence on the protein digestion process.
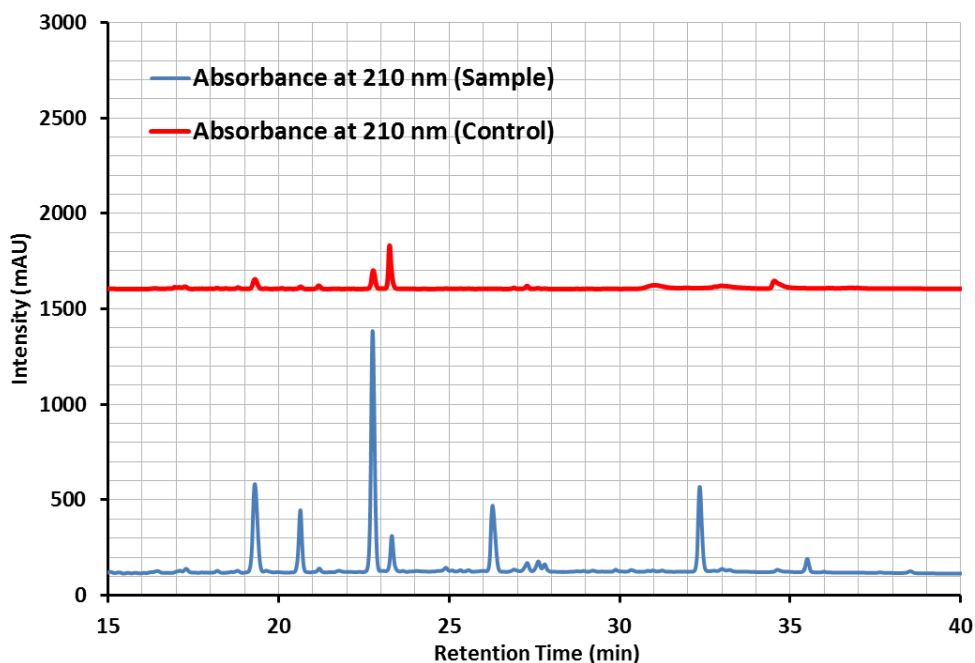

Figure 13. HPLC chromatogram of MNEI after performing gastric phase and intestinal phase. A volume of 20 μL was loaded on C18 column. The chromatogram showing the spectra of protein sample (blue line) and the control (red line) at 210 nm. The HPLC spectra were taken at 25 °C.

2.4 Conclusions

MNEI is a well-characterized sweet protein; however, it is still suffering from lack of some necessary data such as shelf-life and physiological effects. To look closely on these aspects, we performed a prolonged shelf-life study on MNEI and three of its mutants *i.e.* Mut3 (the sweetest protein) [73], Mut4 (more stable protein than MNEI) [50] and Mut9 (super stable protein) [54]. In addition, we carried out an enzymatic degradation experiment on MNEI via simulating a physiological digestion system *i.e.* oral, gastric and intestinal. The outcome of shelf-life study showed that incubational temperature had a big impact on the resistance and oligomerization propensity of the tested sweet proteins. In fact, the proteins were more stable at fridge storage temperature (4 °C) rather than accelerate shelf-life temperature (37 °C). Moreover, the pH of incubated solutions had a limited effect on the resistance and oligomerization tendency of the proteins, where the proteins showed a better resistant in acidic environments. On the other hand, protein concentration was almost ineffective on the resistance and integrity of the proteins in solutions. Among the explored sweet proteins, Mut9 and Mut3 presented a great performance in terms of resistance and oligomerization propensity, although Mut9 was even stronger than Mut3, in particular at pH 2.5 and 6.8.

We also carried out an enzymatic digestion study on MNEI via simulating the human *in vivo* digestive systems through incubation of the protein in the presence of SSF, SGF and SIF that represent the simulated fluids of oral phase, gastric phase and intestinal phase, respectively. Then, the samples obtained after each digestion step were analyzed by HPLC. The HPLC chromatogram of the protein after performing the oral phase showed that the protein remained completely intact (**Fig. 10**). However, MNEI was thoroughly digested into very small pieces of peptide after gastric and pancreatic enzymes treatment (**Fig. 12**). The formed fragments will be identified by MALDI-TOF MS. The peptides were predicted and tested for potential toxicity *in silico* using Expasy and ToxicPred softwares, respectively. In fact, all the

peptide fragments obtained from MNEI digestion by gastric phase were non-toxic (**Table 3**). Also, the peptide pieces formed from gastric and intestinal phase were predicted and their toxicity was evaluated. Again, the data illustrated that all of the produced peptides were free of any toxicity (**Table 4**).

CHAPTER <u>3</u>
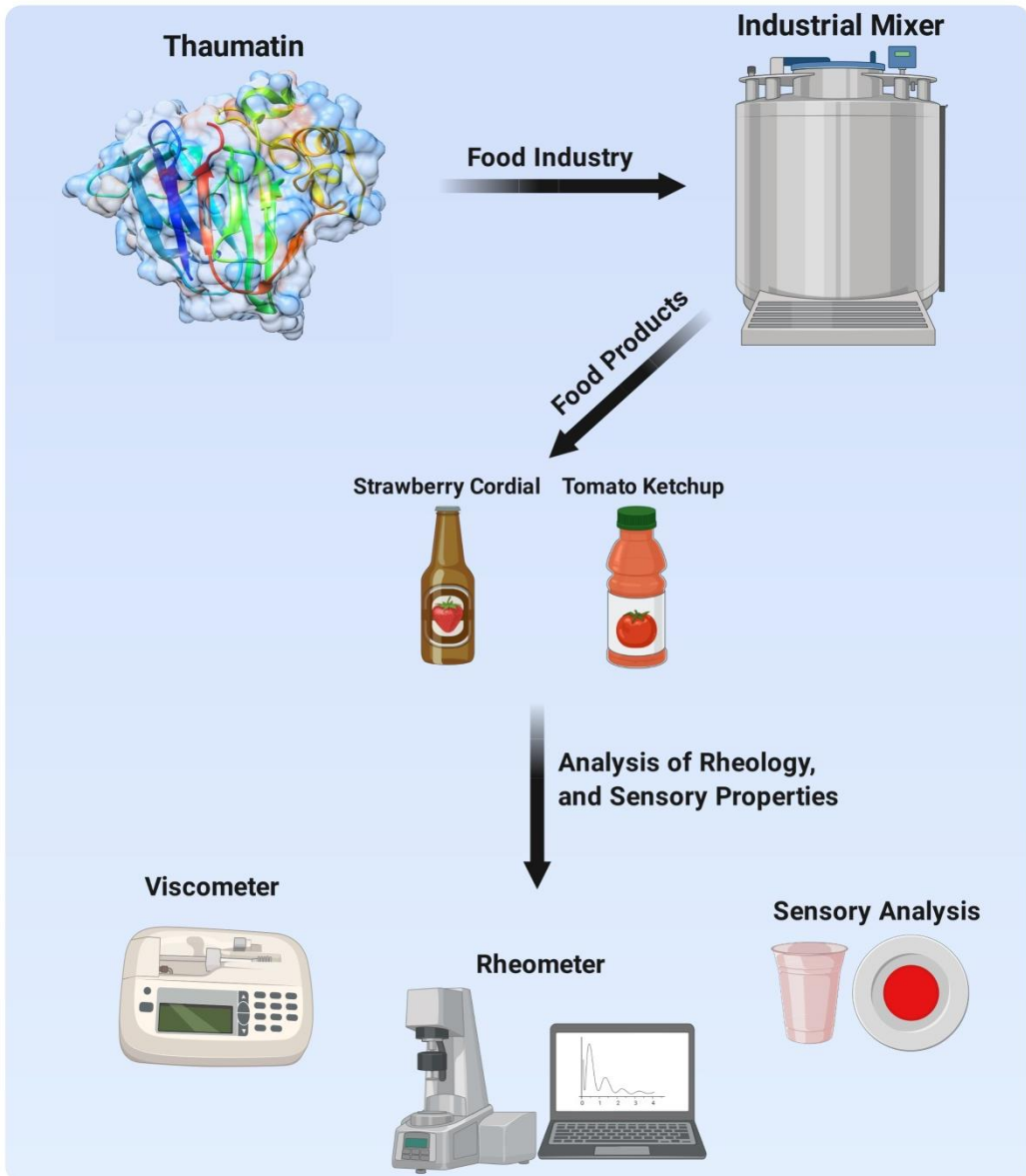
Thaumatin, a Sweet Protein, in Actual Food and Beverage products

Abstract

Thaumatin is a plant-based sweet protein isolated from Katemfe fruit, found in rainforests of West African countries. It is a high-intensity natural sweetener, rated about 3000 times sweeter than sucrose on weight basis. Thaumatin is highly soluble in water and aqueous alcohol reaching to 600 mg/mL. It is also heat and pH-stable with a great synergistic effect upon mixture with other low-calorie sweeteners. Up to this date, Thaumatin is the only sweet protein recognized as Generally Recognized As Safe (GRAS) by the FDA. These characteristics made Thaumatin a promising candidate for a wide range of edible products. For this aim, we included Thaumatin in the recipes of tomato ketchup and strawberry cordial followed by evaluation of sensory analysis and rheological properties. The outcome indicated that Thaumatin lost its functionality in tomato ketchup; instead sourness and bitterness were more revealed by the absence of sweetness. These results suggest that there are some food ingredients, *i.e.* salt, that could cancel the sweetness of Thaumatin. However, cordials prepared with Thaumatin tasted sweet. Worth mentioning, the cordial's sweetness quality was consistent with Thaumatin's sweetness profile itself, which is characterized by a delay in sweetness and liquorice aftertaste. As expected, sucrose played a vital role in rheological properties. Indeed, the viscosity, thickness and consistency were altered in both products after sucrose reduction, although these properties can be modified by addition of some food ingredients, *i.e.* bulky agents. Considering the data obtained, we believe this work open the way to solve the drawbacks in view of possible Thaumatin's applications in food and beverage industries.

3.1 Introduction

Thaumatin is one of the six sweet and sweet taste-modifying proteins with very high sweetness intensity, rated 3000 times sweeter than sucrose on weight basis. It is a plant-based sweet protein extracted from the arils of *Thaumatococcus danielli*, found in the West African countries [9,40]. The sweetness threshold of Thaumatin is ~ 45 nM, suggesting a very strong affinity towards the sweet taste receptor [41,42]. The complex of Thaumatin-receptor is stabilized by electrostatic interactions between positive charge distribution on the external surface of the protein and the complementary negative charges located on the external cleft of the receptor [43,44]. As a matter of fact, some basic amino acids located on the protein's outer surface such as Lys49, Lys67, Lys106, Lys163, Arg76, Arg79 and Arg82 have been identified to be responsible for the sweetness preservation of Thaumatin [69]. The sweetness of Thaumatin in the oral cavity is characterized by late insurgence and persistence up to 30 minutes after taste stimulus. In addition, Thaumatin can exhibit an undesirable liquorice aftertaste [9], which is likely due to the interactions with bitter taste receptors (T2Rs) [96,97].

Thaumatin is composed of 5 α-helices, 13 β-pleated strands and several bends [45]. Structural studies on purified Thaumatin showed that there are six closely related forms of Thaumatin with a molecular weight of ~ 22 kDa, including two major components (Thaumatin I and II) and four minor components (Thaumatin III, a, b and c). The differences in these six variants are net charge variations and sweetness potency with the following order: III > II ≥ I > a > b > c [9]. Thaumatin I and II are the most abundant forms that possess similar structural and functional properties such as amino acid composition, molecular weight, high similarity in amino acid sequences and sweetness. Each one of these two forms of Thaumatin is composed of a single polypeptide chain with 207 amino acid residues, differing by only five amino acids from each other. Thaumatin I and II contain 16 cysteine amino acids in their primary structures, which are oxidized to form 8 intermolecular disulfide bonds

[46]. Further studies on the physicochemical properties of Thaumatin evidenced that the protein is very soluble in water, reaching to 600 mg/mL, and thermostable under acidic conditions, with retained sweetness at 80 °C for several hours [47]. High thermal stability of Thaumatin is attributed to the existence of eight intramolecular disulfide bridges [45]. Thaumatin is considered as a safe ingredient to use in food and beverage applications. In the USA, EU and other countries, Thaumatin has been available in the markets since the mid-1990s under various trade names *i.e.* Talin and San Sweet T-100 as low-calorie sweetener and flavor modifier. In the USA, Thaumatin was granted Generally Recognized As Safe (GRAS) status by FEMA (GRASa No. 3732 [48] and GRASa No. 3814 [49]) as a flavor modifier. In Europe, it is approved as a Sweetener or as a flavor enhancer under EFSA (E 957) for different edible products. In the EU and Japan, the acceptable daily intake limit (ADI) for Thaumatin as a sweetener is "not specified" since the protein is considered non-toxic. However, according to the collected data from preclinical safety studies and human clinical exposure, the preferred maximum level of Thaumatin intake is 1.1 mg/kg-day, which is also recognized by the EU as a highly safe level for all consumers [98]. Thaumatin has already been used in chewing gum, dietary products, some specific drinks and pharmaceuticals.

SteVia rebaudiana (Bertoni) is a shrub of the Asteraceae family that is initially discovered in Paraguay and Brazil. Nowadays, stevia is planted in many regions across Asia, Europe and Canada. Stevia leaves include various diterpene glycosides such as stevioside, rebaudiosides A-F, Steviolbioside and dulcoside A. All of these extracted compositions from stevia leaves elicit a sweet sensation in humans. Rebaudioside A (Reb A) is one of the most abundant constituents of stevia, where 1 % of rebaudioside A was extracted. Stevia Reb A is very sweet being up to 250 times sweeter than sucrose on the weight basis [99]. Stevia rebaudioside M (Reb M), however, is a minor Steviol glycoside that is more potent with very low licorice or bitterness aftertastes; it is sweeter than other Steviol glycosides by several folds [100,101]. Steviol glycosides received a letter of no objection concerning their

GRAS status from FDA [102]. Sucralose, a synthetic trichlorinated disaccharide [103], is a nonnutritive sweetener that has grabbed a particular interest from food manufacturers. Some sensory studies reported that the sweetness profile of sucralose is clean of any bitterness aftertaste [104–106]. Sucralose is very sweet rated approximately 650-fold sweeter than sucrose, on weight basis [107–109]. Moreover, it has a relatively high stability at high temperature (up to 125 °C), therefore it can be used in any food and beverage productions processes [110,111]. Sucralose was approved for all categories of foods and beverages in the United States of America and European Union [112].

Very recently, the prevalence of some hazardous sucrose-correlated diseases raised much more concerns about sucrose consumption, and accordingly the efforts of seeking for healthier replacements of ordinary sweeteners have been widely escalated. In light of this, the idea of using natural sweeteners like sweet proteins attracted the spotlights to substitute table sucrose in food and beverage products [1–3]. Keeping in mind, the experience of using artificial sweeteners instead of sucrose was not very successful due to their association with various dangerous diseases [4,5,7]. In this work, we collaborated with the Kraft-Heinz Company (Heinz Innovation Center, Nijmegen, Netherlands), to investigate the effect of using sweet proteins in two of the company's iconic products, tomato ketchup and strawberry cordial, since the company is the biggest producer of tomato ketchup in the world and they are very keen to eliminate sucrose from this product, while the cordial is characterized by a very different texture and formulation complexity. This selection allowed us to study the protein's effects mainly on sensory analysis in the case of the liquid cordial, and on the sensory analysis and rheological properties of a non-Newtonian fluid preparation, in the case of tomato ketchup. Noteworthy, although Thaumatin is benefitted with some great properties *i.e.* intense sweetness, high stability, thermal resistance and high solubility, however, it suffers from some drawbacks, among which is its taste quality, characterized by a very late insurgence of sweetness with liquorice aftertaste. Nevertheless, the main reason to select

Thaumatin for this project is the approval licenses from FDA and EFSA, which allowed the sensory analysis teams of the Kraft Heinz Company to perform different analysis safely.

3.2 Materials and Methods

3.2.1 Flash Profiling

Flash profiling technique was performed on tomato ketchup samples to evaluate their taste quality and the intensity of the tasted attributes. A team of 7 panelists participated in this sensory analysis. Panelists generated their own list of attributes including sweetness, bitterness, salivating, odor, acidity, thickness, viscosity and overall flavor. We prepared 4 tomato ketchup samples with various sweeteners including TK-NAS (Tomato Ketchup Not Added sucrose) and 3 others containing stevia Reb A, stevia Reb M and Thaumatin with the concentrations of 800 ± 25 ppm, 650 ± 20 ppm and 300 ± 10 ppm, respectively. Of note, TK-NAS is a commercial Kraft Heinz Company's product that includes sucralose as sweetening agent instead of sucrose; therefore, we are obliged to keep its concentration enclosed due to the mutual confidential agreement between the University of Naples Federico II and the Kraft Heinz Company. TK-NAS was labeled by 000 to be recognized as a reference and the other tomato ketchups were labeled by three-digit codes to keep their identity anonymous to the tasters. Panelist received 3 cups of tomato ketchup per code (each includes 40 g) to taste and compare the attributes to the reference product. During the tasting, the panelists only considered the discriminant attributes and ranked the differences between the reference and the samples for each attribute. Prior to sensory analysis, the samples were incubated at room temperature (25.0 ± 1.0 °C) at least for 1 hour. The time duration of this experiment was 2 hours. Duplication of each measurement was performed and the data were analyzed in a comparative way.

3.2.2 Rheology

Rheological properties of tomato ketchup samples were measured using Malvern Kinexus Rheometer (model KNX2100, USA). The experiments were performed under 4 bar compressed air supplied to the rheometer by air motor supplier. To measure the viscoelastic region of tomato ketchups, a medium size spindle (40 mm diameter) was used. All operations and the settings of the experiments were controlled by rSpace software (Malvern Panalytical). To run each measurement, rheometer was calibrated by performing a zero gap test followed by loading 5 g of tomato ketchup on the sample holder. The data were collected from rSpace software and analyzed by Microsoft Excel. Each experiment was repeated twice and the averaged data are presented.

3.2.3 Consistency

The consistency of tomato ketchup samples was determined using the Kraft Heinz Company's designed consistometer. For every measurement, 300 mL of tomato ketchup sample was prepared. The products were preserved at room temperature (25.0 ± 1.0 °C) to prevent any temperature-linked errors. Prior to each measurement, the samples were homogenized by careful stirring to avoid any air bubble formation. A cylinder was loaded with tomato ketchup using a spatula to reach the labeled sign. Then, the cylinder was unloaded into a trough and the flow distance of the sample in the trough was measured in 5 seconds. The sample flow distance is shown by centimeter (cm). The presented results are the average of two independent measurements.

3.2.4 Temporal Dominance of Sensations (TDS)

The dominant taste attributes such as sweetness, sourness, bitterness, artificial sweetener and liquorice taste of different strawberry cordials as function of time

were evaluated by Temporal Dominance of Sensations (TDS) technique. A group of 7 panelists participated in this sensory assessment. Pre-tasting sessions were performed to select 5-10 relevant taste sensations. We prepared a reference strawberry cordial including sucrose and other four strawberry cordials containing diverse sweeteners such as 2500 ± 40 ppm stevia Reb A, 2000 ± 40 ppm stevia Reb M, 1000 ± 30 ppm sucralose and 500 ± 20 ppm Thaumatin. The concentrations of sweeteners were calculated in a way to obtain strawberry cordials with sweetness intensity as close as possible to the reference sample. A volume of 40 mL per sample was prepared to perform TDS. Upon the cordials intake, panelists started describing the sequence of the perceived dominant sensations until they no longer tasted any dominant attributes. TDS was performed on the samples preserved for 1 hour at room temperature (25.0 ± 1.0 °C) before tasting. The presented data are collected from three independent experiments and averaged for each sample.

3.2.5 Time Intensity of Sweetness (TIS)

The sweetness attribute of the strawberry cordials was evaluated as a function of time by a sensory technique called time intensity of sweetness. Seven panelists participated in the evaluation of sweetness intensity of strawberry cordials over 20 seconds. For each tasting, 40 mL of strawberry cordial was prepared in a tester cup. The initial sweetness intensity of each strawberry cordial was assessed out of 100 % sweetness perception of each taster. All the samples were kept at room temperature 1 hour prior to the sensory analysis. The results of each taster were collected from three independent trials and the averaged data are presented.

3.3 Results and Discussion

3.3.1 Tomato Ketchup

3.3.1.1 Flash Profiling

Flash profiling is a widely used descriptive method to characterize the nature and quantify the intensity of sensory properties of food and beverage products [113]. This technique provides very quick and precise sensory assessments on edible products. Perception is a dynamic process with a series of events, in which the intensity and durability of sweetness, bitterness, sourness and overall flavor in various food products are measured [114]. Flash profiling method was selected to describe the sensory attributes of 4 tomato ketchup products: TK-NAS (Tomato Ketchup Not Added Sucrose), which contains sucralose and was used as a reference and 3 other tomato ketchup products prepared with stevia Reb A, stevia Reb M and Thaumatin. The reason for selection TK-NAS as a reference product was to compare tomato ketchup containing a sweetening agent with delayed sweetness to other 3 samples including sweeteners known for their persistent sweetness. In the sensory map (**Fig. 1**), samples closer to the right and left sides of the map are stronger in the attributes loaded on the right and left sides of the graph. This discipline also corresponds to the samples located on the top and bottom sides of the sensory map (**Fig. 1**). According to the obtained results, TK-NAS was the sweetest, most fruity and spicy in comparison to the rest of the samples. Tomato ketchups prepared with stevia Reb A and stevia Reb M showed similar sensory properties. They were less sweet than the reference with a very strong liquorice aftertaste. On the other hand, the sample containing Thaumatin was poorly sweet; instead, it was more bitter, sour and salty with metallic aftertaste (**Fig. 1**). These attributes are not due to the Thaumatin presence, but bitterness and sourness are coming from other tomato ketchup's ingredients *i.e.* vinegar and perceived with higher intensity in the absence of sweetness sensation.
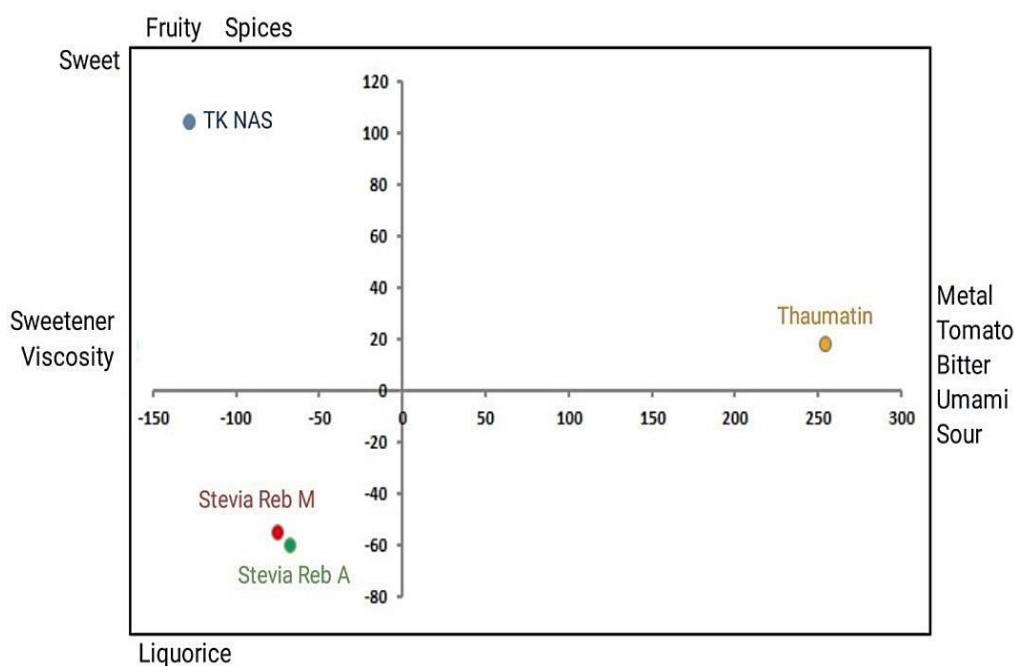
Figure 1. A sensory map presenting the sensory properties of 4 tomato ketchup products: blue) TK-NAS (reference) and tomato ketchups prepared with green) stevia Reb A, red) stevia Reb M and orange) Thaumatin. TK-NAS: Tomato Ketchup Not Added sucrose.

3.3.1.2 Linear Viscoelastic Region

In the past a few decades, the science of rheology attracted much attention in the fields of food acceptability, food processing and food handling [115]. As a matter of fact, semi-liquid foods are complex materials in terms of structure and rheology; therefore, measurement of rheological properties is a challenging process. The reason is that semi-liquid foods are mostly prepared from mixtures of solid and fluid structural components. In this regard, rheology gives insights on the flow and deformation of semi-fluid food products and most importantly, it monitors their behavior in the transient area between solid and liquid states. Rheology data can be also exploited to provide a relationship between the shear stress induced to semi-fluid foods and the resulting deformation and/or flow [116]. Linear viscoelasticity is

one of the rheological properties that is greatly important for obtaining information on the unperturbed state of food products and characterize their microstructures. In addition, the knowledge of the linear viscoelastic region gives the ability to predict the viscos flow upon the development of suitable non-linear viscoelasticity models [117]. Herein, we measured the linear viscoelastic regions of 5 tomato ketchup products: TK-Ref (Tomato Ketchup-Reference) and other 4 tomato ketchups sweetened by 50 % sucrose, full Thaumatin, 50 % sucrose + 50 % Thaumatin and without any sweeteners (negative control) using rheometer. The rheogram (**Fig. 2**) is presented with storage modulus value as a function of the shear strain percentage. According to the results, TK-Ref is the thickest sample among all the samples as it has the highest storage modulus value (**Fig. 2**). Tomato ketchups containing 50 % sucrose + 50 % Thaumatin, 50 % sucrose, full Thaumatin and the negative control follow the TK-Reference in terms of thickness from the highest to the lowest, respectively. Further, the graph indicated that the viscoelastic regions of the tomato ketchup including Thaumatin and the negative control were more linear than the rest of the samples. The reason is that these two samples have less storage modulus value differences between solid and liquid states than the other 3 tomato ketchup products (**Fig. 2**). According to these data, it is quite clear that sucrose had a big impact on the thickness of the products.
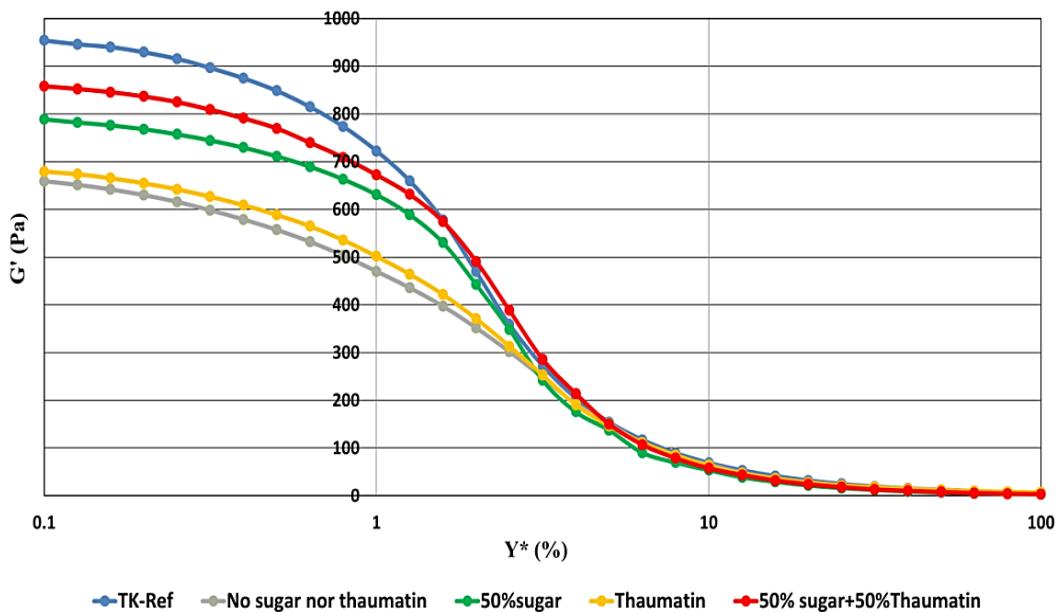
Figure 2. Rheogram presenting the linear viscoelastic regions of TK-Ref (blue line), tomato ketchup containing 50 % sucrose (green line), full Thaumatin (yellow line), 50 % sucrose + 50 % Thaumatin (red line) and without sucrose or Thaumatin – negative control (gray line). The rheogram is shown with storage modulus G' (Pa) as a function of shear strain Y*(%). TK-Ref: Tomato Ketchup-Reference.

3.3.1.3 Consistency

Consistency of foods and thickened liquids is another rheological property that is involved in swallowing impairment [118,119]. It is related to non-Newtonian or semi-liquid fluids *i.e.* sauces, purees and pastes that include soluble and insoluble molecules. Consistency can be measured by flowing the product on a flat surface as a function of time (s) [120]. Observations of the flowing the same tomato ketchup samples in 5 seconds within the trough of the consistometer (designed by Kraft Heinz Company) were measured to quantify their consistency (**Fig. 3**). The reference tomato ketchup resulted in a consistency of 12.2 cm, which is in a good agreement to the standard tomato ketchup consistency range (11.5 – 12.5 cm). Surprisingly, tomato ketchup sweetened by Thaumatin showed a consistency value

of 16.7 cm in 5 second, even lower consistency with respect to the negative control. On the other hand, Thaumatin free products such as tomato ketchup including 50 % sucrose or without any sweeteners (negative control) showed slightly less consistency in comparison to the reference product (**Fig. 3**).
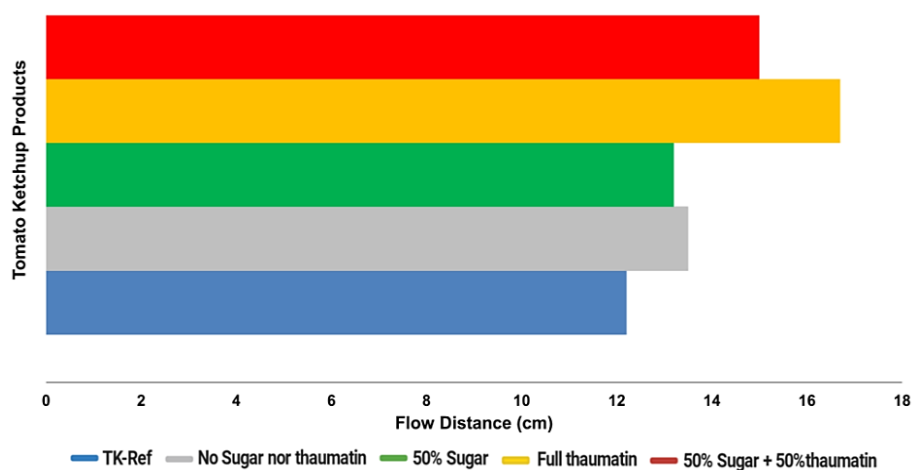

Figure 3. Bar chart presenting the consistency measurement of TK-Ref (blue bar), tomato ketchup without sucrose or Thaumatin – negative control (gray bar) and tomato ketchups containing 50 % sucrose (green bar), full Thaumatin (yellow bar) and 50 % sucrose + 50 % Thaumatin (red bar). TK-Ref: Tomato Ketchup Reference.

3.3.2 Cordial

3.3.2.1 Temporal Dominance of Sensations (TDS)

Temporal dominance of sensations (TDS) is a sensory analysis technique that provides the opportunity to record a sequence of the dominant sensations among a list of sensory attributes perceived during tasting of food and beverage products [121]. It is a descriptive approach that recognizes the dominant sensation at each specific time after tasting of food and beverage products and the assessment continues until the end of sensations. Moreover, TDS method determines the intensity of each dominant attribute by intensity scores [122–125]. This technique

was selected to evaluate the taste quality of 5 cordials with strawberry flavor including full sucrose cordial as a reference sample, and 4 other strawberry cordials prepared with stevia Reb A, stevia Reb M, sucralose and Thaumatin. The TDS graphs are commonly divided into 3 levels: dominant level, significant level and chance level, from which only the data shown in dominant and significant levels are reliable. According to the reference TDS graph (**Fig. 4A**), sweetness is the dominant taste in the first 10 seconds followed by sourness that remains the dominant attribute till the end of sensations. Also, minor bitterness could be observed after 20 seconds of the sample intake. On the other hand, the strawberry cordial prepared with Thaumatin showed a completely different behavior (**Fig. 4B**). Indeed, sourness was the dominant attribute that perceived after ~ 6 seconds of tasting. Before 2 seconds of sourness perception, sweetness with lower intensity was tasted followed by perception of sweetener and liquorice attributes at 14 and 20 seconds, respectively. In the **Figure 4C**, a summary of TDS results of all 5 cordial samples is presented with attributes color-coded attributes during 30 seconds of tasting. The TDS data of the strawberry cordials prepared with stevia Reb A and stevia Reb M showed a sweet peak in the beginning followed by sweetener attribute. The main difference between these two cordials is the sweetness sensation of the cordial including stevia Reb M that remains the dominant attribute for a longer period of time. In the case of the sample containing sucralose, the taste is dominated by sweetness attribute only. To clarify, the sensory team at the Kraft Heinz Company defines the artificial sweetness as sweetener.
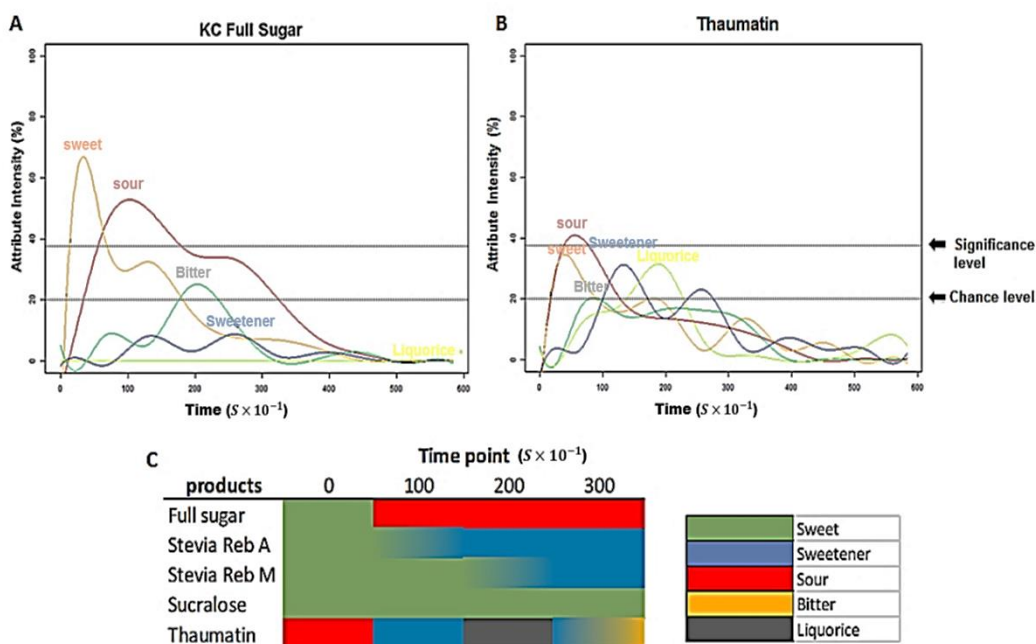
Figure 4. TDS graphs of A) strawberry cordial full sucrose and B) strawberry cordial prepared with Thaumatin. C) A table presenting a summary of TDS results of 5 cordial samples: strawberry cordial full sucrose and cordials with stevia Reb A, stevia Reb M, sucralose and Thaumatin, during 30 seconds of tasting. Each attribute is presented with a color coding shown on the right panel. TDS: Temporal Dominance of Sensations.

3.3.2.2 Time-Intensity of Sweetness

Time-intensity (TI) methodology is a commonly used technique to evaluate the evolution of the attributes intensities over time for any sensory analysis of food and beverage products. This is a useful approach to study the temporal aspects of the perception of single or multiple sensory sensations in a product [126,127]. In addition, the lingering taste perceptions triggered by sweeteners [128], bitter compounds [129] and trigeminal compounds such as menthol [130] could be evaluated by TI methodology [131,132]. This approach was adapted by sensory team of the Kraft Heinz Company to assess the evolution of sweetness intensity over 20 seconds. Time-intensity of sweetness (TIS) was performed on 5 strawberry

cordials such as full sucrose cordial as a reference and 4 other strawberry cordials containing stevia Reb A, stevia Reb M, sucralose and Thaumatin. Based on the results obtained from TIS graph (**Fig. 5**), the reference sample experienced the fastest drop in the sweetness intensity. Strawberry cordials prepared with stevia Reb A, stevia Reb M and sucralose exhibited a very similar sweetness profile over time and the sweetness was more persistent compared to the reference cordial. Worth mentioning, these data are in a good agreement to TDS results (**Fig. 4**). On the other hand, the strawberry cordial prepared with Thaumatin presented a totally diverse behavior. TIS graph indicated that the sweetness intensity of Thaumatin slightly increased over time (**Fig. 5**). These observations were expected due to the sweetness profile of Thaumatin itself, which is defined by development of sweetness over time and lingering for a while.
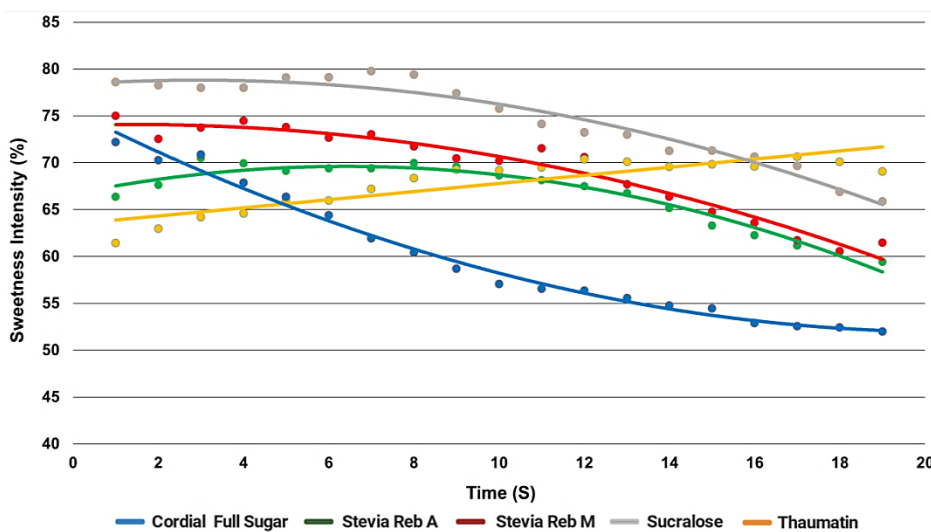

Figure 5. The graph presenting time-intensity of sweetness (TIS) of 5 strawberry cordial samples. The sweetness intensity of full sucrose cordial (blue line) and strawberry cordials containing stevia Reb A (green line), stevia Reb M (red line), sucralose (gray line) and Thaumatin (yellow line) is presented as a function of time (20 seconds).

3.4 Conclusions

In the recent years, as the research of new low-calorie sweeteners for different food and beverage applications attracted much attention [18]. Sweet proteins have a great potential as alternative high intensity sweeteners, however, there are still no systematic studies on their applications in actual food and beverage products. Among sweet proteins, Thaumatin is one of the sweetest proteins with very high thermal stability, suitable for common thermal treatments in food preparations [41,133,134]. It is also the only approved for human ingestion, therefore it was selected as representative of the sweet proteins category in this study performed in the Kraft Heinz Company. Thaumatin shares some common features with the other sweet protein, MNEI, largely investigated in this thesis. The common features consist of similar mode of interaction to the sweet taste receptor, T1R2-T1R3, high thermal stability and late insurgence of sweetness. It is worth a mention, MNEI has less persistence of sweet taste with much lower intensity of liquorice aftertaste with respect to Thaumatin [6,7,18]. We used Thaumatin as a sweetener in the standard recipes of tomato ketchup and strawberry cordial, two of the Kraft Heinz Company's iconic products, followed by performing sensory and texture analyses on the prepared products. According to the sensory analysis data, Thaumatin completely lost its sweetness in tomato ketchup and the samples perceived more sour and bitter. These attributes are not due to the Thaumatin itself but they were more revealed in the absence of sweetness (**Fig. 1**). Moreover, rheological properties of the tomato ketchup containing Thaumatin were greatly altered because of sucrose removal. Indeed, the tomato ketchup was less thick and viscose with respect to the standard tomato ketchup (**Fig. 2**). Consistency is another texture property of the tomato ketchup that was changed by sucrose reduction. In fact, the flow distance of tomato ketchup prepared with Thaumatin increased by 5 cm with respect to the standard tomato ketchup, which is another indication of less thickness and viscosity (**Fig. 3**). On the other hand, the sensory analysis of the strawberry cordial prepared

with Thaumatin showed different results. The sweetness of Thaumatin was clearly perceived in the cordials. Indeed, the sweetness was tasted with the known sweetness profile of Thaumatin, which is delay in the sweetness with liquorice aftertaste (**Fig. 4** and **5**). In this case, the sweetness profile of Thaumatin could be modified by some strategies such as mixing Thaumatin with other low-calorie sweeteners such as sucralose to compensate the sweetness delay of Thaumatin. As a matter of fact, sucrose had a big impact on some rheological properties of both products including viscosity and elasticity. This is due to the very little amount of Thaumatin needed to reach to the same sweetness intensity of sugar-based products. Since Thaumatin has the same sweetness intensity with respect to MNEI [18], thus most probably the same results will be observed for the products prepared with MNEI as a sweetener. However, these properties could be easily compromised by addition of some food additives such as bulky agents. This study requires more time and attention to investigate different strategies to solve these drawbacks and open the way for Thaumatin's applications in food and beverage industries.

CHAPTER <u>4</u>
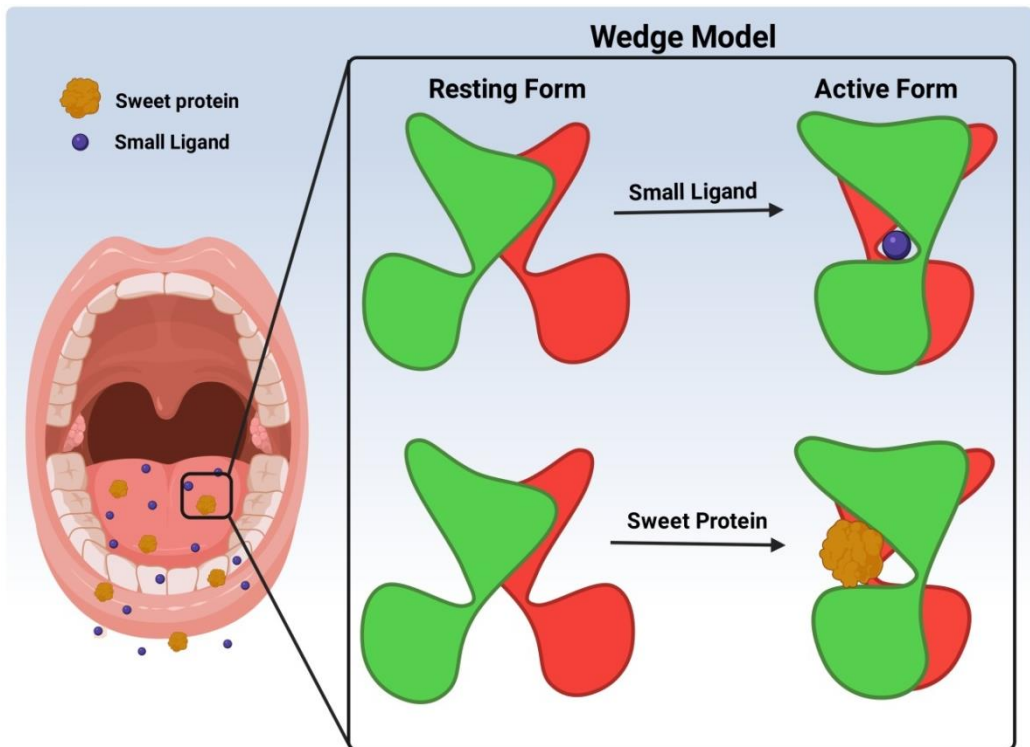
The Effects of Ionic Species on the Sweetness Intensity of Sweet Proteins

Abstract

Naturally occurring sweet proteins are among the best candidates to replace sucrose and artificial sweeteners in edible products. However, industrial applications of sweet proteins encounter some hurdles such as uneven sweetness potency in various commercial waters. In this research work, we used 4 sweet proteins *i.e.* MNEI, Mut3, Mut9 and Thaumatin, in 4 commercial waters with different mineral residue levels to study the effects of different types of waters on the sweetness intensities and the structure of these sweet proteins. Based on the collected data, all of the tested sweet proteins showed a similar behavior in terms of sweetness intensity in various commercial waters. Indeed, more mineral residue amounts resulted in less sweetness power of sweet proteins. Instead, the sweetness levels of drinking samples including sucrose, sucralose and aspartame remained almost identical for all types of waters. The structural analysis of proteins checked by CD and NMR spectroscopies evidenced that the 3D structure of sweet proteins was preserved in various types of waters. According to these results, we believe that the decrease in the sweetness intensity of sweet proteins in waters containing higher amounts of mineral residues are not due to the protein's structural changes, but to the presence of ionic compounds that could hamper the bindings between the sweet proteins and sweet taste receptors.

4.1 Introduction

Nowadays, sucrose consumption is one of the most controversial and hot topics in all over the world and more seriously in the developed countries [135–140]. It is due to the sucrose's association with increased risk of obesity [141–143] and some other factors leading to cardiovascular disease [144], dyslipidemia [145,146], increased blood pressure [147–149], diabetes [150–152] and non-alcoholic fatty liver disease [153,154]. Indeed, some attempts have already been made to reduce or substitute sucrose with natural or artificial sweeteners in food and beverage products. However, the trials of sucrose's substitution with artificial sweeteners were not very successful after many evidences recorded about the severe consequences of consuming artificial sweeteners [4]. In fact, sucrose reduction/substitution in sweet foods and beverages is still a challenging matter due to the impact of this food ingredient on texture and sensory properties including sweetness and thickness. According to this fact, sucrose reduction might alter the final product's quality affecting consumer's perception [155].

A relatively new class of natural sweeteners is sweet proteins that have been found in the late 1960s from the berries and seeds of some unrelated tropical plants of West Africa [7,18]. Due to the intense sweetness and plant origin of sweet proteins, they are considered a promising group of natural sweeteners that could replace ordinary sweeteners in the markets [18]. Among sweet proteins, Thaumatin is the only sweet protein that was approved by FDA and used in some specific edible products such as chewing gum, dietary products and pharmaceuticals. However, the applications of sweet proteins as sweeteners in actual food industries did not occur due to some drawbacks. For instance, in some attempts to prepare home-made beverages with sweet proteins as sweeteners, we realized that the sweetness intensity varied upon using various commercial waters. This inconvenience could be resulted from either protein's structural changes or disturbance in the protein-receptor bindings. To understand the circumstances of this ambiguous behavior of this type

of natural sweeteners, we used 4 well characterized sweet proteins, *i.e.* MNEI, Mut3, Mut9 and Thaumatin to prepare drinking samples in 4 commercial waters *i.e.* HPLC grade, Sant'Anna, Rocchetta and Lieve, which have different mineral residue amounts and conductivities. Then, the drinking samples were subjected to sensory analysis by running blind tasting sessions and structural analysis using CD and NMR spectroscopies. Also, we prepared sweet drinking samples by sucrose, sucralose and aspartame in the same commercial waters to control the sweetness intensity.

4.2 Materials and Methods

4.2.1 Materials

MNEI [34] and two of its mutants such as Mut3 [73] and Mut9 [54] were obtained in our laboratory, while Thaumatin was ordered from sigma (Sigma-Aldrich, USA). The commercial sucrose, sucralose and aspartame were purchased from the markets. Protein concentration was assessed by UV absorbance at 280 nm using a value of the absorbance at 0.1% of 1.41 for MNEI and Mut9, 1.29 for Mut3 and 1.33 for Thaumatin. The water analysed were HiPerSolv CHROMANORM HPLC grade (VWR), henceforth synthetically indicated as "HPLC", and commercial mineral waters (Sant'Anna, Rocchetta and Lieve) selected on the basis of the mineral residue amounts, conductivity, pH and the NaCl concentration corresponding to the conductivity values as indicated in **Table 1**.

Table 1. Physicochemical properties (mineral residue amount, conductivity, pH and the NaCl concentration corresponding to the conductivity values) of the 4 commercial waters used in this study.

Water	Mineral amount (mg/l)	Conductivity (μs/cm)	pH	NaCl concentration (mM)
HPLC	≤ 1	≤ 1	5.90	N.A.
Sant'Anna	22	25	7.25	0.0096
Rocchetta	182	298	7.86	0.383
Lieve	294	445	7.81	1.262

4.2.2 Protein expression and purification

The recombinant proteins including MNEI, Mut3 and Mut9 were produced as described in the Materials and Methods section of Chapter 1.

4.2.3 Sensory Analysis

The drinking samples were prepared with MNEI, Mut3, Mut9 and Thaumatin, in the four waters, as indicated above. A group of 5 panellists participated in these blind tasting sessions. Two paper cups, one containing 5 mL of protein-based drink and the other 5 mL of commercial water were provided for the tasting and recording their evaluation from 0 to 5. The definitions of the values are 0: (no taste), 1: unidentified taste, 2: slightly sweet, 3: sweet, 4: very sweet and 5: extremely sweet. MNEI, Mut3, Mut9 and Thaumatin samples were prepared with the concentrations of 2, 4, 6, 8 and 10 mg/L. In the case of Mut3, lower concentrations (0.5 and 1 mg/L) were also prepared due to the very high sweetness intensity [73]. The concentrations of the used proteins were selected according to their sweetness intensities, starting from a little higher the concentration of known sweetness thresholds of the proteins to the maximum sweetness perception limitation. In another experiment, MNEI and Thaumatin with a concentration of 10 mg/L were dissolved in HPLC water containing a NaCl concentration calculated to reproduce the ionic strength of the three mineral waters (**Table 1**). Also, control samples of 40 g/L sucrose, 67 mg/L sucralose and 0.2 g/L aspartame in the same types of waters were prepared. The subjects tasted the sample solutions without any time constrains

followed by spitting it out and rinsing their mouth thoroughly with mineral water within 1 min interval.

4.2.4 Circular Dichroism Spectroscopy (CD)

CD measurements were performed on a Jasco J-1500 spectropolarimeter (Jasco, Essex, UK), equipped with a Peltier temperature control system (CTU-100), using a 1.0 cm quartz cell. The diluted samples were obtained starting from concentrated protein solution (2.5 mg/mL in 5 mM HCl). The spectra measured in the far UV-range 195-250 nm (50 nm/min scan speed), and each experiment performed with 3 accumulations. Molar ellipticity per mean residue [θ] was calculated according to the formula:

$$[\theta] = [\theta]_{obs} \, mrw / (10 \times l \times C), \quad deg \, cm^2 \, dmol^{-1}$$

where $[\theta]_{obs}$ is the raw ellipticity values measured in degrees, mrw is the mean residue molecular weight of each protein (Da), C is the protein concentration in g/mL and l is the optical path length of the quartz cell in cm.

4.2.5 NMR Spectroscopy

^{1}H NMR spectra were recorded with a Bruker AVANCE 700 MHz spectrometer equipped with a cryo-probe, using excitation sculpting water suppression pulse sequence on resonance with the water signal. The protein samples were prepared in 90 % commercial water (as indicated in the captions) and 10 % D_2O at the protein concentration of 3 mg/mL for MNEI and 6 mg/mL for Thaumatin, respectively. The spectra were acquired at 25 °C, with the following settings: 64k fid points, 128 scans, 2 seconds recycle delay.

4.3 Results and Discussion

4.3.1 MNEI

The effects of various commercial waters on the sweetness intensity and the secondary structure of single-chain Monellin, MNEI, were carefully assessed by blind sensory analysis and CD spectroscopy, respectively. MNEI was used to prepare sweet drinking samples with 4 types of commercial waters containing different amounts of mineral residues. According to the sensory analysis, MNEI at the lowest protein concentration (2 mg/L) in HPLC grade and Sant'Anna waters that contain the least mineral residues (1 and 22 mg/L, respectively) evaluated between the levels of unidentified taste and slightly sweet. The sweetness intensity of both drinking samples developed by increasing the protein concentration to maximum 10 mg/L, where the sweetness potency of both samples fell in the range of very sweet and extremely sweet (**Fig. 1A**). On the other hand, the other 2 sweet drinking samples prepared with Rocchetta and Lieve waters including higher amounts of mineral residues (182 mg/L and 294 mg/L, respectively) tasted less sweet. In fact, the drinking samples with 2 mg/L protein concentration were totally tasteless and upon increasing the protein concentration to 10 mg/L, the sweetness intensity was assessed between slightly sweet and sweet levels (**Fig. 1A**). The secondary structure of MNEI with the protein concentration of 10 mg/L in 4 types of commercial waters was also analyzed to detect any possible structural changes. The folding patterns of MNEI in all 4 types of commercial waters were very alike (**Fig. 1B**). The only mentionable differences in the secondary structures recorded by deconvolution of MNEI spectra using the BestSel online tool [74] were variations in the β-sheet (antiparallel) and α-helix contents by a few percentages (**Fig. 1C**). These differences are smaller than intrinsic errors in the deconvolution procedure [156].
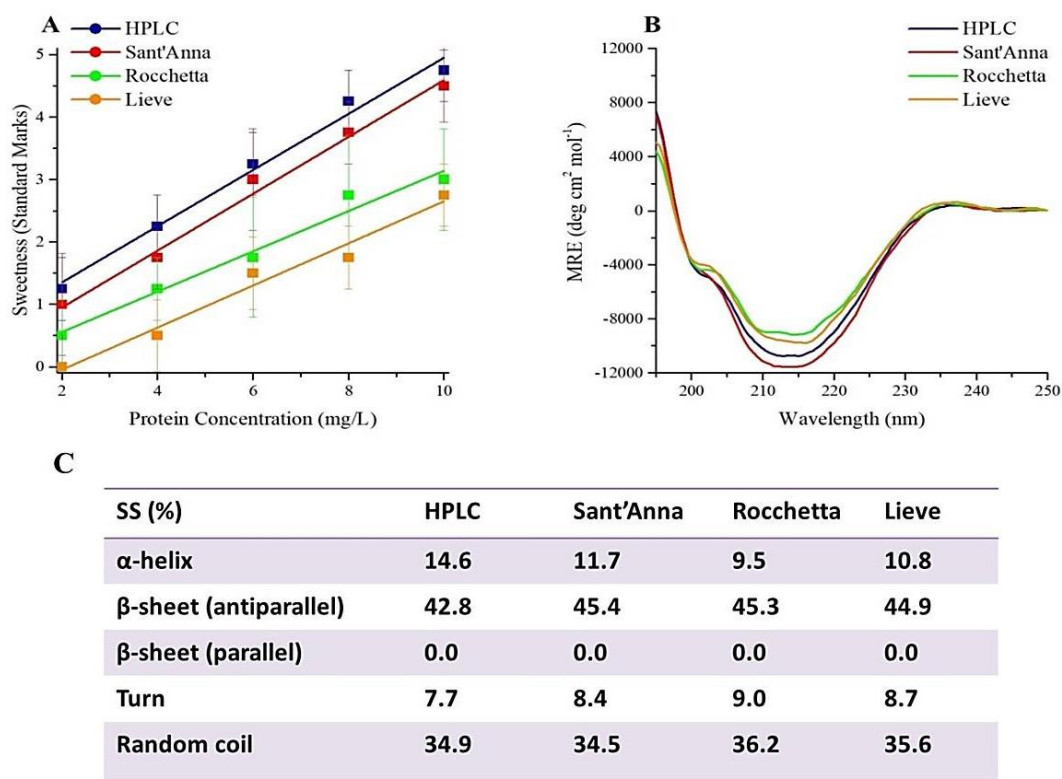
Figure 1. A) Sensory analysis of MNEI at 2, 4, 6, 8 and 10 mg/L in 4 commercial waters: blue) HPLC grade, red) Sant'Anna, green) Rocchetta and orange) Lieve. B) The secondary structure spectra of MNEI at 10 mg/L in 4 commercial waters: blue) HPLC grade, red) Sant'Anna, green) Rocchetta and orange) Lieve. C) A table presenting the secondary structure contents of MNEI in different commercial waters by spectral deconvolution [74].

4.3.2 Mut3

Mut3 is one of MNEI's constructs with the highest sweetness power among all known sweet proteins up to this date [73]. Herein, the sweetness intensity of Mut3 from the protein concentration of 0.5 to 10 mg/L was carefully controlled by a blind tasting session. At the lowest protein concentration (0.5 mg/L), all of the Mut3 drinking samples that prepared with 4 different types of commercial waters were tasteless. The sweetness intensity of Mut3 drinking samples escalated upon

increasing the protein concentration to maximum 10 mg/L. Based on the obtained data, the sweetness intensity of Mut3 with the maximum protein concentration in HPLC grade and Sant'Anna was close to extremely sweet, although the sample prepared with HPLC grade water was slightly sweeter (**Fig. 2A**). Very similar to MNEI data, Mut3 in Rocchetta and Lieve waters perceived less sweet than Mut3 in HPLC grade and Sant'Anna. Indeed, the sweetness potency of Mut3 in Rocchetta and Lieve resulted within the levels of sweet and very sweet (**Fig. 2A**). Also, the secondary structure of Mut3 in 4 commercial waters was measured to control the changes in Mut3's folding pattern upon using various types of waters. In fact, the spectra of Mut3 were highly superimposable and no noticeable differences could be observed (**Fig. 2B**). Worth mentioning, only a few percentages of variation in the β-sheet (antiparallel) and α-helix contents could be recorded (**Fig. 2C**), which are negligible with respect to intrinsic errors in the deconvolution procedure [156].
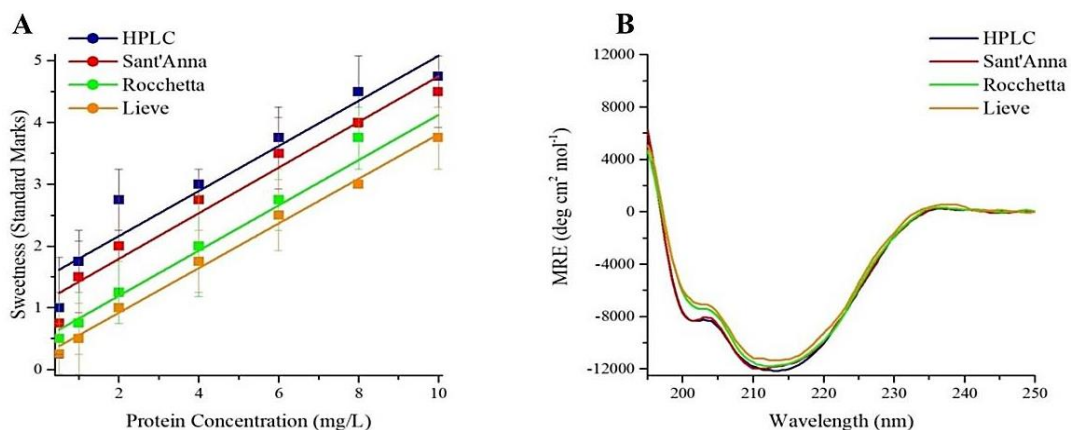

SS (%)	HPLC	Sant'Anna	Rocchetta	Lieve
α-helix	14.5	17.9	16.3	17.4
β-sheet (antiparallel)	43.0	40.0	42.1	41.6
β-sheet (parallel)	0.0	0.0	00	0.0
Turn	7.4	6.6	5.8	7.3
Random coil	35.1	35.5	35.7	33.8

Figure 2. A) Sensory analysis of Mut3 at 0.5, 1, 2, 4, 6, 8 and 10 mg/L in 4 commercial waters: blue) HPLC grade, red) Sant'Anna, green) Rocchetta and orange) Lieve. B) The secondary structure of Mut3 at 10 mg/L in 4 commercial waters: blue) HPLC grade, red) Sant'Anna, green) Rocchetta and orange) Lieve. C) A table presenting the secondary structure contents of Mut3 in different commercial waters by spectral deconvolution [74].

4.3.3 Mut9

Mut9 is another mutant of MNEI with an extraordinary thermal and chemical stability endowed with a double sweetness power compared to its parent protein [54]. To screen the changes of the protein's sweetness potency in 4 various commercial waters, Mut9 drinking samples with increased concentration starting from 2 to 10 mg/L were prepared and subjected to a blind sensory analysis. At 2 mg/L protein concentration, only the samples prepared with HPLC grade and Sant'Anna waters tasted slightly sweet and the remaining samples were between tasteless and unidentified taste levels (**Fig. 3A**). At the maximum protein concentration (10 mg/L), the sweetness intensity of Mut9 in HPLC grade and Sant'Anna was evaluated near to the maximum level. While, the sweetness of Mut9 at 10 mg/L concentration in Rocchetta and Lieve waters was between sweet and very sweet levels (**Fig. 3A**). Moreover, secondary structure of Mut9 in different types of commercial waters was screened. The outcome demonstrated that Mut9's spectra were very similar and highly superimposable (**Fig. 3B**), but slight differences in the β-sheet and the α-helix contents could be observed (**Fig. 3C**). These variations are far smaller than intrinsic errors in the deconvolution procedure [156]
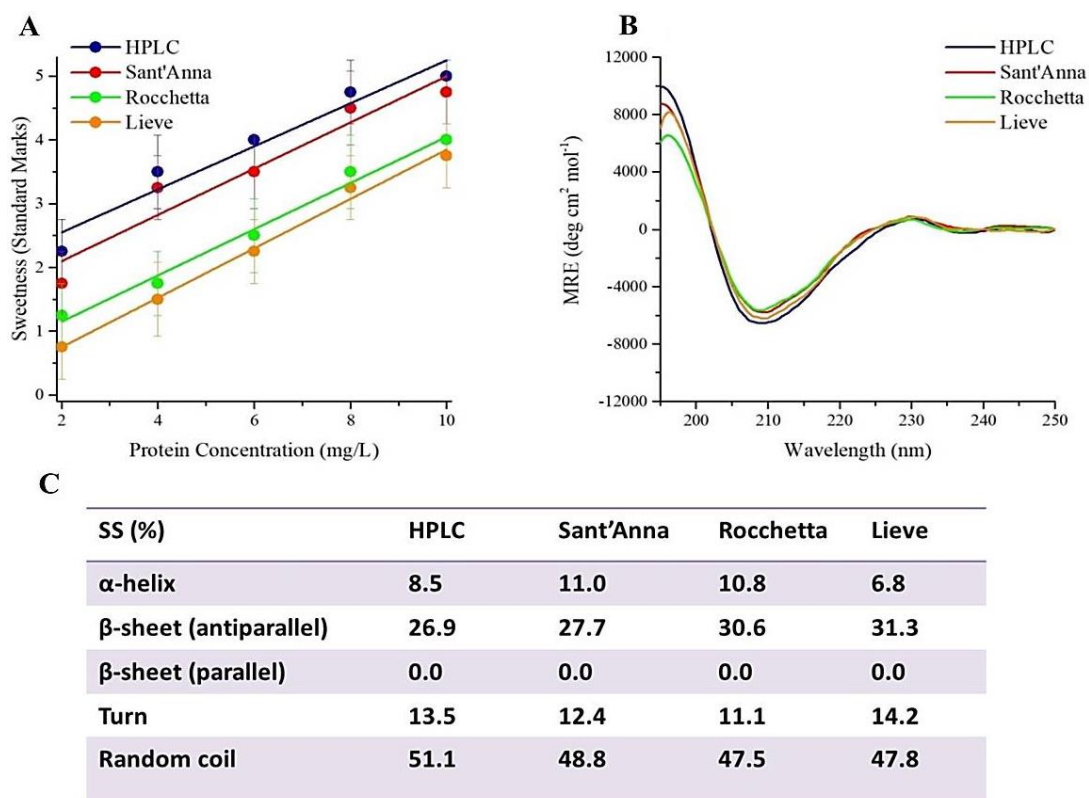
Figure 3. A) Sensory analysis of Mut9 at 2, 4, 6, 8 and 10 mg/L in 4 commercial waters: blue) HPLC grade, red) Sant'Anna, green) Rocchetta and orange) Lieve. B) The secondary structure of Mut9 at 10 mg/L in 4 commercial waters: blue) HPLC grade, red) Sant'Anna, green) Rocchetta and orange) Lieve. C) A table presenting the secondary structure contents of Mut9 in different commercial waters by spectral deconvolution [74].

4.3.4 Thaumatin

Thaumatin was the last sweet protein selected for this study. A blind sensory analysis was performed on Thaumatin-based drinking samples with protein concentration ranging from 2 to 10 mg/L. At 2 mg/L protein concentration, only Thaumatin prepared in HPLC grade and Sant'Anna tasted slightly sweet and the other two samples were almost tasteless (**Fig. 4A**). The sweetness potency of Thaumatin at the highest concentration (10 mg/L) in HPLC grade and Sant'Anna

was assessed to be within the levels of very sweet and extremely sweet, while in Rocchetta and Lieve, it tasted one unit less sweet (**Fig. 4A**). Like the other three sweet proteins, the secondary structure of Thaumatin at 10 mg/L in different commercial waters was also analyzed by CD spectroscopy. The results showed that the spectra of Thaumatin in 4 types of waters were very similar and superimposable (**Fig. 4B**), except minor variations in the secondary structure contents (**Fig. 4C**) that are far below the intrinsic error values of deconvolution procedure [156]


SS (%)	HPLC	Sant'Anna	Rocchetta	Lieve
α-helix	4.8	5.0	6.3	4.4
β-sheet (antiparallel)	34.5	35.1	36.0	36.9
β-sheet (parallel)	0.0	0.0	0.0	0.0
Turn	14.5	14.1	13.2	14.4
Random coil	46.2	45.8	44.5	44.3
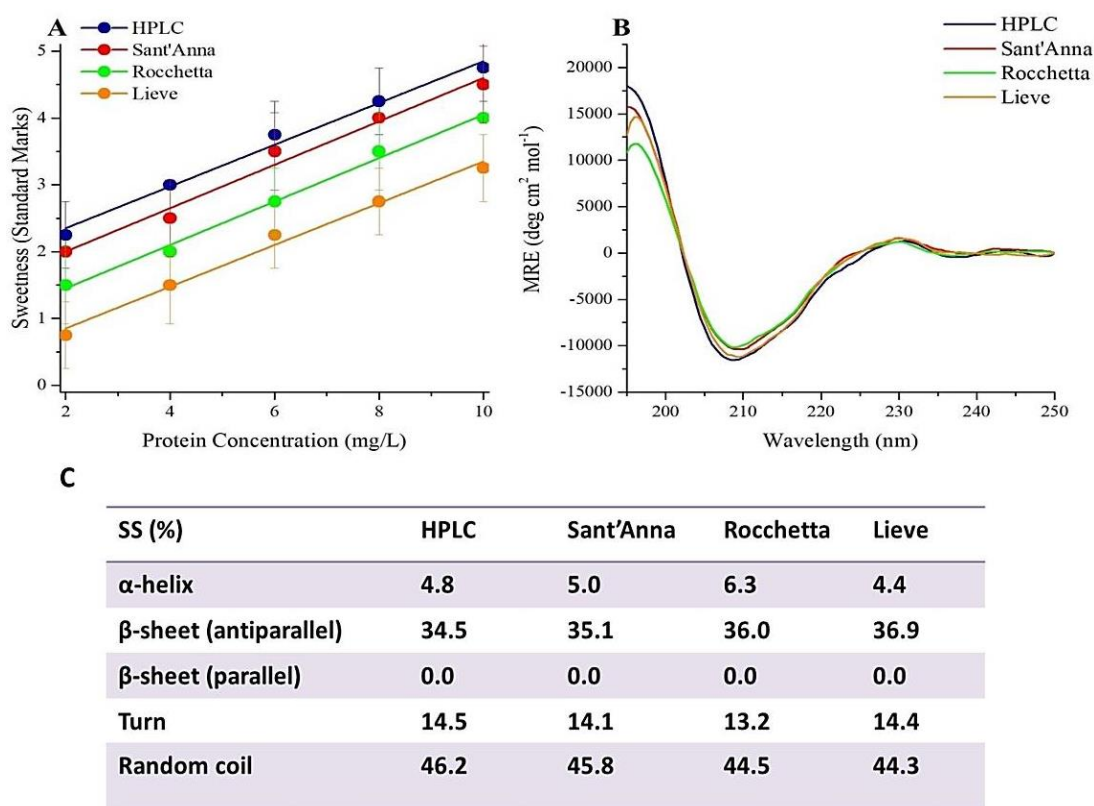
Figure 4. A) Sensory analysis of Thaumatin at 2, 4, 6, 8 and 10 mg/L in 4 commercial waters: blue) HPLC grade, red) Sant'Anna, green) Rocchetta and orange) Lieve. B) The secondary structure of Thaumatin at 10 mg/L in 4 commercial waters: blue) HPLC grade, red) Sant'Anna, green) Rocchetta and orange) Lieve. C) A table presenting the secondary structure contents of Thaumatin in different commercial waters by spectral deconvolution [74].

4.3.5 Sensory analysis on MNEI and Thaumatin at increasing NaCl concentrations

Our study of water effects on the sweetness of MNEI, Mut3, Mut9 and Thaumatin confirmed that ionic content of mineral waters can have a profound influence on sweetness potency. As a further control, we dissolved MNEI and Thaumatin in HPLC water in which we had previously added different amounts of NaCl in order to reproduce the ionic strength of the commercial mineral waters (**Table 1**). Remarkably, the sweetness trend was confirmed when we analysed the sweetness of the examined sweet proteins (**Fig. 5A** and **5B**). Interestingly, the sweetness intensities of MNEI and Thaumatin observed in different commercial waters (**Fig. 1A** and **4A**) were almost consistent with the data obtained after reproducing the ionic strength of the same waters by addition of NaCl to HPLC water (**Fig. 5A** and **5B**).
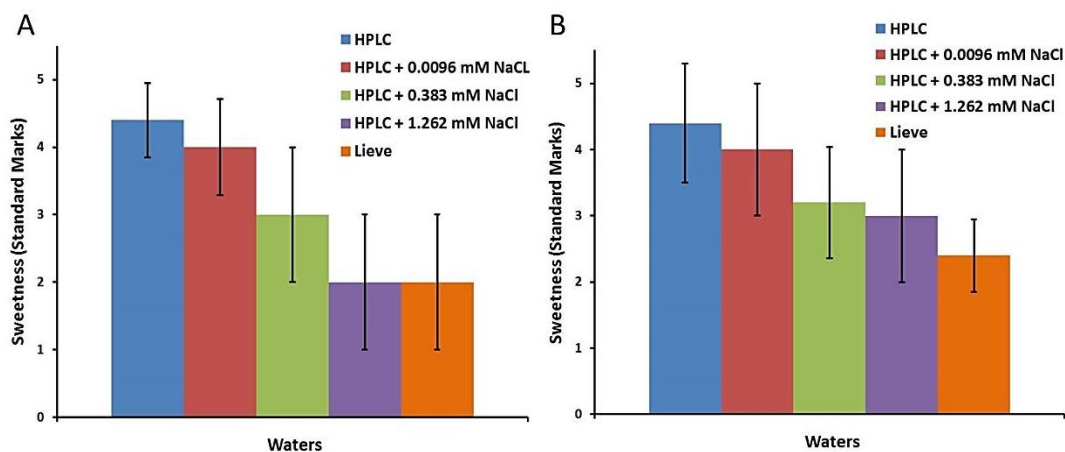

Figure 5. Sensory analysis performed on 10 mg/L samples of A) MNEI and B) Thaumatin when dissolved in HPLC water with increasing concentration of NaCl, calculated to match the commercial water conductivity.

4.3.6 NMR Spectroscopy on MNEI and Thaumatin

We also used NMR spectroscopy technique to detect possible structural changes of MNEI and Thaumatin in HPLC water (containing the least amount of mineral residues) and Lieve water (containing the highest amount of mineral residue). According to the CD spectroscopy data (**Fig. 4B** and **4C**), Thaumatin presented a very low structural sensitivity to the different commercial waters. These results were also confirmed by running ^{1}H-NMR spectroscopy (**Fig. 6A**). Indeed, the ^{1}H-NMR spectra in HPLC and Lieve waters are completely superimposable (**Fig. 6A**). Again, we performed the same control experiment on MNEI using 4 commercial waters: HPLC, Sant'Anna, Rocchetta and Lieve. As a result, some differences in the NMR spectra were noticed, but all the typical signatures of 2D and 3D structure (*i.e.* the amide protons signal dispersion, the β-sheet diagnostic signals between 5 and 6 ppm and the shielded signal below 0.5 ppm) were well evident (**Fig. 6B** and **6C**). These differences are not counted as significant structural alterations; therefore, we believe that the existence of various amounts of ionic strengths in waters did not affect the structures of the sweet proteins.
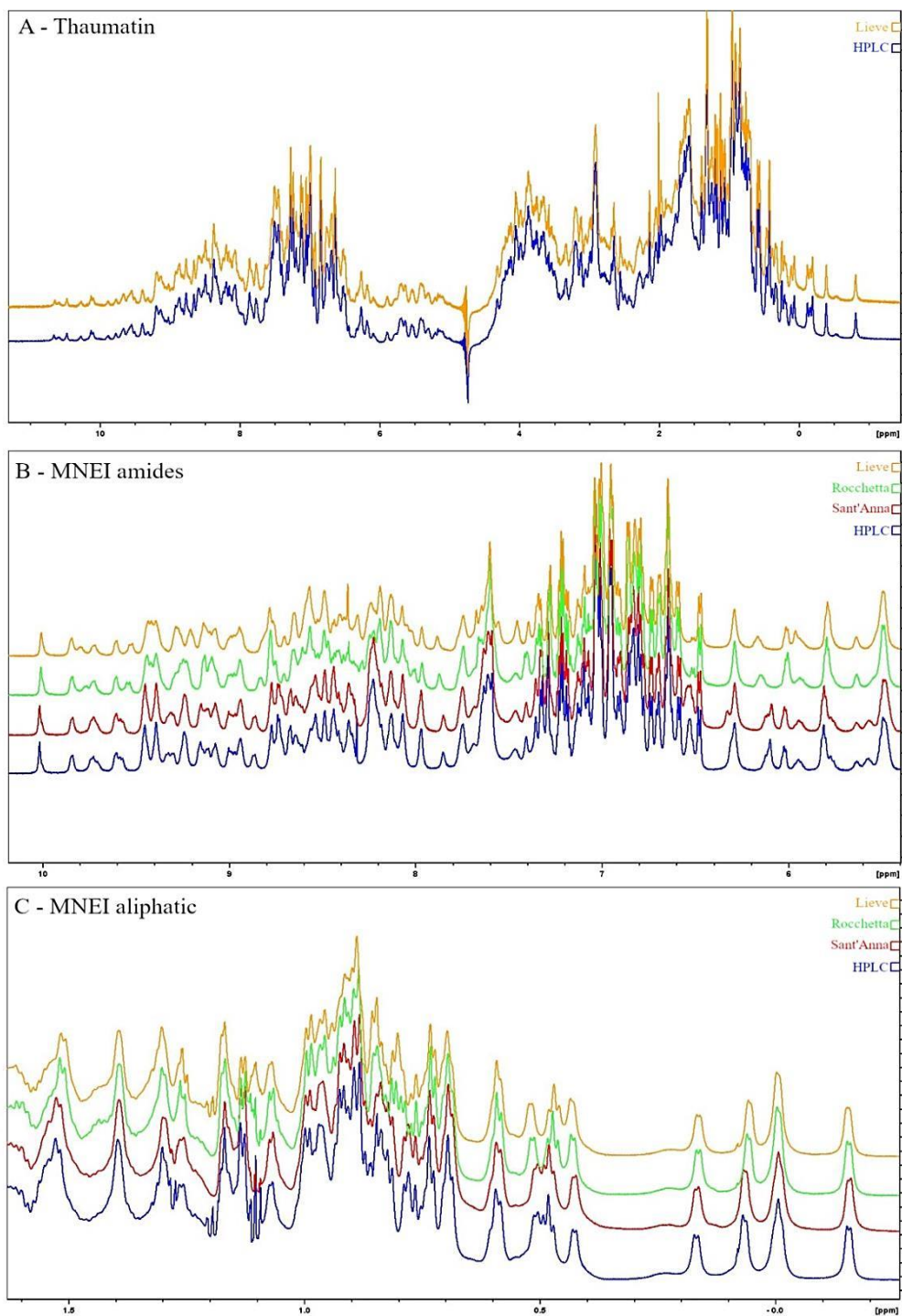
Figure 6. ^{1}H NMR spectra of 6 mg/ml Thaumatin samples in HPLC (blue line) and Lieve (orange line) waters (A). Amide (B) and aliphatic (C) regions of ^{1}H NMR spectra of 3 mg/ml MNEI samples in HPLC (blue line), Sant'Anna (red line), Rocchetta (green line) and Lieve (orange line) waters.

4.3.7 Sucrose

Sucrose is a commonly consumed low molecular weight sweetener in all types of food and beverage products worldwide. This is why, it was selected as a reference low molecular weight sweetener to investigate the effects of 4 various commercial waters *i.e.* HPLC grade, Sant'Anna, Rocchetta and Lieve on its sweetness intensity. These commercial waters were sweetened by equal amounts (40 g/L) of sucrose followed by running a blind sensory analysis on the drinking samples to determine the sweetness intensity. The concentration of sucrose was selected based on the previous sensory analysis studies reported at [157]. The sensory analysis data showed that the sweetness intensity of all prepared sucrose-based drinks resulted within the levels of sweet and very sweet (**Fig. 7**). There are, however, minor differences in the sweetness intensity of these samples, where the sweetness power slightly increased from HPLC grade water that includes the least mineral residues to Lieve with the highest amount of minerals (**Fig. 7**). These variations are not necessarily due to the real differences in the sweetness potency of the drinking samples; instead, they could be experimental errors resulted from the sensory analysis experiment.
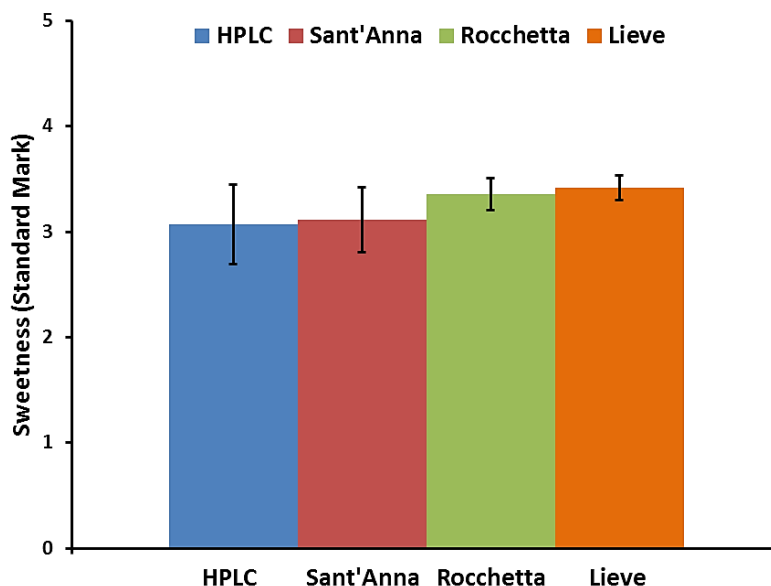
Figure 7. Sensory analysis of 40 g/L sucrose in 4 commercial waters: blue) HPLC grade, red) Sant'Anna, green) Rocchetta and orange) Lieve.

4.3.8 Sucralose

In this study, sucralose with the concentration of 67 mg/L was used as another low molecular weight sweetener to assess the influence of various commercial waters on the sweetness intensity of this type of sweeteners. The sucralose concentration was selected according to the equivalent sweetness intensity of 40 g/L sucrose (sucralose is ~ 600 times sweeter than sucrose). The data clearly indicated that the sweetness potency of sucralose was unaffected in different commercial types of waters that contain various amounts of mineral residues and conductivities. The sweetness intensity of all the samples was evaluated between the levels of sweet and very sweet (**Fig. 8**). Although sucralose was slightly less sweet in Sant'Anna water, however, this diversity is negligible and can fall in the experimental error range (**Fig. 8**).
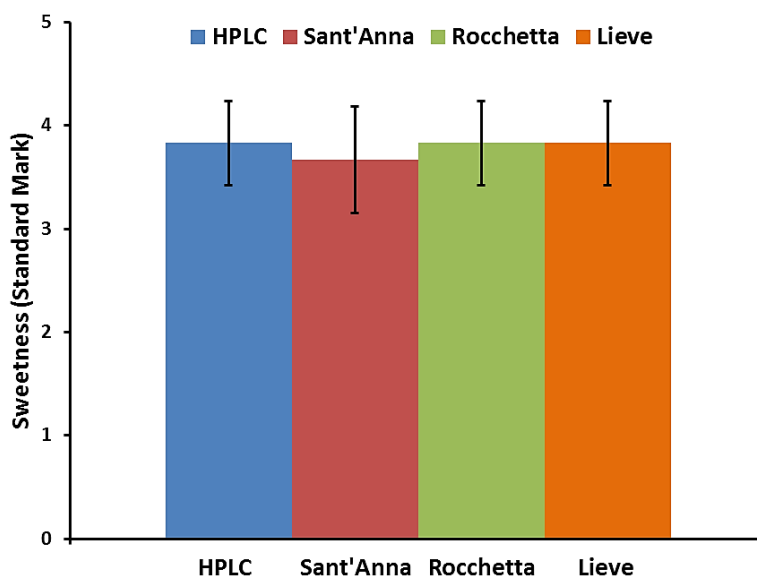
Figure 8. Sensory analysis of 67 mg/L sucralose in 4 commercial waters: blue) HPLC grade, red) Sant'Anna, green) Rocchetta and orange) Lieve.

4.3.9 Aspartame

Aspartame was also used to prepare sweet drinking solutions to evaluate the possible influence of different commercial waters on the sweetness intensity of a charged low molecular weight sweetener. In this sensory analysis, aspartame-based drinking samples with an equal concentration of 0.2 g/L were prepared. The reason for selecting this concentration for aspartame was to obtain the same sweetness intensity with respect to that of 40 g/L sucrose (aspartame is ~ 200 times sweeter than sucrose). According to the sensory analysis data of aspartame, all the drinking samples were tasted between sweet and very sweet levels (**Fig. 9**). In fact, using different types of waters did not affect the sweetness intensity of aspartame. Small differences in the sweetness intensity could be observed, however, these differences do not follow any trend *i.e.* the existence amount of mineral residues (**Fig. 9**). Therefore, the observed differences could be considered as experimental errors of sensory analysis.
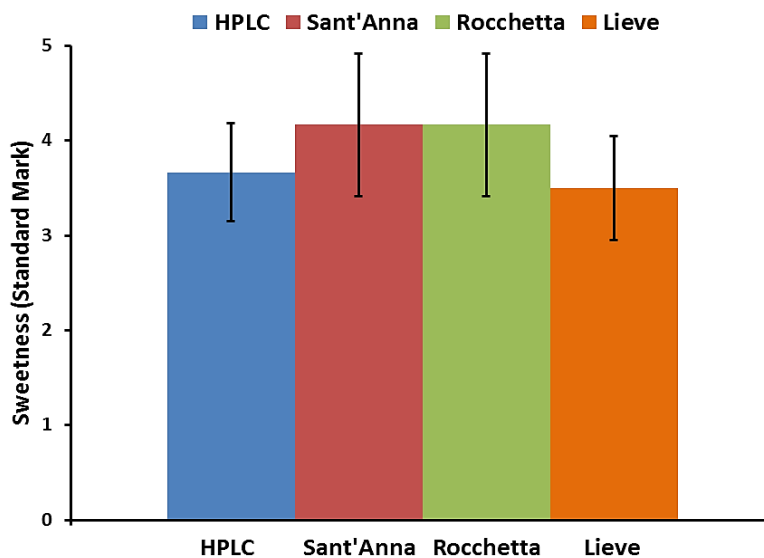
Figure 9. Sensory analysis of 0.2 g/L aspartame in 4 commercial waters: blue) HPLC grade, red) Sant'Anna, green) Rocchetta and orange) Lieve.

4.4 Conclusions

During preparing home-made beverages using sweet proteins, we ran into inequality issue in the sweetness intensity of this type of sweeteners upon different commercial waters. In this study, we used 4 sweet proteins including MNEI, Mut3, Mut9 and Thaumatin to prepare sweet drinking samples in 4 commercial waters with different mineral residue amounts. Then, the sweetness intensity of the proteins was analyzed by blind sensory analysis and the structure by CD and NMR spectroscopies. Also, low molecular weight sweeteners such as sucrose, sucralose and aspartame were used to prepare drinking samples in the same types of waters for control purposes. According to the outcome, all of the explored sweet proteins behaved similarly in terms of sensory analysis. Indeed, the sweetness intensities of the sweet proteins decreased noticeably from HPLC grade (the lowest mineral residues amount) to Lieve (the highest mineral residues amount). Diversely, only slight variations in the structures of the proteins could be detected, which are smaller than intrinsic

experimental errors (**Fig. 1**, **2**, **3**, **4** and **6**). In fact, the CD and NMR spectra of the sweet proteins were almost superimposable in different commercial waters. On the other hand, the sweetness potency of the drinking samples containing sucrose, sucralose and aspartame in various commercial waters was almost identical.

According to the wedge model, low molecular weight sweeteners occupy the orthosteric cavities of the Venus flytrap domain and activate the sweet taste receptor. On the other hand, sweet proteins bind to the external cleft between both subunits of the sweet taste receptor and activate it. The bindings between sweet proteins and the sweet taste receptors are relatively strong due to many specific electrostatic interactions between the positive charged residues of the sweet proteins from one side and the complementary negative charged residues located on the external surface of the receptor accepting the sweet proteins from the other side [24,26,27,52]. By considering the mechanism of action of sweet taste receptor in wedge model, we believe that the decrease in the sweetness intensity of sweet proteins is due to the presence of ionic mineral residues, which could hinder the proper protein-receptor bindings (**Fig. 10**). In the case of low molecular weight sweeteners, since there is a different mode of interaction with the receptor due to their small size, therefore, the binding activities between the sweet taste receptor and small molecular weight sweeteners including the charged ones remained undisturbed; and the sweetness power was unaffected in the presence of ionic compounds (**Fig. 7**, **8**, **9** and **10**).
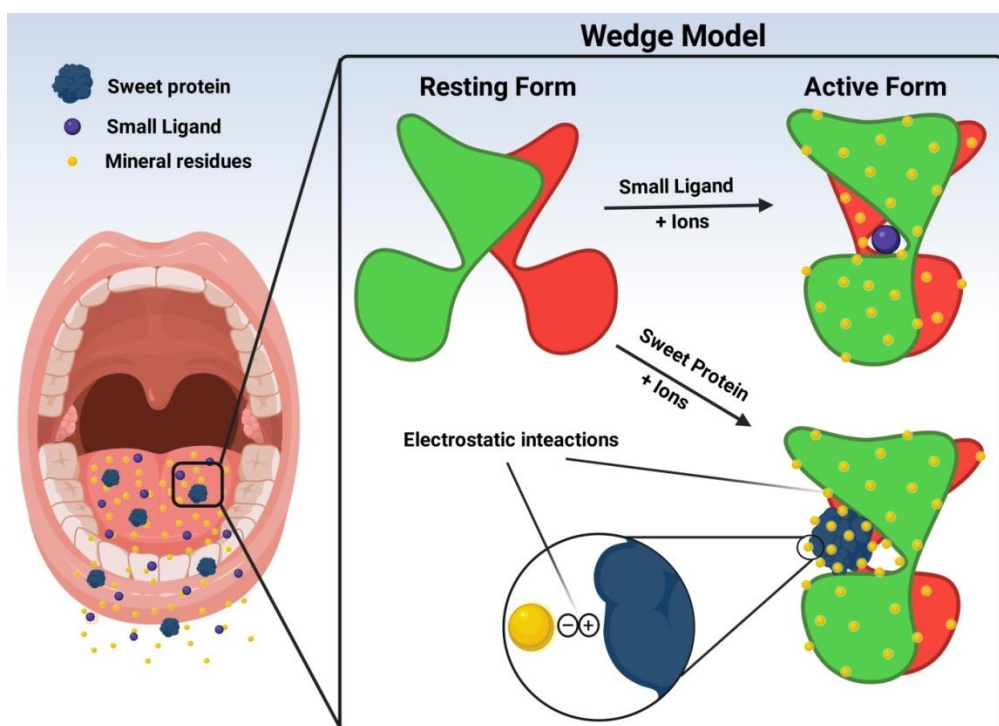
Figure 10. Schematic presentation of wedge model and the activation process of sweet taste receptor by low molecular weight sweeteners or sweet proteins in presence of ionic compounds.

CHAPTER <u>5</u>
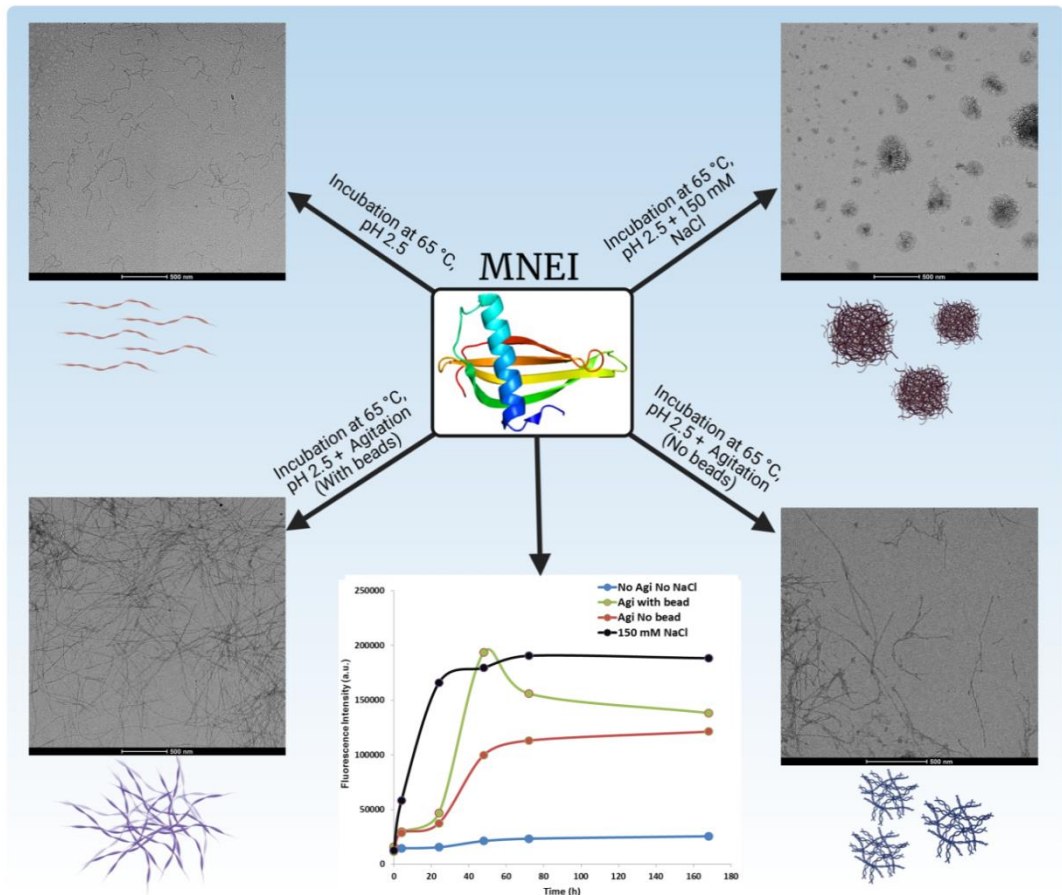
Aggregation study on MNEI

Abstract

The promising potential of single-chain Monellin, MNEI, as a sweetener in food industries is counterbalanced by its high aggregation propensity, which represents a drawback not only for the protein function, but also for the potential toxicity, associated to the amyloidogenic aggregation processes. In this study, we performed a careful investigation on the influence of some parameters such as temperature, intensive mechanical agitation, protein concentration and ionic strength on the aggregation kinetics and the mechanism of MNEI aggregation. These experimental parameters were selected to screen the protein's behavior when treated with possible stressing conditions during food processing or prolonged storage. Here, MNEI at pH 2.5 was incubated at 65 °C and subjected to an intensive mechanical agitation or addition of 150 mM NaCl. These two factors increased the aggregation kinetics of MNEI exponentially. Transmission electron microscopy confirmed the formation of protein fibrils with several micrometers length in both cases, although the morphologies of the formed fibrils were totally diverse. Moreover, conformational differences of the final aggregates obtained from MNEI solutions subjected to intensive mechanical agitation or addition of salt were clearly detected by FTIR. Further, MNEI soluble oligomers induced by mechanical agitation were observed by native PAGE, while no trace of soluble aggregates could be detected in the sample solution containing NaCl. In addition, the cytotoxicity data on MNEI aggregates showed that only soluble aggregates formed after 24 hours of incubation at 65 °C and under mechanical agitation (with and without PTFE beads) were toxic. These findings emphasized the possibility of controlling the aggregation process of MNEI through regulation of some physicochemical conditions that could increase the possibility to prevent the formation of toxic species.

5.1 Introduction

Over the past a few decades, spontaneous conversion of soluble proteins into soluble/insoluble aggregates with different morphologies was one of the most challenging issues in biology and medical sciences [158–160]. So far, much effort has been made to understand and probably control the factors associated in the formation of insoluble aggregates, known as amyloid fibrils. In the recent years, insoluble aggregates were extensively studied due to their correlation with over 30 diseases [161]. There are also a few diagnosed diseases which have been found that soluble aggregates, rather than amyloid fibrils, formed during very early stages of fibrillar aggregation played the determinant role in their establishment[162,163].

Amyloid-linked diseases are majorly established by the deposits of some specific variants of polypeptides. However, by looking closely to this type of polypeptides and other peptides or proteins, some common traits could be observed. For instance, in not so long time ago amyloidogenesis was thought to occur merely for a few proteins, but very recent data demonstrated that under certain conditions, a large number of soluble proteins undergo amyloidogenesis. Worthy of note, even some globular proteins *i.e.* muscle myoglobin and Monellin which are not involved in any protein-folding diseases and with totally diverse amino acid sequences, structures and functions could under specific physicochemical conditions *in vitro* convert into fibrillar aggregates with some structural properties that cannot be distinguished from those found in the amyloidosis [162,164,165].

The results of several studies indicated that Monellin and its single-chain derivatives possess high aggregation propensity [55–58]. This feature represents a drawback not only for the protein function, but also for the protein acceptance as food ingredient. Very recent data showed that some physicochemical conditions such as pH, temperature and ionic strength have a significant influence on the aggregation kinetics and the morphologies of the formed MNEI aggregates. As a matter of fact, formation of ordered or disordered aggregates, at a temperature close to T_m, can be

only controlled by pH regulation [58]. While, ionic strength has a significant effect on the kinetics of the aggregation process [78]. In this study, we investigated the effect of new experimental parameters such as different temperatures, intensive mechanical agitation with and without PTFE beads, protein concentration, different buffering compositions, extended pH and ionic strength on the aggregation kinetics and the morphologies of the formed aggregates. These incubational conditions were selected to monitor the behavior of MNEI in various conditions to which the protein could be exposed during storage, transport or food processing.

5.2 Materials and Methods

5.2.1 Protein expression and purification

The recombinant protein, MNEI, was produced as described in the Materials and Methods section of Chapter 1.

5.2.2 Thioflavin T (ThT) binding assay

Aliquots of MNEI incubated under different experimental conditions were withdrawn from the glass vials at different time points. A final protein concentration of 10 μM in 400 μL of solution was used for each measurement. Protein aliquots were diluted in 20 mM sodium phosphate buffer followed by addition of ThT with a final concentration of 30 μM. Fluorescence emission spectra were acquired in the range of 460-600 nm after excitation at 440 nm using a HORIBA Fluoromax spectrofluorimeter, with a scan speed of 100 nm/min. Excitation as well as emission slits were adjusted at 5 nm.

5.2.3 Transmission electron microscopy (TEM)

TEM images were obtained in bright field mode using a FEI Tecnai G2 200 kV transmission electron microscope with an accelerating voltage of 120 kV. Aliquots of MNEI at different time points were taken from each solution and diluted ten times with deionized water. A 3 µL drop was deposited on carbon coated copper TEM grid (200 mesh) for 2 minutes. Then, the excess solution was removed by gently touching the remaining portion of the drop using the edge of a filter paper sheet and air dried. Images were collected avoiding negative staining of the samples, therefore they were free from the artifacts that could arise, for instance, from uneven staining or dye crystallization. TEM analysis was performed on different regions of each specimen to check the uniformity of the morphology over the macroscopic area of the support and for independent samples. Average fibril thicknesses were calculated from the TEM images using ImageJ software (https://imagej.nih.gov/ij/). At least 200 independent measurements were taken at different locations of the TEM image.

5.2.4 Fourier-transform infrared (FTIR) spectroscopy

Conformational changes of MNEI were monitored by ATR-FTIR measurements as described [79,166,167]. Briefly, 2 µL of the samples were deposited on the single reflection diamond crystal of the ATR device (Quest, Specac, USA) and dried at room temperature in order to obtain a protein hydrated film. ATR-FTIR spectra were acquired on a Varian 670-IR spectrometer (Varian Australia Pty Ltd., Mulgrave VIC, Australia) under the following conditions: resolution of 2 cm^{-1}, scan speed of 25 kHz, 1000 scan coadditions nitrogen-cooled Mercury Cadmium Telluride detector. Spectra were smoothed using the Savitsky-Golay method before the second derivative analysis. Spectral collection and analysis were performed with the Resolution-Pro software (Varian Australia Pty Ltd., Mulgrave VIC, Australia).

5.2.5 Native gel electrophoresis analysis

MNEI at a concentration of 2.5 mg/mL was incubated at 65 °C under four different experimental conditions: control, agitation without bead, agitation with bead, and in presence of 150 mM NaCl. The pH of all conditions was adjusted to 2.5, by addition of sodium phosphate at pH 2.5 (20 mM final concentration). Identical aliquots (10 µg) of each sample were loaded on 10 % polyacrylamide gel under native conditions. This experiment was performed with the incubation interval of 24 hours for three days on the control and the agitated samples (with and without beads), and with the incubation interval of 1 hour for 5 hours on the sample including 150 mM NaCl.

5.2.6 Cell cultures and treatments

SH-SY5Y human neuroblastoma cells (ATCC# CRL-2266) were cultured in Eagle's Minimum Essential Medium (EMEM) supplemented with 10 % fetal bovine serum, 3.0 mM glutamine, 50 units/mL penicillin and 50 mg/mL streptomycin in a 5.0 % CO_2 humidified environment at 37 °C. For toxicity experiments, the cells were plated at a density of 200,000 cells/well in 24-well plates and, after 24 hours, cells were exposed to 30 µM protein samples for 24 hours. For FLIM experiments, the cells were plated at a density of 100,000 cells/well in a 35 mm glass-bottom dish (Ibidi). After 24 hours, cells were exposed to 30 µM protein samples for 24 hours and then incubated with 10 µM Bodipy FL 12 (ThermoFisher) in cell medium for 20 minutes. Before FLIM measurements, the cells were rinsed twice with phosphate buffer solution PBS and incubated with fresh cell medium.

5.2.7 Cell viability assay

Cell viability was assessed as the inhibition of the ability of cells to reduce MTT (Metabolic dye 3-[4,5-dimethylthiazol-2-yl]-2,5-diphenyltetrazolium bromide to a blue formazan product [168]. After incubation with MNEI samples, cells were rinsed with PBS. A stock solution of MTT (5 mg/mL in PBS) was diluted ten times

in cell medium and incubated with cells for 3 hours at 37 °C. After removing the medium, cells were treated with isopropyl alcohol, 0.1 M HCl for 20 minutes. Levels of reduced MTT were assayed by measuring the difference in absorbance between 570 and 690 nm. Data are expressed, as average percentage reduction of MTT with respect to the control ± S.D. Data are an average from five independent experiments carried out in triplicate. Statistical analysis was performed using Stata software (Version 13.0, StataCorp LP., College Station, TX, USA). Turkey's post hoc test was used if the treatment was significant on analysis of variance (ANOVA). All data are presented as the mean ± SE. Statistical significance was set at $p < 0.05$.

5.2.8 Fluorescence lifetime imaging microscopy (FLIM)

FLIM was performed on SH-SY5Y living cells using an ISS Alba frequency domain confocal FLIM microscope (ISS, Champaign, IL). The microscope optics included a $60\times$, N.A. = 1.2 water immersion objective mounted in a Nikon TE-2000 V inverted microscope. Excitation was from 468 nm diode laser amplitude modulated at 20, 40, 60, 80, 100 and 120 MHz and fluorescence emission was detected using TTL avalanche photodiodes. Confocal scanning optics was an ISS proprietary design. Regions of interest comprising about 500 pixels each within the images of twenty cells each in multiple fields at six frequencies were collected and analyzed. Pixel fits to the lifetime data were performed using the manufacturer software (Vista Vision 4.0). Calibration of Bodipy FL C12 was performed by measuring the fluorescence lifetime of different methanol/glycerol mixtures (0, 50, 60, 70, 80 and 90 % glycerol) with known viscosity [169,170].

5.3 Results and Discussion

5.3.1 ThT binding assay

Thioflavin T (ThT) is a very common and feasible assay to study the *in vitro* amyloid fibril formation. ThT, upon binding to amyloid fibrils, displays a dramatic fluorescence rise from 445 to 482 nm when excited in the range of 385 to 450 nm [171]. The strong shift of fluorescence occurs due to the rotational immobilization of the central C-C bond of ThT which connect benzothiazole ring to aniline ring [172–174]. Although, there are different structural models of amyloid fibrils, however, it is strongly suggested that ThT binds to a common structural features among amyloid fibrils. Since amyloid fibrils are formed from parallel or anti-parallel alignments of β-strands, therefore, they share the cross-β architecture that is most probably the target of ThT-binding [175]. Here, we used ThT binding assay to evaluate the influence of some parameters such as temperature, intensive mechanical agitation with and without PTFE beads, protein concentration, pH, different buffers and ionic strength on the aggregation kinetics of MNEI.

Earlier data demonstrated that MNEI produced fibrillar aggregates upon incubation at acidic pH and controlled temperature (60 °C). Fibrillization process of MNEI could be also accelerated by elevating the temperature to a little below the protein melting temperature (T_m = 73 °C, at pH 2.5) [58]. Furthermore, fibrillar aggregation of MNEI can be significantly fastened at increasing concentration of NaCl [79]. Worth mentioning, mechanical agitation is another parameter that is reported to increase fibrillar growth of some peptides and proteins [176–178]. Although the precise mechanism of peptides and proteins fibrillar aggregation induced by controlled mechanical agitation is an obscure procedure up to date, however, it is hypothesized that increase in collisions of monomeric and oligomeric species with the both ends of already formed fibrils or fragmentations result in fibrillar growth [179]. Moreover, enhance in the air-water interface through agitation that can simulate the hydrophobic surface is assumed to elevate the fibrillation rate [180]. In this study, the aggregation study of MNEI was begun by a prolonged incubation (up to 3 months) of the protein at 37 °C (to simulate the accelerated shelf-life conditions). In addition to explore the influence of temperature on the aggregation

kinetics of MNEI, we also investigated the effects of pH and mechanical agitation by running an extended experiment. In this experiment, samples of MNEI at pH 2.5, 5.0 and 6.8 were incubated with and without mechanical agitation. The protein concentration for all the samples was adjusted on 2.5 mg/mL. The obtained results indicate that temperature played the determinant role in the aggregation process of MNEI, since at a low temperature (37 °C), the protein did not aggregate upon incubation for 3 months (**Fig. 1**). These observations did not change even after introducing mechanical agitation. In spite of the fact that MNEI is known to have high aggregation propensity at neutral pH, however, incubation at 37 °C and pH 6.8 did not lead to aggregate formation (**Fig. 1**). Small growth in the florescence intensity of the protein at pH 6.8 could be detected, but it cannot be counted for protein aggregation.
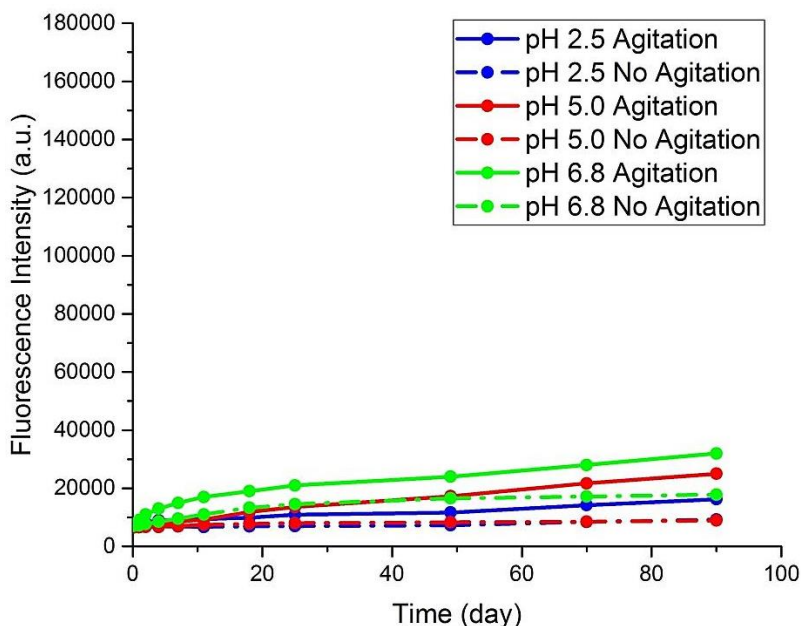

Figure 1. Time course of the ThT binding assay of MNEI incubated under mechanical agitation at 37 °C, protein concentration of 2.5 mg/mL and pH 2.5, 5.1 and 6.8. Fluorescence values were recorded at 485 nm at the indicated times. The symbols and color codes of the curves are reported on the inset.

The effect of temperature on the aggregation process of MNEI was further checked by increasing the temperature to 65 °C. MNEI at pH 2.5 with the concentration of 2.5 mg/mL was incubated under intensive mechanical agitation at 250 rpm on an orbital shaker (VWR 3500 orbital shaker) with or without poly(tetrafluoroethylene) (PTFE) beads (Sigma, 1 bead every 500 µL of solution). According to the results, intensive mechanical agitation in presence or absence of PTFE beads significantly increased the aggregation process (**Fig. 2**). In the case of using PTFE beads, the fluorescence intensity reached a peak after 48 hours of incubation and slightly decreased for the rest of the incubation time. Whereas, for MNEI agitated without PTFE beads, the fluorescence intensity reached a plateau after 2 days of incubation without experiencing any decrease in the intensity (**Fig. 2**). On the other hand, the fluorescence intensity of MNEI under static condition remained almost constant over 1 week incubation. Only a very slight increase in the intensity could be observe after 48 hours of incubation, which we believe this slight increase in the fluorescence intensity cannot be associated with any aggregate formation (**Fig. 2**).
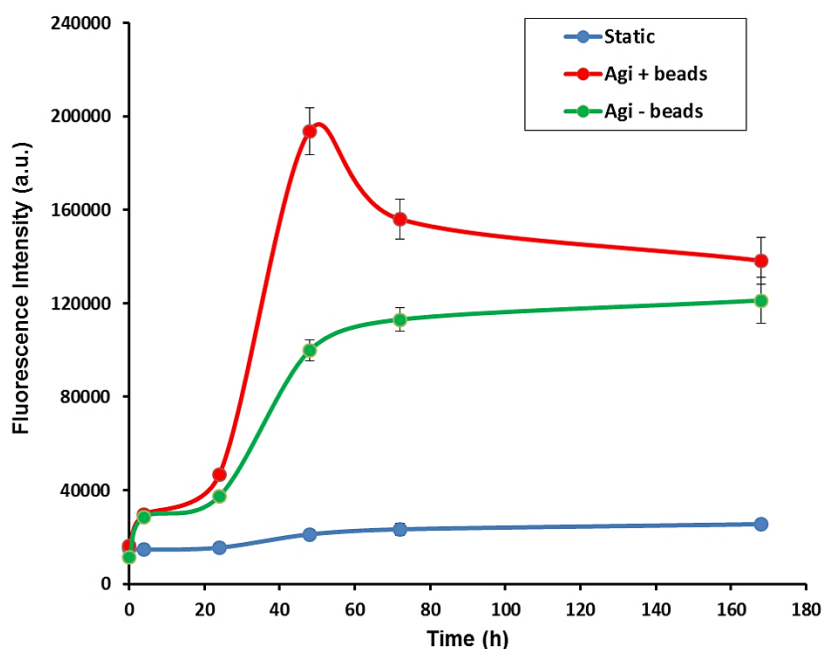
Figure 2. Time course of the ThT binding assay of MNEI incubated at 65 °C, protein concentration of 2.5 mg/mL and pH 2.5. Fluorescence values were recorded at 485 nm at the indicated times. The symbols and color codes of the curves are reported on the inset. This figure is adapted from [59].

To extend the aggregation study, MNEI with different protein concentrations in the range of 0.5 – 5.0 mg/mL were incubated at 65 °C upon strong and mild acidic pH. The graphs (**Fig. 3A** and **3B**) demonstrated that protein concentration had a big impact on the kinetics of aggregation process of MNEI at strong and slightly acidic pH. In fact, it is evident that by increasing protein concentration the fluorescence intensity grows exponentially; it can be a sign of fast aggregate formation (**Fig. 3A** and **3B**). The only observable difference among these two graphs is the aggregation kinetics of MNEI at pH 5.5 (**Fig. 3B**), which was a little higher than that of MNEI at pH 2.5 (**Fig. 3B**) in the early stages of aggregation process.
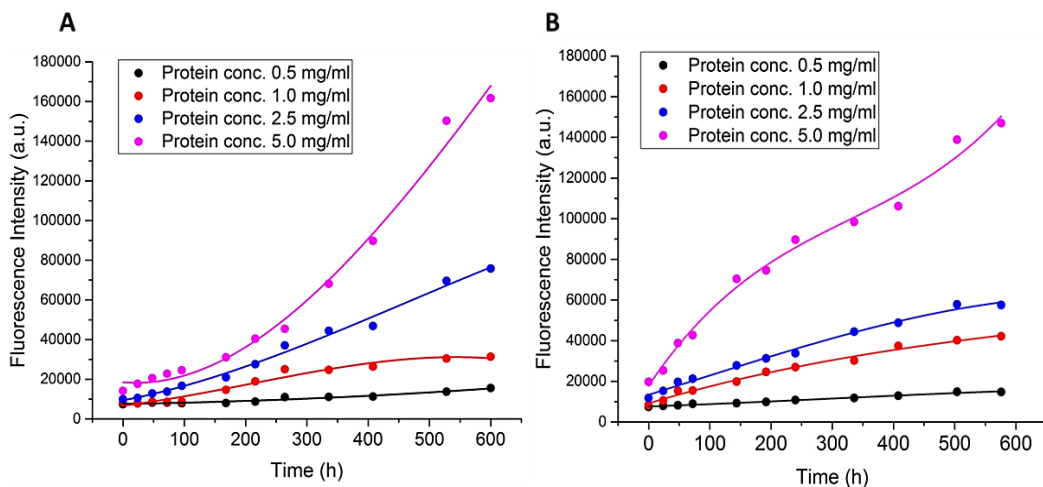
Figure 3. Time course of the ThT fluorescence binding assays of MNEI incubated at 65 °C, and pH A) 2.5, B) 5.5. Fluorescence values were recorded at 485 nm for different protein concentrations as indicated on the insets.

The influence of different salts with a wide range of concentration on the aggregation procedure of MNEI have been thoroughly discussed before [78]. A new experiment was designed to screen the behavior of MNEI with the same protein concentration (2.5 mg/mL) upon incubation at 65 °C, in two different buffering solutions (sodium phosphate and sodium acetate) with a pH value of 5.0 and in presence of 150 mM NaCl. The obtained results indicate that the fluorescence intensity of both buffering solutions increased significantly in the presence of salt (**Fig. 4A**). In more detail, both buffering solutions containing NaCl reached a plateau after six days of incubation, while no considerable rise in the fluorescence intensity could be observed for the samples prepared without any addition of salt even after two weeks of incubation. Moreover, the explored buffers displayed a similar behavior after monitoring the aggregation process of MNEI (**Fig. 4A**). In addition, MNEI solutions with the same protein concentration (2.5 mg/mL) including 150 mM NaCl were incubated at two various temperatures 65 °C and 37 °C to examine the influence of incubational temperature on the aggregation process.

The outcome clearly evidenced that the incubational temperature had a striking impact on the aggregation procedure of MNEI. In the case of MNEI incubated at 65 °C, the fluorescence intensity reached a plateau after only 48 hours of incubation, whereas MNEI at 37 °C did not aggregate upon incubating over 1 week (**Fig. 4B**).
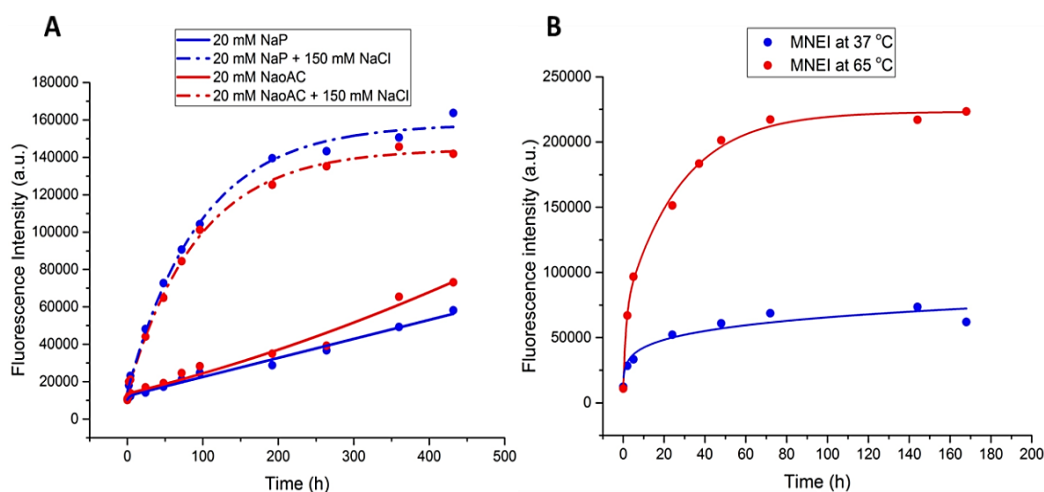

Figure 4. Time course of the ThT fluorescence binding assay of 2.5 mg/mL MNEI incubated at A) 20 mM NaP or 20 mM NaOAc pH 5.0, with and without 150 mM NaCl and T= 65 °C; and B) 20 mM NaP pH 2.5, T= 65 or 37 °C and 150 mM NaCl. Fluorescence values were recorded at 485 nm. The symbols and color codes of the curves are reported on the inset.

5.3.2 Transmission Electron Microscopy (TEM)

Transmission electron microscopy (TEM) was used to monitor the resulting morphology of the formed aggregates after MNEI incubation at some newly selected physicochemical conditions with higher influence on the aggregation process of MNEI. TEM images of MNEI's aggregates found in static conditions (without NaCl and agitation), with 150 mM NaCl, agitation without and with PTFE beads. Samples of MNEI at pH 2.5 with the concentration of 2.5 mg/mL were incubated at 65 °C up to 1 week. According to TEM images, MNEI after 1 week of incubation in static conditions resulted in the formation of short and bent fibrils with a length of 100 –

200 nm and a width of 9 nm (**Fig. 5A**). While in the presence of 150 mM NaCl, very dense nest-shape conglomerates fibrils with the length of 70 – 200 nm and thickness of ~ 8 nm were detected after 24 hours of incubation (**Fig. 5B**). In the case of MNEI agitated with PTFE beads, long fibrils formed by one (7 ± 1 nm), two (14 ± 3 nm) or three filaments (22 ± 3 nm) were observed after 7 days (**Fig. 5D**). On the other hand, the sample agitated without any beads produced twisted fibrils with an average thickness of 11 ± 2 nm and a periodicity of 44 ± 4 nm (**Fig. 5C**). The collected results indicated that NaCl and mechanical agitation greatly uplifted the aggregation kinetics of MNEI.
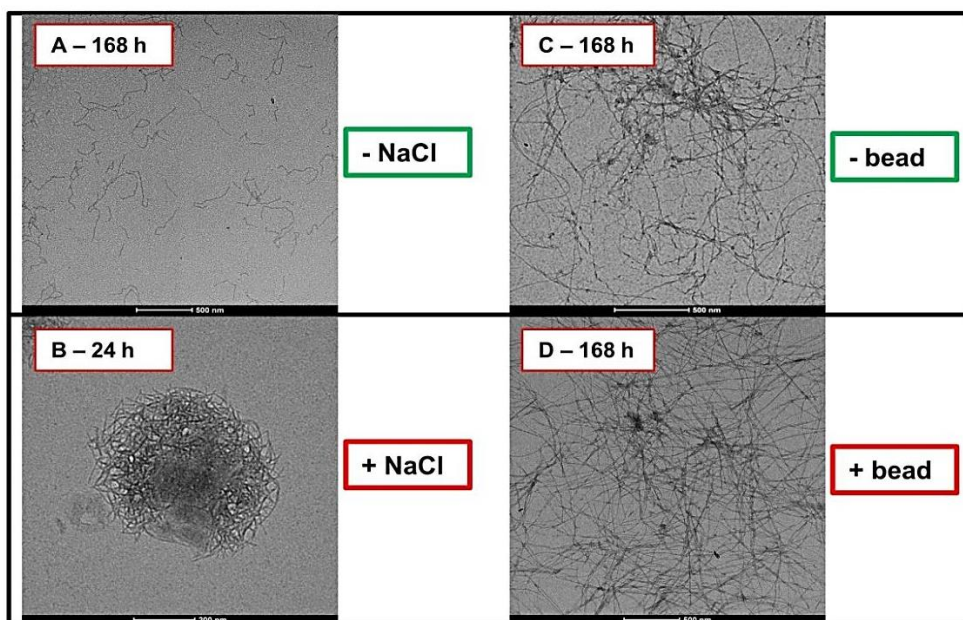
**Figure 5**. Transmission electron microscopy images of MNEI. Samples of 2.5 mg/mL MNEI incubated in 20 mM sodium phosphate buffer at pH 2.5 and 65 °C. The samples are incubated in: (A) static, (B) presence of 150 mM NaCl, (C) agitation without PTFE beads, and (D) agitation with beads. The samples were deposited on carbon-coated copper TEM grids and observed without any staining procedure. Several regions of the grids were

analyzed to ensure the uniformity of samples and two independent experiments were performed for each condition. This figure is adapted with permission from [79].

5.3.3 Fourier-transform infrared (FTIR) spectroscopy

To detect possible changes in the protein secondary structure after incubation of the protein under different physicochemical conditions we used Fourier transform infrared (FTIR) spectroscopy in attenuated total reflection (ATR). This experiment was performed with the collaboration of Professor Antonino Natalello's research group, Department of Biotechnology and Biosciences of the University of Milano-Bicocca, Milan, Italy. Previously we observed that upon fibril formation in the presence or absence of NaCl, distinct and characteristic spectral features could be detected for the monomeric and aggregated forms [181]. Here, 2.5 mg/mL MNEI at pH 2.5 was incubated at 65 °C up to 1 week and aliquots from the samples solutions were withdrawn and analyzed by FTIR at various time points. Under native conditions, the second derivatives of MNEI absorption spectra displayed (in the Amide I band), three main negative peaks, which can be assigned to the protein secondary structures as follow: ~1691 cm^{-1} and ~1635 cm^{-1} to β-sheets and ~1659 cm^{-1} to α-helix (**Fig. 6**, 0 h) [181]. For the sample including 150 mM NaCl, decrease in the peaks were noticed after 24 hours of the incubation, which are most likely due to the α-helix and native β-sheets and the concomitant appearance of the IR signatures of intermolecular β-sheets (peak at ~1695 cm^{-1} and ~1621 cm^{-1}) (**Fig. 6**). In the agitated samples, a progressive down shift of the peak position of the native β-sheets from 1635 cm^{-1} to about 1627 cm^{-1} were observed after 1 week of incubation (**Fig. 6**). At 24 hours of incubation, the down shift of the native β-sheet peak and the increase in intensity of the peak at ~1615 cm^{-1} were more evident in the agitated sample in the presence of PTFE beads with respect to the sample agitated without beads. At this incubation time (24 hours), the main β-sheet component in the agitated solutions displayed an intermediate peak positioned between the peak of native MNEI (~1635 cm^{-1}) and the peak of the final aggregates (~1627 cm^{-1}).

However, the protein in the presence of 150 mM NaCl was characterized by remarkable different spectral features: a higher intensity of the ~1695 cm^{-1} peak and a main β-sheet component at ~1621 cm^{-1} (**Fig. 6**, 24 hours). These differences were also observed upon longer incubation times. From literature data, peaks in the 1627–1615 cm^{-1} spectral region can be assigned to the β-sheet structures of the protein aggregates [167,181,182]. Noteworthy, the protein aggregates obtained at the end of incubation from various experimental conditions displayed marked features (**Fig. 6**, 1 Week and pellet). The aggregates formed in the agitated samples showed two β-sheet components in the low-wavenumbers range, the peak with higher intensity is at 1615 cm^{-1} for the sample agitated with PTFE beads. Moreover, these aggregates displayed a peak at about 1661 cm^{-1} that could not be detected in the protein solution containing 150 mM of NaCl. The peak at ~1661 cm^{-1} cannot be assigned unequivocally, since it can be due to the existence of turns, loops and/or α-helices in the protein structure.
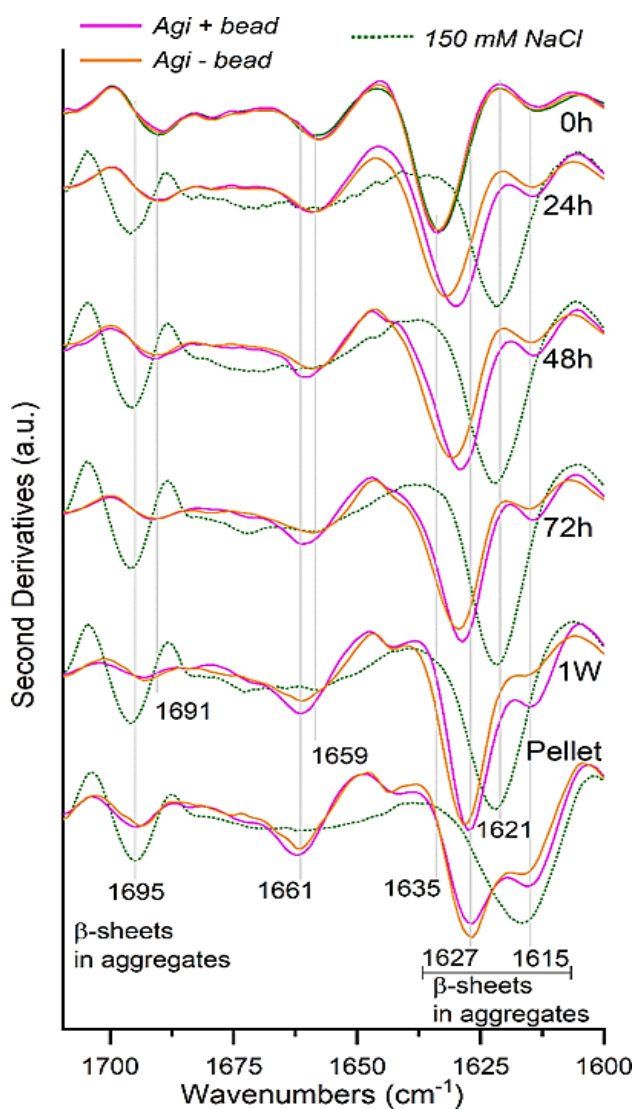
Figure 6. Time course of MNEI aggregation process studied by ATR-FTIR spectroscopy. Second derivatives of the absorption spectra of 2.5 mg/mL MNEI at different times of incubation at pH 2.5 and 65 °C, up to 1 week (1 W), in agitation with (magenta) or without PTFE bead (orange) or under static conditions with 150 mM NaCl (green). The second derivatives of the absorption spectra of the pellet obtained by centrifugation of the samples after 1 week incubation are also reported. The wavenumbers of the main peaks and their assignment to β-sheet structures in protein aggregates are indicated. This figure is reprinted from [59].

5.3.4 Native gel electrophoresis analysis

The different morphologies of MNEI fibrils obtained at acidic pH could be the result of alternative aggregation mechanisms, possibly involving different intermediates in solutions *i.e.* at diverse stages of unfolding and/or oligomerization. To explore this hypothesis, we examined the population of soluble species during the early stages of MNEI aggregation process by native acidic PAGE (**Fig. 7**). This experiment was performed on 2.5 mg/mL MNEI solutions at pH 2.5 incubated at 65 °C and in the presence or absence of 150 mM NaCl. Protein samples were analyzed within the first 5 hours of incubation. The native PAGE gel in in **Figure 7A** showed that in the free-salt sample, the protein remained soluble and a small amount (~ 5 %) of dimer was always observed during 5 hours of incubation. On the other hand, upon MNEI incubation with 150 mM NaCl, the dimeric band of the protein quickly disappeared from the solution (**Fig. 7B**). In parallel, the intensity of the monomeric band of MNEI decreased, indicating fast aggregation and/or precipitation. This suggests that while the aggregation kinetics of the protein in the presence of NaCl is significantly faster than that of free-salt sample, it is more likely involves the monomeric protein in solution only, as soluble dimers or higher multimers could not be detected even shortly after the beginning of the incubation.
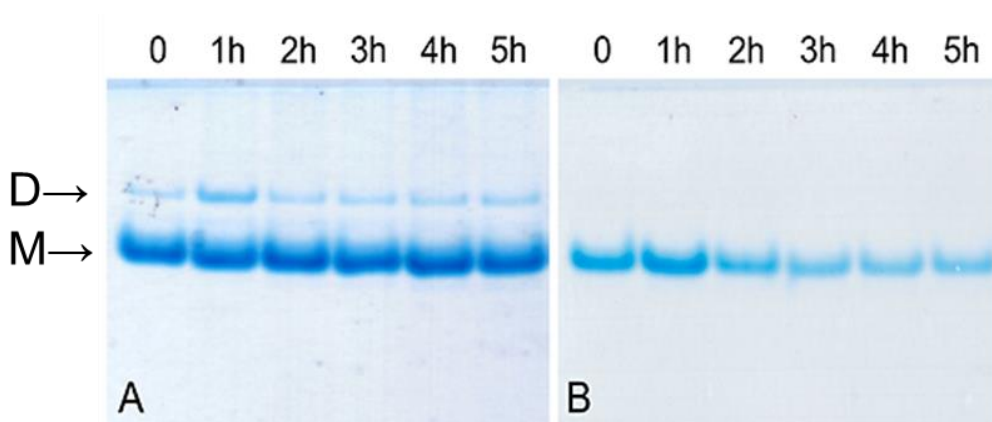
Figure 7. Native acidic PAGE of 2.5 mg/mL MNEI incubated at pH 2.5 and 65 °C (A) without or (B) with 150 mM NaCl. The samples loaded on the gels were withdrawn from MNEI solutions at the early time points of incubation. In each lane, 10 µg of sample was loaded. This figure is adapted with permission from [79].

The native gel electrophoresis analysis was also performed on MNEI subjected to an extensive mechanical agitation with and without PTFE beads for 3 days with an interval of 24 hours (**Fig. 8**). The Results illustrated that mechanical agitation promoted the formation of soluble oligomers (O1 and O2) after 24 hours of incubation. Although, the amount of oligomer 1 is very little in a way that barely can be detected by naked eyes (**Fig. 8A**). Noteworthy, the formed oligomers (O1 and O2) were not observed either under static conditions or in the samples including 150 mM NaCl, at least within the analyzed incubation time (**Fig. 7A** and 7**B**). Furthermore, dimeric form of MNEI could be detected only in the agitated samples after 24 hours of incubation (**Fig. 8A**). The amount of monomers, dimers and oligomers (O1 and O2) diminished upon longer incubation time (48 h) (**Fig. 8B**). This is most likely due to the accelerated aggregation process of MNEI under mechanical agitation. Important to mention, there is always ~ 5 % of oligomer 2 could be detected in the agitated samples regardless of presence of beads (**Fig. 8A, 8B and 8C**).
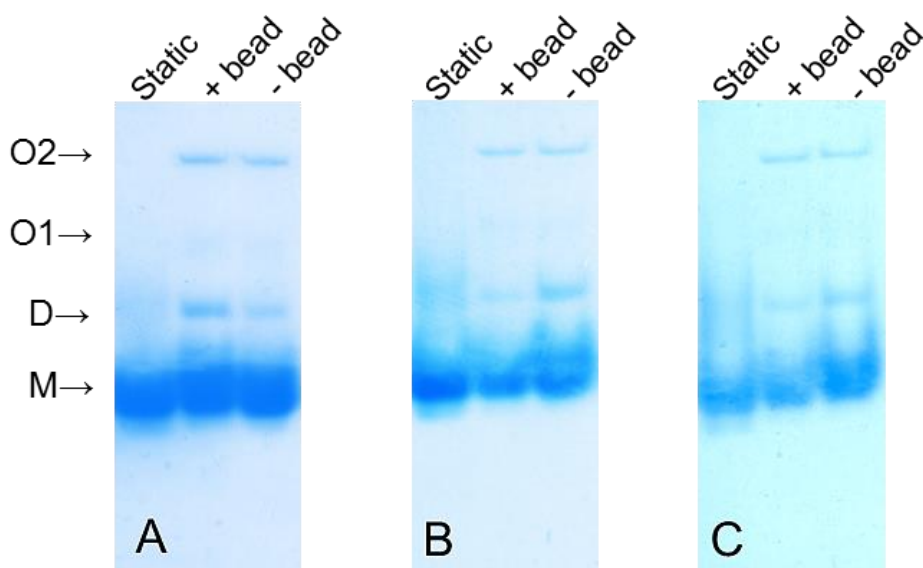
Figure 8. Native PAGE of MNEI soluble species loaded after (A) 24 h, (B) 48 h and (C) 72 h of incubation. MNEI with the concentration of 2.5 mg/mL was incubated at pH 2.5 and 65 °C under static condition or intensive mechanical agitation with and without PTFE beads. Monomeric protein (M), dimers (D) and at least two kinds of different oligomers (O1 and O2) are visible depending on the incubation conditions. In each lane, 10 µg of sample was loaded. This figure is adapted from [59].

5.3.5 Cell viability assay

In order to investigate the cytotoxicity status of different structural/morphological MNEI species formed in various aggregation conditions, we evaluated the cell viability of cultured human neuroblastoma SH-SY5Y cells by the MTT assay, which measures the cellular metabolic activity. This experiment was performed with the collaboration of Professor Clara Iannuzzi's research group, Department of Precision Medicine of the University of Campania "L. Vanvitelli", Naples, Italy. MTT assay showed that amyloid cytotoxicity could be also induced by early formed oligomeric aggregates [183,184]. Amyloid fibrils are often harmless, although examples of cytotoxic amyloid fibrils are available *i.e.* in the case of α-syn fibrillar aggregates

that the fibrils were found to bind and permeabilize cell membranes [185]. Also it is known that not all prefibrillar aggregates cause cytotoxicity, and the toxicity is a result of several features, including their size and hydrophobicity [186–188]. To this aim, the cells were exposed for 24 hours to 30 μM MNEI at pH 2.5 incubated for 24, 48 and 72 hours at 65 °C in different aggregation conditions *i.e.* static, agitation without beads, agitation with PTFE beads and with 150 mM NaCl. Interestingly, only MNEI samples incubated for 24 hours under agitation (with and without PTFE beads) reduced the cell viability by approximately 40 % with respect to the untreated cells. Unexpectedly, MNEI fibrils formed in the presence of 150 mM NaCl were almost harmless, since only about 10 % cell death could be detected, which is far from known toxicity limit (more than 40 %). Moreover, no toxicity was observed for all of the samples after 48, 72 hours or one week of incubation under the explored conditions. Thus, these results suggest that at these time points the formation of ultrastructured fibrils were not able to affect the cell viability (**Fig. 9**). Notably, analysis of the soluble fractions by native PAGE (**Fig. 8A, 8B, and 8C**) proved that mechanical agitation promoted the formation of soluble oligomers (O1 and O2), which were detectable neither in the static conditions nor in the sample containing NaCl. Either of these aggregates could be responsible for the observed cytotoxic effects. Of note, MNEI incubated at static condition, in acidic environment and temperature of 65 °C did not result in any toxicity during 1 week incubation, deduced from less than 10 % cell death (**Fig. 9**).
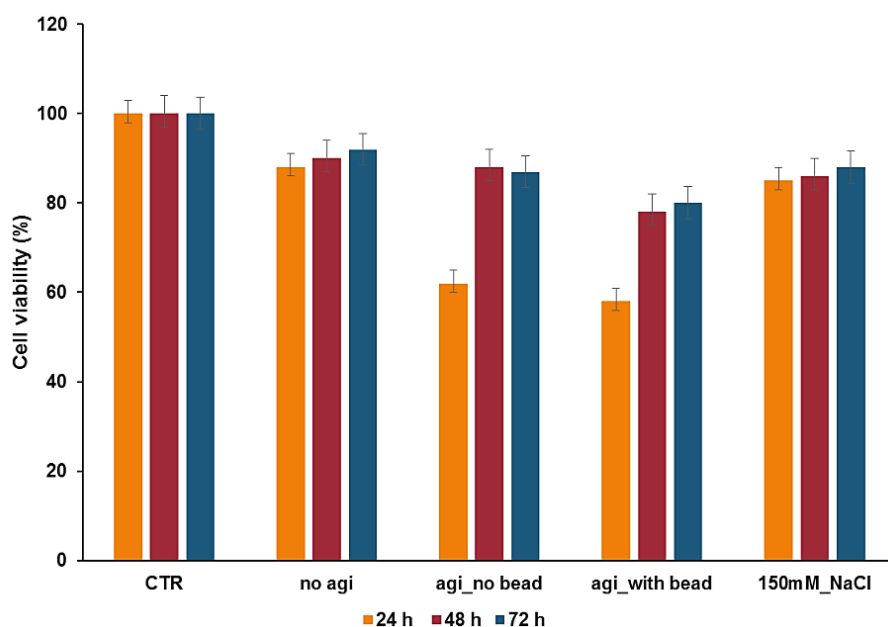
Figure 9. Cytotoxicity of MNEI aggregates formed at pH 2.5 and 65 °C in different conditions: no agitation (Static), agitation_no bead (− bead), agitation_with bead (+ bead) and 150 mM NaCl (+ NaCl). SH-SY5Y human neuroblastoma cells were exposed for 24 hours to 30 μM MNEI incubated for 24, 48 and 72 hours in aggregating conditions and the cell viability was evaluated by the MTT assay. Control represents untreated cells. Other experimental details are described in the Methods section. This figure is reprinted from [59].

5.3.6 Fluorescence Lifetime Imaging Microscopy (FLIM)

In order to understand whether the cytotoxicity was mediated by a direct interaction of the protein aggregates with the cell membrane or not, we monitored the ability of MNEI incubated under different conditions to induce perturbation on cell membrane. To this aim, Fluorescence Lifetime Imaging Microscopy (FLIM) was performed to map the cell membrane viscosity in SH-SY5Y human neuroblastoma cells exposed to MNEI aggregates as this is strictly related to cell dysfunction in amyloid toxicity [189,190]. This experiment was also carried out with the collaboration of Professor Clara Iannuzzi's research group. In particular, FLIM was

used to estimate the fluorescence lifetime of the molecular rotor 4,4-difluoro- 5,7-dimethyl-4-bora-3a,4a-diaza-s-indacene-3-dodecanoic acid (Bodipy FL C12) in cells exposed for 24 hours to MNEI samples, the same protein samples that were already incubated for 24 hours in different experimental conditions (**Fig. 10**). Bodipy FL C12 is a dye widely used to monitor membrane perturbation as its fluorescence lifetime is directly related to the membrane viscosity *i.e.* shorter lifetimes are associated to a low membrane viscosity while longer lifetimes suggest a higher membrane viscosity [169,170,191,192]. Following the calibration of the fluorescence lifetime of Bodipy FL C12 as a function of viscosity in methanol/glycerol mixtures, we performed FLIM to map the spatial variations of viscosity in cells. Upon incubation of living cells with the probe, a punctate dye distribution was observed in the fluorescence images and this is consistent with previously reported data [170,193]. Mapping the fluorescence lifetime is independent of the fluorescence intensity, thus allowing the separation of probe concentration and viscosity effects. In the color-coded images for mean lifetime, the average lifetimes appeared shorter for SH-SY5Y cells treated with MNEI incubated in agitation (around 1.8 ns) compared to those treated with the protein incubated without agitation (around 2.6 ns) and with 150 mM NaCl (around 2.4 ns). These data suggested that only MNEI aggregates formed at pH 2.5, and 65 °C under intensive mechanical agitation for 24 h (both: with and without PTFE beads) induced cell membrane perturbation, strongly reducing the membrane viscosity (**Fig. 10C and 10D**). Indeed, no strong variation of membrane viscosity was observed for MNEI incubated at pH 2.5, 65 °C and under static condition and the other sample that includes sodium chloride (**Fig. 10B and 10E**). Overall, the obtained results demonstrated that MNEI fibrillar self-assembly in the agitated conditions occurred by formation of soluble aggregates that were able to directly interact with the cell membrane and induce a strong perturbation, affecting cell viability.
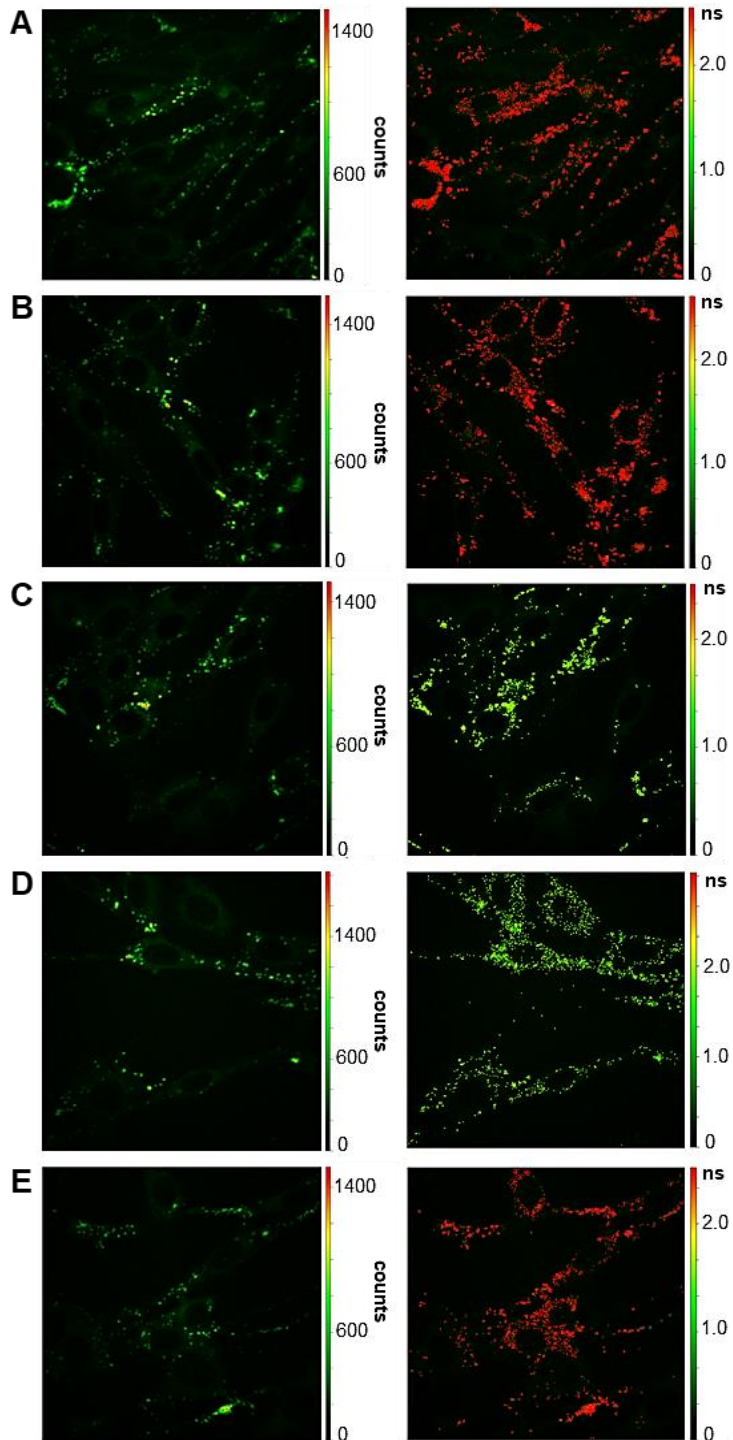
Figure 10. FLIM images illustrating the effect of MNEI amyloid aggregates on the cell's membrane viscosity. Fluorescence intensity (left panels) and average lifetime (right panels) for live SH-SY5Y human neuroblastoma cells incubated with 5 μM BODIPY FL C12. Cells were previously exposed for 24 hours to 30 μM MNEI aggregates formed after 24 hours of incubation at pH 2.5 and 65 °C in different conditions: untreated cells (panel A), no agitation (panel B), agitation without bead (panel C), agitation with bead (panel D) and no agitation with 150 mM NaCl (panel E). The discrete color scale shows shorter lifetimes in green and longer lifetimes in red. Other experimental details are described in the Methods section. This figure is reprinted from [59].

5.4 Conclusions

MNEI has been introduced not only as a protein sweetener for food industries [53,55,65,73,194], but also it has been accepted as a protein model for folding/unfolding and aggregation studies [35–39]. Herein, we modified/added new experimental parameters such as temperature, intensive mechanical agitation, protein concentration and buffering solutions to assess their effect on the kinetics of protein aggregation and morphology of the formed aggregates, also to check if any possible toxic species were formed during the process. Based on the collected results from ThT binding assay, temperature, mechanical agitation and protein concentration had a big impact on the aggregation kinetics of MNEI at acidic pH. Notably, MNEI at low temperature *i.e.* 37 °C did not aggregate during 3 months of incubation, even if mechanical agitation was introduced (**Fig. 1**). However at higher temperature (65 °C), intensive mechanical agitation with and without PTFE beads increased the aggregation kinetics of MNEI (**Fig. 2**), although the aggregation process of MNEI induced by mechanical agitation was slower in comparison to MNEI solution containing 150 mM NaCl incubated at the same temperature (**Fig. 4B**). The morphologies of the formed aggregates were detected by TEM, from which we could observe that mechanical agitation with and without PTFE beads induced fast fibrillization (**Fig. 5C** and **5D**). Under both conditions, masses of

fibrillar populations with different morphologies could be observed, indicating acceleration in the ordered aggregates rather than amorphous aggregates. Samples from different incubation times were withdrawn and loaded on native gels to detect possible presence of soluble oligomers. Indeed, only in the agitated samples, with and without PTFE beads, high molecular weight soluble species were found at the early stages of incubation (**Fig. 8A**, **8B** and 8**C**). The cytotoxicity of MNEI aggregates formed under various conditions such as static (neither agitation nor NaCl_control), mechanical agitation (with and without PTFE beads) and in presence of 150 mM NaCl were assessed as well. It was found that only soluble MNEI aggregates formed after 24 hours of incubation at 65 °C and under mechanical agitation (with and without PTFE beads) were toxic. Interestingly, the soluble aggregates detected after 48 and 72 hours of incubations were nontoxic (**Fig. 9**). Worth mentioning, mature MNEI fibrils were also free of any toxicity [59]. This study was strongly in favor of MNEI applications in food and beverage industries, since it ruled-out any possible toxic effect because the toxicity was developed only when the protein was intensively agitated at high temperature 65 °C and protein concentration (2.5 mg/ml) for 24 hours. Overall, the obtained data clearly demonstrated that MNEI keeps a native, soluble structure for several months unless extreme treatments (*i.e.* at least 2 days of incubation at high protein concentration, temperature above 60 °C, and intensive mechanical agitation or presence of salt with high concentration) are introduced, thus pointing to a safe storage, transport and use of the protein for food and beverages preparations

Final Remarks and Future Perspectives

Sweet proteins are a new class of natural sweeteners that showed a great potential to substitute sugar in different industrial applications. However, these sweeteners suffer from some drawbacks such as limited availability of the natural sweet prtoeins, low thermal/chemical stability, their sweetness profile characterized by late insurgence and lack of data useful for real industrial applications, including sensorial analysis and shelf-life. Nevertheless, there is a possibility to use biotechnological approaches to overcome some drawbacks and also to combine it with protein engineering technique, although in this case there are some limitations *i.e.* lack of data about the safety/physiological and sensorial analyses. Monellin and Thaumatin are the sweetest proteins known up to this date. Thanks to their sweetness power, they have received a special attention from food customers and manufacturers. In this project we focused on the main topics; from one side we designed a sweeter and stronger mutant of MNEI, single-chain Monellin, and from the other side we further characterized MNEI in terms of shelf-life, enzymatic degradation, protein-receptor binding in presence of ionic compounds and aggregation. Also, we monitored the behavior of sweet proteins in real food products after replacing sugar with Thaumatin as a sweetening agent in the recipes of 2 products, tomato ketchup and strawberry cordial, and analyzing the taste quality and rheological properties of the products.

In the beginning, we rationally designed and produced a new mutant of MNEI, called Mut9, with an extraordinary thermal and chemical stability endowed with doubled sweetness power. Interestingly, the thermal stability of Mut9 at neutral pH increased by 21 °C compared to its parent protein, MNEI. Moreover, Mut9 showed a great resistance upon boiling at acidic and neutral pH up to 10 minutes. Again, the sweetness power of Mut9 was doubled with the sweetness threshold of only 0.80 mg/L, where the sweetness threshold of MNEI is known to be 1.64 mg/L. For the future, it is highly recommended to use Mut9 in real food and beverage products and

analyze their taste quality and texture. Since Mut9 is benefitted with an astonishing thermal and chemical stability, it is of great importance to find out whether the improvement of protein's stability is reflected on the aggregation propensity or not.

The characterization studies of MNEI was carried out by running a 6-month shelf-life study on MNEI and three of its mutants including Mut3, Mut4 and Mut9 at a wide range of physicochemical conditions including different temperatures, pHs and protein concentrations. Among these parameters, incubational temperature had a big impact on the resistance and oligomerization propensity of the proteins. Based on the data, Mut9 and Mut3 were the most resistant proteins with respect to other tested sweet proteins.

Enzymatic degradation experiment was also performed on MNEI by simulating the human *in vivo* digestive system through using fluids containing digestive enzymes. The results indicated that the protein remained fully intact after the oral phase; however, it was completely digested into very small pieces after gastric and intestinal phases including pepsin and pancreatic enzymes, respectively. The identification study of the formed peptides using mass spectrometry is still in progress. In this regard, we made *in silico* studies for peptide identification and toxicity assessment and it was found that the obtained peptides were non-toxic. It is suggested to study the cytotoxicity effect of the formed peptide fragments on human cells.

We also investigated the effects of different commercial waters with various mineral residue amounts on the sweetness intensity of sweet proteins. In this study, we used 4 sweet proteins *i.e.* MNEI, Mut3, Mut9 and Thaumatin in 4 types of waters, and monitored the secondary structure and the sweetness intensity of the proteins. The conformational structures of all sweet proteins remained unchanged in various types of waters, however, the sweetness intensity changed significantly based on the existed amounts of ionic compounds in waters. This behavior could not be observed with the low molecular weight sweeteners, even the charged one (Aspartame). These

data indicated that ionic compounds could hinder protein-receptor binding leading to less sweetness power.

To further characterize MNEI, we studied its aggregation process upon introducing/modifying some incubational parameters such as intensive mechanical agitation, protein concentration, temperature, ionic strength and different buffering solutions. The aim of this study was to observe the behavior of the protein upon possible industrial treatments. According to the obtained data, temperature played the determinant role on the aggregate formation, where the protein aggregated only at high temperature (above 60 °C). Mechanical agitation and high ionic strength increased the aggregation kinetics exponentially and led to the formation of amyloid fibrils, although the morphologies of the formed aggregates differed. The cytotoxicity study on the formed aggregates indicated that mature fibrils are free of toxicity, whereas soluble aggregates formed after 24 hours of incubation under intensive mechanical agitation were toxic.

Thaumatin was used in the recipes of two edible products, tomato ketchup and strawberry cordial, followed by analyzing their taste quality and rheological properties. The results showed that Thaumatin lost its sweetness in tomato ketchup. On the other hand, cordial-based Thaumatin perceived sweet with late insurgence and liquorice aftertaste. Also, the rheological properties of both products were disturbed by sugar reduction. For the future, it is highly recommended to make some trials using blends of low-calorie sweeteners including Thaumatin with other intense sweet proteins *i.e.* Mut3 and Mut9, or low molecular weight sweeteners *i.e.* sucralose to cover the delayed sweetness of Thaumatin in some selected food products. To compensate the altered rheological properties, it is also suggested to run a series of trials using food additives *i.e.* bulky agents.

The studies performed during this Ph.D. project were aimed to improve the sweet protein variants or to solve the problems on the way of industrial applications of

sweet proteins. The whole contribution of this thesis is a small step toward the real use of sweet proteins in actual foods and beverages.

References

[1]   F.B. Hu, Resolved: there is sufficient scientific evidence that decreasing sugar-sweetened beverage consumption will reduce the prevalence of obesity and obesity-related diseases, Obes. Rev. 14 (2013) 606–619.

[2]   S. Park, F. Xu, M. Town, H.M. Blanck, Prevalence of sugar-sweetened beverage intake among adults-23 states and the District of Columbia, 2013, Morb. Mortal. Wkly. Rep. 65 (2016) 169–174.

[3]   I. Faus, Recent developments in the characterization and biotechnological production of sweet-tasting proteins, Appl. Microbiol. Biotechnol. 53 (2000) 145–151.

[4]   J. Suez, T. Korem, D. Zeevi, G. Zilberman-Schapira, C.A. Thaiss, O. Maza, D. Israeli, N. Zmora, S. Gilad, A. Weinberger, Artificial sweeteners induce glucose intolerance by altering the gut microbiota, Nature. 514 (2014) 181–186.

[5]   S.S. Schiffman, Rationale for further medical and health research on high-potency sweeteners, Chem. Senses. 37 (2012) 671–679.

[6]   P.A. Temussi, Natural sweet macromolecules: how sweet proteins work, Cell. Mol. Life Sci. C. 63 (2006) 1876–1888.

[7]   R. Kant, Sweet proteins–potential replacement for artificial low calorie sweeteners, Nutr. J. 4 (2005) 5.

[8]   J.A. Morris, R.H. Cagan, Purification of monellin, the sweet principle of Dioscoreophyllum cumminsii, Biochim. Biophys. Acta (BBA)-General Subj. 261 (1972) 114–122.

[9]   H. van der Wel, K. Loeve, Isolation and characterization of thaumatin I and II, the sweet-tasting proteins from Thaumatococcus daniellii Benth, Eur. J. Biochem. 31 (1972) 221–225.

[10]   D. Ming, G. Hellekant, Brazzein, a new high-potency thermostable sweet protein from Pentadiplandra brazzeana B, FEBS Lett. 355 (1994) 106–108.

[11]   X. Liu, S. Maeda, Z. Hu, T. Aiuchi, K. Nakaya, Y. Kurihara, Purification, complete amino acid sequence and structural characterization of the heat-stable sweet protein, mabinlin II, Eur. J. Biochem. 211 (1993) 281–287.

[12]   S. Theerasilp, H. Hitotsuya, S. Nakajo, K. Nakaya, Y. Nakamura, Y. Kurihara, Complete amino acid sequence and structure characterization of the taste-modifying protein, miraculin., J. Biol. Chem. 264 (1989) 6655–

6659.

[13]   H. Yamashita, S. Theerasilp, T. Aiuchi, K. Nakaya, Y. Nakamura, Y. Kurihara, Purification and complete amino acid sequence of a new type of sweet protein taste-modifying activity, curculin., J. Biol. Chem. 265 (1990) 15770–15775.

[14]   X. Song, Y. Yi, L. Liu, M. He, S. Deng, H. Tian, W. Yao, X. Gao, Design and development of a high temperature stable sweet protein base on monellin, Process Biochem. 89 (2020) 29–36.

[15]   J.A. Morris, Sweetening agents from natural sources, Lloydia. 39 (1976) 25–38.

[16]   K. Kurihara, L.M. Beidler, Taste-modifying protein from miracle fruit, Science. 161 (1968) 1241–1243.

[17]   H. Yamashita, T. Akabane, Y. Kurihara, Activity and stability of a new sweet protein with taste-modifying action, curculin, Chem. Senses. 20 (1995) 239–243.

[18]   D. Picone, P.A. Temussi, Dissimilar sweet proteins from plants: Oddities or normal components?, Plant Sci. 195 (2012) 135–142.

[19]   X. Li, L. Staszewski, H. Xu, K. Durick, M. Zoller, E. Adler, Human receptors for sweet and umami taste, Proc. Natl. Acad. Sci. 99 (2002) 4692–4696.

[20]   G. Nelson, M.A. Hoon, J. Chandrashekar, Y. Zhang, N.J.P. Ryba, C.S. Zuker, Mammalian sweet taste receptors, Cell. 106 (2001) 381–390.

[21]   P.A. Temussi, New insights into the characteristics of sweet and bitter taste receptors, in: Int. Rev. Cell Mol. Biol., Elsevier, (2011) pp. 191–226.

[22]   J. Chandrashekar, M.A. Hoon, N.J.P. Ryba, C.S. Zuker, The receptors and cells for mammalian taste, Nature. 444 (2006) 288–294.

[23]   M. Cui, P. Jiang, E. Maillet, M. Max, R.F. Margolskee, R. Osman, The heterodimeric sweet taste receptor has multiple potential ligand binding sites, Curr. Pharm. Des. 12 (2006) 4591–4600.

[24]   G. Morini, A. Bassoli, P.A. Temussi, From small sweeteners to sweet proteins: anatomy of the binding sites of the human T1R2_T1R3 receptor, J. Med. Chem. 48 (2005) 5520–5529.

[25]   R. Yoshida, Y. Ninomiya, Taste information derived from T1R-expressing taste cells in mice, Biochem. J. 473 (2016) 525–536.

[26]   K. Masuda, A. Koizumi, K. Nakajima, T. Tanaka, K. Abe, T. Misaka, M.

Ishiguro, Characterization of the modes of binding between human sweet taste receptor and low-molecular-weight sweet compounds, PLoS One. 7 (2012).

[27]   P.A. Temussi, Why are sweet proteins sweet? Interaction of brazzein, monellin and thaumatin with the T1R2-T1R3 receptor, FEBS Lett. 526 (2002) 1–4.

[28]   G.E. Inglett, J.F. May, Serendipity berries–source of a new intense sweetener, J. Food Sci. 34 (1969) 408–411.

[29]   C. Ogata, M. Hatada, G. Tomlinson, W.C. Shin, S.H. Kim, Crystal structure of the intensely sweet protein monellin, Nature. 328 (1987) 739–742.

[30]   J.R. Somoza, F. Jiang, L. Tong, C.H. Kang, J.M. Cho, S.H. Kim, Two Crystal Structures of a Potently Sweet Protein: Natural Monellin at 2.75 Å Resolution and Single-Chain Monellin at 1.7 Å Resolution, J. Mol. Biol. 234 (1993) 390–404.

[31]   W.F. Xue, O. Szczepankiewicz, M.C. Bauer, E. Thulin, S. Linse, Intra-versus intermolecular interactions in monellin: Contribution of surface charges to protein assembly, J. Mol. Biol. 358 (2006) 1244–1255.

[32]   S.H. Kim, C.H. Kang, R. Kim, J.M. Cho, Y.B. Lee, T.K. Lee, Redesigning a sweet protein: increased stability and renaturability, Protein Eng. Des. Sel. 2 (1989) 571–575.

[33]   T. Tancredi, H. Iijima, G. Saviano, P. Amodeo, P.A. Temussi, Structural determination of the active site of a sweet protein A 1H NMR investigation of pMNEI, FEBS Lett. 310 (1992) 27–30.

[34]   S. Leone, F. Sannino, M.L. Tutino, E. Parrilli, D. Picone, Acetate: friend or foe? Efficient production of a sweet protein in Escherichia coli BL21 using acetate as a carbon source, Microb. Cell Fact. 14 (2015) 106.

[35]   R.R. Goluguri, J.B. Udgaonkar, Rise of the Helix from a Collapsed Globule during the Folding of Monellin, Biochemistry. 54 (2015) 5356–5365.

[36]   S.K. Jha, J.B. Udgaonkar, Direct evidence for a dry molten globule intermediate during the unfolding of a small protein, Proc. Natl. Acad. Sci. 106 (2009) 12289–12294.

[37]   T. Kimura, A. Maeda, S. Nishiguchi, K. Ishimori, I. Morishima, T. Konno, Y. Goto, S. Takahashi, Dehydration of main-chain amides in the final folding step of single-chain monellin revealed by time-resolved infrared spectroscopy, Proc. Natl. Acad. Sci. 105 (2008) 13391–13396.

[38]   P. Malhotra, J.B. Udgaonkar, High-energy intermediates in protein unfolding

characterized by thiol labeling under nativelike conditions, Biochemistry. 53 (2014) 3608–3620.

[39] A.K. Patra, J.B. Udgaonkar, Characterization of the folding and unfolding reactions of single-chain monellin: Evidence for multiple intermediates and competing pathways, Biochemistry. 46 (2007) 11727–11743.

[40] R.B. Iyengar, P. Smits, F. Van Der Ouderaa, H. Van Der Wel, J. Van Brouwershaven, P. Ravestein, G. Richters, P.D. Van Wassenaar, The complete amino-acid sequence of the sweet protein thaumatin I, Eur. J. Biochem. 96 (1979) 193–204.

[41] H.V.D. Wel, Some thoughts about Thaumatin binding, Sweet Tast. Chemorecept. (1993) 365–372.

[42] P. Jiang, Q. Ji, Z. Liu, L.A. Snyder, L.M.J. Benard, R.F. Margolskee, M. Max, The cysteine-rich region of T1R3 determines responses to intensely sweet proteins, J. Biol. Chem. 279 (2004) 45068–45075.

[43] K. Ohta, T. Masuda, F. Tani, N. Kitabatake, Introduction of a negative charge at Arg82 in thaumatin abolished responses to human T1R2–T1R3 sweet receptors, Biochem. Biophys. Res. Commun. 413 (2011) 41–45.

[44] K. Ohta, T. Masuda, F. Tani, N. Kitabatake, The cysteine-rich domain of human T1R3 is necessary for the interaction between human T1R2–T1R3 sweet receptors and a sweet-tasting protein, Thaumatin, Biochem. Biophys. Res. Commun. 406 (2011) 435–438.

[45] S.H. Kim, A. de Vos, C. Ogata, Crystal structures of two intensely sweet proteins, Trends Biochem. Sci. 13 (1988) 13–15.

[46] T. Suami, L. Hough, T. Machinami, N. Watanabe, R. Nakamura, Molecular mechanisms of sweet taste 7: The sweet protein, Thaumatin I, Food Chem. 60 (1997) 277–285.

[47] R. Kaneko, N. Kitabatake, Sweetness of sweet protein thaumatin is more thermoresistant under acid conditions than under neutral or alkaline conditions, Biosci. Biotechnol. Biochem. 65 (2001) 409–413.

[48] B.L. Oser, R.A. Ford, B.K. Bernard, Recent progress in the consideration of flavoring ingredients under the Food Additives Amendment. 13. GRAS substances, Food Technol. 38 (1984) 65–89.

[49] R.L. Smith, P. Newberne, T.B. Adams, R.A. Ford, J.B. Hallagan, F.E. Panel, Correction to GRAS flavoring substances 17, Food Technol. 50 (1996) 72–78.

[50] S. Leone, D. Picone, Molecular dynamics driven design of pH-stabilized

mutants of MNEI, a sweet protein, PLoS One. 11 (2016).

[51]   N. Aghera, I. Dasgupta, J.B. Udgaonkar, A buried ionizable residue destabilizes the native state and the transition state in the folding of monellin, Biochemistry. 51 (2012) 9058–9066.

[52]   V. Esposito, R. Gallucci, D. Picone, G. Saviano, T. Tancredi, P.A. Temussi, The importance of electrostatic potential in the interaction of sweet proteins with the sweet taste receptor, J. Mol. Biol. 360 (2006) 448–456.

[53]   T. Weiffert, S. Linse, Protein stabilization with retained function of monellin using a split GFP system, Sci. Rep. 8 (2018) 1–11.

[54]   M. Delfi, A. Emendato, S. Leone, E.A. Lampitella, P. Porcaro, G. Cardinale, L. Petraccone, D. Picone, A Super Stable Mutant of the Plant Protein Monellin Endowed with Enhanced Sweetness, (2021) 1–13.

[55]   M.F. Rega, R. Di Monaco, S. Leone, F. Donnarumma, R. Spadaccini, S. Cavella, D. Picone, Design of sweet protein based sweeteners: Hints from structure–function relationships, Food Chem. 173 (2015) 1179–1186.

[56]   V. Esposito, F. Guglielmi, S.R. Martin, K. Pauwels, A. Pastore, R. Piccoli, P.A. Temussi, Aggregation mechanisms of cystatins: a comparative study of monellin and oryzacystatin, Biochemistry. 49 (2010) 2805–2810.

[57]   T. Konno, Multistep nucleus formation and a separate subunit contribution of the amyloidgenesis of heat-denatured monellin, Protein Sci. 10 (2001) 2093–2101.

[58]   A. Pica, S. Leone, R. Di Girolamo, F. Donnarumma, A. Emendato, M.F. Rega, A. Merlino, D. Picone, pH driven fibrillar aggregation of the super-sweet protein Y65R-MNEI: A step-by-step structural analysis, Biochim. Biophys. Acta (BBA)-General Subj. 1862 (2018) 808–815.

[59]   M. Delfi, S. Leone, A. Emendato, D. Ami, M. Borriello, A. Natalello, C. Iannuzzi, D. Picone, Understanding the self-assembly pathways of a single chain variant of monellin: A first step towards the design of sweet nanomaterials, Int. J. Biol. Macromol. 152 (2020) 21–29.

[60]   J.-P. Montmayeur, S.D. Liberles, H. Matsunami, L.B. Buck, A candidate taste receptor gene near a sweet taste locus, Nat. Neurosci. 4 (2001) 492–498.

[61]   T. Tancredi, A. Pastore, S. Salvadori, V. Esposito, P.A. Temussi, Interaction of sweet proteins with their receptor: a conformational study of peptides corresponding to loops of brazzein, monellin and thaumatin, Eur. J. Biochem. 271 (2004) 2231–2240.

References

[62]   N. Kunishima, Y. Shimada, Y. Tsuji, T. Sato, M. Yamamoto, T. Kumasaka, S. Nakanishi, H. Jingami, K. Morikawa, Structural basis of glutamate recognition by a dimeric metabotropic glutamate receptor, Nature. 407 (2000) 971–977.

[63]   D. Bordo, P. Argos, Suggestions for "safe" residue substitutions in site-directed mutagenesis, J. Mol. Biol. 217 (1991) 721–729.

[64]   W.F. Xue, O. Szczepankiewicz, E. Thulin, S. Linse, J. Carey, Role of protein surface charge in monellin sweetness, Biochim. Biophys. Acta (BBA)-Proteins Proteomics. 1794 (2009) 410–420.

[65]   Q. Liu, L. Li, L. Yang, T. Liu, C. Cai, B. Liu, Modification of the sweetness and stability of sweet-tasting protein monellin by gene mutation and protein engineering, Biomed Res. Int. (2016).

[66]   J.R. Somoza, J.M. Cho, S.H. Kim, The taste-active regions of monellin, a potently sweet protein, Chem. Senses. 20 (1995) 61–68.

[67]   T. Masuda, K. Ohta, N. Ojiro, K. Murata, B. Mikami, F. Tani, P.A. Temussi, N. Kitabatake, A hypersweet protein: removal of the specific negative charge at Asp21 enhances thaumatin sweetness, Sci. Rep. 6 (2016) 1–9.

[68]   R. Kaneko, N. Kitabatake, Structure–sweetness relationship in thaumatin: importance of lysine residues, Chem. Senses. 26 (2001) 167–177.

[69]   K. Ohta, T. Masuda, N. Ide, N. Kitabatake, Critical molecular regions for elicitation of the sweetness of the sweet-tasting protein, thaumatin I, FEBS J. 275 (2008) 3644–3652.

[70]   F.M. Assadi-Porter, M. Tonelli, E.L. Maillet, J.L. Markley, M. Max, Interactions between the human sweet-sensing T1R2–T1R3 receptor and sweeteners detected by saturation transfer difference NMR spectroscopy, Biochim. Biophys. Acta (BBA)-Biomembranes. 1798 (2010) 82–86.

[71]   D.E. Walters, T. Cragin, Z. Jin, J.N. Rumbley, G. Hellekant, Design and evaluation of new analogs of the sweet protein brazzein, Chem. Senses. 34 (2009) 679–683.

[72]   S.Y. Yoon, J.N. Kong, D.H. Jo, K.H. Kong, Residue mutations in the sweetness loops for the sweet-tasting protein brazzein, Food Chem. 129 (2011) 1327–1330.

[73]   S. Leone, A. Pica, A. Merlino, F. Sannino, P.A. Temussi, D. Picone, Sweeter and stronger: enhancing sweetness and stability of the single chain monellin MNEI through molecular design, Sci. Rep. 6 (2016) 34045.

[74]   A. Micsonai, F. Wien, L. Kernya, Y.H. Lee, Y. Goto, M. Réfrégiers, J.

Kardos, Accurate secondary structure prediction and fold recognition for circular dichroism spectroscopy, Proc. Natl. Acad. Sci. 112 (2015) E3095–E3103.

[75] B. Pagano, A. Randazzo, I. Fotticchia, E. Novellino, L. Petraccone, C. Giancola, Differential scanning calorimetry to investigate G-quadruplexes structural stability, Methods. 64 (2013) 43–51.

[76] J. Ghiso, O. Jensson, B. Frangione, Amyloid fibrils in hereditary cerebral hemorrhage with amyloidosis of Icelandic type is a variant of gamma-trace basic protein (cystatin C), Proc. Natl. Acad. Sci. 83 (1986) 2974–2978.

[77] A.G. Murzin, Sweet-tasting protein monellin is related to the cystatin family of thiol proteinase inhibitors, J. Mol. Biol. 230 (1993) 689–694.

[78] F. Donnarumma, A. Emendato, S. Leone, C. Ercole, G. D'Errico, D. Picone, Salt modulated fibrillar aggregation of the sweet protein MNEI in aqueous solution, J. Solution Chem. 47 (2018) 939–949.

[79] F. Donnarumma, S. Leone, M. Delfi, A. Emendato, D. Ami, D.V. Laurents, A. Natalello, R. Spadaccini, D. Picone, Probing structural changes during amyloid aggregation of the sweet protein MNEI, FEBS J. (2019).

[80] E. van der Linden, P. Venema, Self-assembly and aggregation of proteins, Curr. Opin. Colloid Interface Sci. 12 (2007) 158–165.

[81] H.R. Costantino, R. Langer, A.M. Klibanov, Solid-phase aggregation of proteins under pharmaceutically relevant conditions, J. Pharm. Sci. 83 (1994) 1662–1669.

[82] H.C. Mahler, W. Jiskoot, Analysis of aggregates and particles in protein pharmaceuticals, John Wiley & Sons, 2011.

[83] T. Nicolai, D. Durand, Controlled food protein aggregation for new functionality, Curr. Opin. Colloid Interface Sci. 18 (2013) 249–256.

[84] J. Den Engelsman, P. Garidel, R. Smulders, H. Koll, B. Smith, S. Bassarab, A. Seidl, O. Hainzl, W. Jiskoot, Strategies for the assessment of protein aggregates in pharmaceutical biotech product development, Pharm. Res. 28 (2011) 920–933.

[85] W.F. Weiss IV, T.M. Young, C.J. Roberts, Principles, approaches, and challenges for predicting protein aggregation rates and shelf life, J. Pharm. Sci. 98 (2009) 1246–1277.

[86] W. Wang, Protein aggregation and its inhibition in biopharmaceutics, Int. J. Pharm. 289 (2005) 1–30.

[87] E.Y. Chi, S. Krishnan, T.W. Randolph, J.F. Carpenter, Physical stability of proteins in aqueous solution: mechanism and driving forces in nonnative protein aggregation, Pharm. Res. 20 (2003) 1325–1336.

[88] C.M. Dobson, Principles of protein folding, misfolding and aggregation, in: Semin. Cell Dev. Biol., Elsevier, 2004: pp. 3–16.

[89] A. Kumar, I.Y. Galaev, B. Mattiasson, Precipitation of proteins: non specific and specific, Isol. Purif. Proteins. CRC Press. Boca Rat. (2003) 225–276.

[90] M. Minekus, M. Alminger, P. Alvito, S. Ballance, T. Bohn, C. Bourlieu, F. Carriere, R. Boutrou, M. Corredig, D. Dupont, A standardised static in vitro digestion method suitable for food–an international consensus, Food Funct. 5 (2014) 1113–1124.

[91] K.A. Kopf-Bolanz, F. Schwander, M. Gijs, G. Vergeres, R. Portmann, L. Egger, Validation of an in vitro digestive system for studying macronutrient decomposition in humans, J. Nutr. 142 (2012) 245–250.

[92] J. Maldonado-Valderrama, A.P. Gunning, P.J. Wilde, V.J. Morris, In vitro gastric digestion of interfacial protein structures: visualisation by AFM, Soft Matter. 6 (2010) 4908–4915.

[93] U.K. Laemmli, Cleavage of structural proteins during the assembly of the head of bacteriophage T4, Nature. 227 (1970) 680–685.

[94] E. Gasteiger, C. Hoogland, A. Gattiker, M.R. Wilkins, R.D. Appel, A. Bairoch, Protein identification and analysis tools on the ExPASy server, Proteomics Protoc. Handb. (2005) 571–607.

[95] S. Gupta, P. Kapoor, K. Chaudhary, A. Gautam, R. Kumar, G.P.S. Raghava, O.S.D.D. Consortium, In silico approach for predicting toxicity of peptides and proteins, PLoS One. 8 (2013) e73957.

[96] C. Hellfritsch, A. Brockhoff, F. Stähler, W. Meyerhof, T. Hofmann, Human psychometric and taste receptor responses to steviol glycosides, J. Agric. Food Chem. 60 (2012) 6782–6793.

[97] A.N. Pronin, H. Tang, J. Connor, W. Keung, Identification of ligands for two human bitter T2R receptors, Chem. Senses. 29 (2004) 583–593.

[98] Scientific Opinion on the safety of the extension of use of thaumatin (E 957), EFSA J. 13 (2015) 4290.

[99] B. Crammer, R. Ikan, Progress in the chemistry and properties of the rebaudiosides, Dev. Sweeten. 3 (1987) 45–64.

[100] A.D. Kinghorn, D.D. Soejarto, Intensely sweet compounds of natural origin,

Med. Res. Rev. 9 (1989) 91–115.

[101] A.D. Kinghora, D.D. Soejarto, G.E. Inglett, Sweetening agents of plant origin, CRC. Crit. Rev. Plant Sci. 4 (1986) 79–120.

[102] J.D. Perrier, J.J. Mihalov, S.J. Carlson, FDA regulatory approach to steviol glycosides, Food Chem. Toxicol. 122 (2018) 132–142.

[103] M.J. O'Neil, P.E. Heckelman, C.B. Koch, K.J. Roman, The Merck Index 14th, Whitehouse Station. NJ Merck. (2006) 811.

[104] S.G. Wiet, P.K. Beyts, Sensory characteristics of sucralose and other high intensity sweeteners, J. Food Sci. 57 (1992) 1014–1019.

[105] J. Horne, H.T. Lawless, W. Speirs, D. Sposato, Bitter taste of saccharin and acesulfame-K, Chem. Senses. 27 (2002) 31–38.

[106] C. Kuhn, B. Bufe, M. Winnig, T. Hofmann, O. Frank, M. Behrens, T. Lewtschenko, J.P. Slack, C.D. Ward, W. Meyerhof, Bitter taste receptors for saccharin and acesulfame K, J. Neurosci. 24 (2004) 10260–10265.

[107] G.E. Dubois, D.E. Walters, S.S. Schiffman, Z.S. Warwick, B.J. Booth, S.D. Pecore, K. Gibes, B.T. Carr, L.M. Brands, Concentration—Response relationships of sweeteners: A systematic study, in: ACS Publications, 1991.

[108] S.S. Schiffman, E.A. Sattely-Miller, I.E. Bishay, Sensory properties of neotame: Comparison with other sweeteners, in: ACS Publications, 2008.

[109] S.S. Schiffman, C.A. Gatlin, Sweeteners: state of knowledge review, Neurosci. Biobehav. Rev. 17 (1993) 313–345.

[110] D.N. De Oliveira, M. De Menezes, R.R. Catharino, Thermal degradation of sucralose: a combination of analytical methods to determine stability and chlorinated byproducts, Sci. Rep. 5 (2015) 1–5.

[111] H.C. Grice, L.A. Goldsmith, Sucralose-an overview of the toxicity data., Food Chem. Toxicol. 38 (2000).

[112] V.L. Grotz, I.C. Munro, An overview of the safety of sucralose, Regul. Toxicol. Pharmacol. 55 (2009) 1–5.

[113] H. Stone, J. Sidel, S. Oliver, A. Woolsey, R.C. Singleton, Sensory evaluation by quantitative descriptive analysis, Descr. Sens. Anal. Pract. 28 (2008) 23–34.

[114] J.R. Piggott, Understanding flavour quality: difficult or impossible?, Food Qual. Prefer. 5 (1994) 167–171.

[115] G. V Barbosa-Cánovas, J.L. Kokini, L. Ma, A. Ibarz, The rheology of

semiliquid foods, in: Adv. Food Nutr. Res., Elsevier, 1996: pp. 1–69.

[116] E.E. Finney, Elementary concepts of rheology relevant to food texture studies, in: Texture Meas. Foods, Springer, 1973: pp. 33–51.

[117] M.R. Mackley, R.T.J. Marshall, J. Smeulders, F.D. Zhao, The rheological characterization of polymeric and colloidal fluids, Chem. Eng. Sci. 49 (1994) 2551–2565.

[118] J. Robbins, M. Nicosia, J.A. Hind, G.D. Gill, R. Blanco, J. Logemann, Defining physical properties of fluids for dysphagia evaluation and treatment, Perspect. Swallowing Swallowing Disord. 11 (2002) 16–19.

[119] J.M. Garcia, E. ChambersIV, M. Molander, Thickened liquids, Am. J. Speech-Language Pathol. (2005).

[120] W.A. Gould, Tomato, production, processing and quality evaluation, 1974.

[121] N. Pineau, P. Schlich, S. Cordelle, C. Mathonnière, S. Issanchou, A. Imbert, M. Rogeaux, P. Etiévant, E. Köster, Temporal Dominance of Sensations: Construction of the TDS curves and comparison with time–intensity, Food Qual. Prefer. 20 (2009) 450–455.

[122] F.M. Le Révérend, C. Hidrio, A. Fernandes, V. Aubry, Comparison between temporal dominance of sensations and time intensity results, Food Qual. Prefer. 19 (2008) 174–178.

[123] F. Lenfant, C. Loret, N. Pineau, C. Hartmann, N. Martin, Perception of oral food breakdown. The concept of sensory trajectory, Appetite. 52 (2009) 659–667.

[124] D. Labbe, P. Schlich, N. Pineau, F. Gilbert, N. Martin, Temporal dominance of sensations and sensory profiling: A comparative study, Food Qual. Prefer. 20 (2009) 216–221.

[125] N. Pineau, P. Schilch, Temporal dominance of sensations (TDS) as a sensory profiling technique, in: Rapid Sens. Profiling Tech., Elsevier, 2015: pp. 269–306.

[126] N. Larson-Powers, R.M. Pangborn, Paired comparison and time-intensity measurements of the sensory properties of beverages and gelatins containing sucrose or synthetic sweeteners, J. Food Sci. 43 (1978) 41–46.

[127] W.E. Lee III, M. Pangborn, Time-intensity: the temporal aspects of sensory perception, Food Technol. (1986).

[128] M.I. Ujikawa, H.M.A. Bolini, Descriptive profile, time-intensity sweetness profile and affective test of traditional and low-calorie peach (Prunus persica

sp.) nectar, Aliment. Rev. Tecnol. e Hig. Los Aliment. (2004) 85–96.

[129] R.M. Pangborn, M.J. Lewis, J.F. Yamashita, Comparison of time-intensity with category scaling of bitterness of iso-α-acids in model systems and in beer, J. Inst. Brew. 89 (1983) 349–355.

[130] E. Gwartney, H. Heymann, Profiling to describe the sensory characteristics of a simple model menthol solution 1, J. Sens. Stud. 11 (1996) 39–48.

[131] M. Cliff, H. Heymann, Development and use of time-intensity methodology for sensory evaluation: A review, Food Res. Int. 26 (1993) 375–385.

[132] J.R. Piggott, Dynamism in flavour science and sensory methodology, Food Res. Int. 33 (2000) 191–197.

[133] B. Poldermans, J. Matt, Processing aids for the food industry: The state of the art, Boitechnological Innov. Food Process. (1991) 7–44.

[134] S.K. Sathe, D.K. Salunkhe, Solubilization and electrophoretic characterization of the great northern bean (Phaseolus vulgaris L.) proteins, J. Food Sci. 46 (1981) 82–87.

[135] V.J. van Buul, L. Tappy, F.J.P.H. Brouns, Misconceptions about fructose-containing sugars and their role in the obesity epidemic, Nutr. Res. Rev. 27 (2014) 119–130.

[136] L. Tappy, K.A. Lê, Health effects of fructose and fructose-containing caloric sweeteners: where do we stand 10 years after the initial whistle blowings?, Curr. Diab. Rep. 15 (2015) 1–12.

[137] J.M. Rippe, T.J. Angelopoulos, Sucrose, high-fructose corn syrup, and fructose, their metabolism and potential health effects: what do we really know?, Adv. Nutr. 4 (2013) 236–245.

[138] J.S. White, Straight talk about high-fructose corn syrup: what it is and what it ain't, Am. J. Clin. Nutr. 88 (2008) 1716S-1721S.

[139] J.S. White, Challenging the fructose hypothesis: new perspectives on fructose consumption and metabolism, Adv. Nutr. 4 (2013) 246–256.

[140] D.M. Klurfeld, J. Foreyt, T.J. Angelopoulos, J.M. Rippe, Lack of evidence for high fructose corn syrup as the cause of the obesity epidemic, Int. J. Obes. 37 (2013) 771–773.

[141] N.J. Olsen, B.L. Heitmann, Intake of calorically sweetened beverages and obesity, Obes. Rev. 10 (2009) 68–75.

[142] V.S. Malik, M.B. Schulze, F.B. Hu, Intake of sugar-sweetened beverages and weight gain: a systematic review, Am. J. Clin. Nutr. 84 (2006) 274–288.

References

[143] V.S. Malik, B.M. Popkin, G.A. Bray, J.P. Després, F.B. Hu, Sugar-sweetened beverages, obesity, type 2 diabetes mellitus, and cardiovascular disease risk, Circulation. 121 (2010) 1356–1364.

[144] G.A. Bray, Fructose and risk of cardiometabolic disease, Curr. Atheroscler. Rep. 14 (2012) 570–578.

[145] P. Marckmann, Dietary treatment of thrombogenic disorders related to the metabolic syndrome, Br. J. Nutr. 83 (2000) S121–S126.

[146] G.A. Bray, B.M. Popkin, Calorie-sweetened beverages and fructose: what have we learned 10 years later, Pediatr. Obes. 8 (2013) 242–248.

[147] J.J. Di Nicolantonio, S.C. Lucan, The wrong white crystals: not salt but sugar as aetiological in hypertension and cardiometabolic disease, Open Hear. 1 (2014) e000167.

[148] D.I. Feig, B. Soletsky, R.J. Johnson, Effect of allopurinol on blood pressure of adolescents with newly diagnosed essential hypertension: a randomized trial, Jama. 300 (2008) 924–932.

[149] S. Nguyen, H.K. Choi, R.H. Lustig, C. Hsu, Sugar-sweetened beverages, serum uric acid, and blood pressure in adolescents, J. Pediatr. 154 (2009) 807–813.

[150] J.J. Di Nicolantonio, J.H. O'Keefe, S.C. Lucan, Added fructose: a principal driver of type 2 diabetes mellitus and its consequences, in: Mayo Clin. Proc., Elsevier, 2015: pp. 372–381.

[151] S. Basu, P. Yoffe, N. Hills, R.H. Lustig, The relationship of sugar to population-level diabetes prevalence: an econometric analysis of repeated cross-sectional data, PLoS One. 8 (2013) e57873.

[152] M.I. Goran, S.J. Ulijaszek, E.E. Ventura, High fructose corn syrup and diabetes prevalence: a global perspective, Glob. Public Health. 8 (2013) 55–64.

[153] J.M. Clark, The epidemiology of nonalcoholic fatty liver disease in adults, J. Clin. Gastroenterol. 40 (2006) S5–S10.

[154] A.J. McCullough, Update on nonalcoholic fatty liver disease, J. Clin. Gastroenterol. 34 (2002) 255–262.

[155] M. Stieger, Texture-taste interactions: Enhancement of taste intensity by structural modifications of the food matrix, Procedia Food Sci. 1 (2011) 521–527.

[156] G. Nagy, H. Grubmüller, How accurate is circular dichroism-based model

validation?, Eur. Biophys. J. 49 (2020) 497–510.

[157] R. Di Monaco, N.A. Miele, S. Volpe, D. Picone, S. Cavella, Temporal sweetness profile of MNEI and comparison with commercial sweeteners, J. Sens. Stud. 29 (2014) 385–394.

[158] F.U. Hartl, M. Hayer-Hartl, Converging concepts of protein folding in vitro and in vivo, Nat. Struct. Mol. Biol. 16 (2009) 574.

[159] R. Mezzenga, P. Schurtenberger, A. Burbidge, M. Michel, Understanding foods as soft materials, Nat. Mater. 4 (2005) 729–740.

[160] Y. Wang, A. Lomakin, J.J. McManus, O. Ogun, G.B. Benedek, Phase behavior of mixtures of human lens proteins Gamma D and Beta B1, Proc. Natl. Acad. Sci. 107 (2010) 13282–13287.

[161] R.S. Harrison, P.C. Sharpe, Y. Singh, D.P. Fairlie, Amyloid peptides and proteins in review, in: Rev. Physiol. Biochem. Pharmacol., Springer, 2007: pp. 1–77.

[162] M. Bucciantini, E. Giannoni, F. Chiti, F. Baroni, L. Formigli, J. Zurdo, N. Taddei, G. Ramponi, C.M. Dobson, M. Stefani, Inherent toxicity of aggregates implies a common mechanism for protein misfolding diseases, Nature. 416 (2002) 507–511.

[163] M.D. Kirkitadze, G. Bitan, D.B. Teplow, Paradigm shifts in Alzheimer's disease and other neurodegenerative disorders: the emerging role of oligomeric assemblies, J. Neurosci. Res. 69 (2002) 567–577.

[164] M. Fändrich, M.A. Fletcher, C.M. Dobson, Amyloid fibrils from muscle myoglobin, Nature. 410 (2001) 165–166.

[165] T. Konno, K. Murata, K. Nagayama, Amyloid-like aggregates of a plant protein: a case of a sweet-tasting protein, monellin, FEBS Lett. 454 (1999) 122–126.

[166] F. Bisceglia, A. Natalello, M.M. Serafini, R. Colombo, L. Verga, C. Lanni, E. De Lorenzi, An integrated strategy to correlate aggregation state, structure and toxicity of Aß 1–42 oligomers, Talanta. 188 (2018) 17–26.

[167] A. Natalello, P.P. Mangione, S. Giorgetti, R. Porcari, L. Marchese, I. Zorzoli, A. Relini, D. Ami, G. Faravelli, M. Valli, Co-fibrillogenesis of wild-type and D76N β2-Microglobulin the crucial role of fibrillar seeds, J. Biol. Chem. 291 (2016) 9678–9689.

[168] C. Iannuzzi, V. Carafa, L. Altucci, G. Irace, M. Borriello, R. Vinciguerra, I. Sirangelo, Glycation of Wild-Type Apomyoglobin Induces Formation of Highly Cytotoxic Oligomeric Species, J. Cell. Physiol. 230 (2015) 2807–

2820.

[169] M.K. Kuimova, G. Yahioglu, J.A. Levitt, K. Suhling, Molecular rotor measures viscosity of live cells via fluorescence lifetime imaging, J. Am. Chem. Soc. 130 (2008) 6672–6673.

[170] J.A. Levitt, M.K. Kuimova, G. Yahioglu, P.H. Chung, K. Suhling, D. Phillips, Membrane-bound molecular rotors measure viscosity in live cells via fluorescence lifetime imaging, J. Phys. Chem. C. 113 (2009) 11634–11642.

[171] H. Naiki, K. Higuchi, M. Hosokawa, T. Takeda, Fluorometric determination of amyloid fibrils in vitro using the fluorescent dye, thioflavine T, Anal. Biochem. 177 (1989) 244–249.

[172] A. Srivastava, P.K. Singh, M. Kumbhakar, T. Mukherjee, S. Chattopadyay, H. Pal, S. Nath, Identifying the bond responsible for the fluorescence modulation in an amyloid fibril sensor, Chem. Eur. J. 16 (2010) 9257–9263.

[173] V.I. Stsiapura, A.A. Maskevich, V.A. Kuzmitsky, K.K. Turoverov, I.M. Kuznetsova, Computational study of thioflavin T torsional relaxation in the excited state, J. Phys. Chem. A. 111 (2007) 4829–4835.

[174] E.S. Voropai, M.P. Samtsov, K.N. Kaplevskii, A.A. Maskevich, V.I. Stepuro, O.I. Povarova, I.M. Kuznetsova, K.K. Turoverov, A.L. Fink, V.N. Uverskii, Spectral properties of thioflavin T and its complexes with amyloid fibrils, J. Appl. Spectrosc. 70 (2003) 868–874.

[175] M. Biancalana, K. Makabe, A. Koide, S. Koide, Aromatic cross-strand ladders control the structure and stability of β-rich peptide self-assembly mimics, J. Mol. Biol. 383 (2008) 205–213.

[176] F. Grigolato, C. Colombo, R. Ferrari, L. Rezabkova, P. Arosio, Mechanistic origin of the combined effect of surfaces and mechanical agitation on amyloid formation, ACS Nano. 11 (2017) 11358–11367.

[177] A. Tiiman, A. Noormägi, M. Friedemann, J. Krishtal, P. Palumaa, V. Tõugu, Effect of agitation on the peptide fibrillization: Alzheimer's amyloid-β peptide 1-42 but not amylin and insulin fibrils can grow under quiescent conditions, J. Pept. Sci. 19 (2013) 386–391.

[178] A. Sicorello, S. Torrassa, G. Soldi, S. Gianni, C. Travaglini-Allocatelli, N. Taddei, A. Relini, F. Chiti, Agitation and high ionic strength induce amyloidogenesis of a folded PDZ domain in native conditions, Biophys. J. 96 (2009) 2289–2298.

[179] T.R. Serio, A.G. Cashikar, A. S. Kowal, G.J. Sawicki, J.J. Moslehi, L. Serpell, M.F. Arnsdorf, S.L. Lindquist, Nucleated conformational conversion

and the replication of conformational information by a prion determinant, Science. 289 (2000) 1317–1321.

[180] V. Sluzky, J.A. Tamada, A.M. Klibanov, R. Langer, Kinetics of insulin aggregation in aqueous solutions upon agitation in the presence of hydrophobic surfaces., Proc. Natl. Acad. Sci. 88 (1991) 9377–9381.

[181] F. Donnarumma, S. Leone, M. Delfi, A. Emendato, D. Ami, D. V. Laurents, A. Natalello, R. Spadaccini, D. Picone, Probing structural changes during amyloid aggregation of the sweet protein MNEI, FEBS J. (2019).

[182] A. Dong, J. Matsuura, M.C. Manning, J.F. Carpenter, Intermolecular β-sheet results from trifluoroethanol-induced nonnative α-helical structure in β-sheet predominant proteins: infrared and circular dichroism spectroscopic study, Arch. Biochem. Biophys. 355 (1998) 275–281.

[183] M. Fändrich, Oligomeric intermediates in amyloid formation: structure determination and mechanisms of toxicity, J. Mol. Biol. 421 (2012) 427–440.

[184] K.E. Marshall, R. Marchante, W.F. Xue, L.C. Serpell, The relationship between amyloid structure and cytotoxicity, Prion. 8 (2014) 192–196.

[185] L. Pieri, K. Madiona, L. Bousset, R. Melki, Fibrillar α-synuclein and huntingtin exon 1 assemblies are toxic to the cells, Biophys. J. 102 (2012) 2894–2905.

[186] M. Vivoli Vega, R. Cascella, S.W. Chen, G. Fusco, A. De Simone, C.M. Dobson, C. Cecchi, F. Chiti, The toxicity of misfolded protein oligomers is independent of their secondary structure, ACS Chem. Biol. 14 (2019) 1593–1600.

[187] S. Campioni, B. Mannini, M. Zampagni, A. Pensalfini, C. Parrini, E. Evangelisti, A. Relini, M. Stefani, C.M. Dobson, C. Cecchi, A causative link between the structure of aberrant protein oligomers and their toxicity, Nat. Chem. Biol. 6 (2010) 140–147.

[188] C. Capitini, J.R. Patel, A. Natalello, C. D'Andrea, A. Relini, J.A. Jarvis, L. Birolo, A. Peduzzo, M. Vendruscolo, P. Matteini, Structural differences between toxic and nontoxic HypF-N oligomers, Chem. Commun. 54 (2018) 8637–8640.

[189] E. Drolle, A. Negoda, K. Hammond, E. Pavlov, Z. Leonenko, Changes in lipid membranes may trigger amyloid toxicity in Alzheimer's disease, PLoS One. 12 (2017) e0182194.

[190] E. Evangelisti, R. Cascella, M. Becatti, G. Marrazza, C.M. Dobson, F. Chiti, M. Stefani, C. Cecchi, Binding affinity of amyloid oligomers to cellular membranes is a generic indicator of cellular dysfunction in protein

misfolding diseases, Sci. Rep. 6 (2016) 32721.

[191] G. Hungerford, A. Allison, D. McLoskey, M.K. Kuimova, G. Yahioglu, K. Suhling, Monitoring sol-to-gel transitions via fluorescence lifetime determination using viscosity sensitive fluorescent probes, J. Phys. Chem. B. 113 (2009) 12067–12074.

[192] C. Iannuzzi, M. Borriello, A. D'Agostino, D. Cimini, C. Schiraldi, I. Sirangelo, Protective effect of extractive and biotechnological chondroitin in insulin amyloid and advanced glycation end product-induced toxicity, J. Cell. Physiol. 234 (2019) 3814–3828.

[193] K. Suhling, J.A. Levitt, P.H. Chung, M.K. Kuimova, G. Yahioglu, Fluorescence lifetime imaging of molecular rotors in living cells, JoVE (Journal Vis. Exp. (2012) e2925.

[194] D. Castiglia, S. Leone, R. Tamburino, L. Sannino, J. Fonderico, C. Melchiorre, A. Carpentieri, S. Grillo, D. Picone, N. Scotti, High-level production of single chain monellin mutants with enhanced sweetness and stability in tobacco chloroplasts, Planta. 248 (2018) 465–476.

Publications (include submitted manuscript)

1- F. Donnarumma, S. Leone, M. Delfi, A. Emendato, D. Ami, D. V. Laurents, A. Natalello, R. Spadaccini, D. Picone, Probing structural changes during amyloid aggregation of the sweet protein MNEI, FEBS J. 2020. https://doi.org/10.1111/febs.15168

2- M. Delfi, S. Leone, A. Emendato, D. Ami, M. Borriello, A. Natalello, C. Iannuzzi, D. Picone, Understanding the self-assembly pathways of a single chain variant of Monellin: A first step towards the design of sweet nanomaterials, *Int. J. Biol. Macromol*. 152 (2020) 21–29. doi.org/10.1016/j.ijbiomac.2020.02.229

3- M. Delfi, A. Emendato, S. Leone, E.A. Lampitella, P. Porcaro, G. Cardinale, L. Petraccone, D. Picone, A Super Stable Mutant of the Plant Protein Monellin Endowed with Enhanced Sweetness, *life* (2021) 1–13. doi.org/10.3390/life11030236

4- M. Delfi, A. Emendato, P. A. Temussi, D. Picone, Striking dependence of protein sweetness on water quality: the role of the ionic strength, *Frontier in Molecular Biosciences*. 6 (2021) 677. doi.org/10.3389/fmolb.2021.705102

5- M. Delfi, M. Ghomi, A. Zarrabi, R. Mohammadinejad, Z.B. Taraghdari, M. Ashrafizadeh, E.N. Zare, T. Agarwal, V.V.T. Padil, B. Mokhtari, Functionalization of polymers and nanomaterials for biomedical applications: Antimicrobial platforms and drug carriers, *Prosthesis*. 2 (2020) 117–139. doi.org/10.3390/prosthesis2020012

6- M. Delfi, R. Sartorius, M. Ashrafizadeh, E. Sharifi, Y. Zhang, P. De Berardinis, A. Zarrabi, R.S. Varma, F.R. Tay, B.R. Smith, Self-assembled peptide and protein nanostructures for anti-cancer therapy: Targeted delivery, stimuli-responsive devices and immunotherapy, *Nano Today*. 38 (2021) 101119. doi.org/10.1016/j.nantod.2021.101119

7- M. Ashrafizade, M. Delfi, F. Hashemi, A. Zabolian, H. Saleki, M. Bagherian, N. Azami, M.V. Farahani, S. omid Sharifzadeh, S. Hamzehlou, Biomedical application of chitosan-based nanoscale delivery systems: Potential usefulness

in siRNA delivery for cancer therapy, Carbohydr. Plyme. (2021) 117809. doi.org/10.1016/j.carbpol.2021.117809

8- P. Makvandi, U. Josic, M. Delfi, F. Pinelli, V. Jahed, E. Kaya, M. Ashrafizadeh, A. Zarepour, F. Rossi, A. Zarrabi, T. Agarwal, E.N. Zare, M. Ghomi, T. Kumar Maiti, L. Breschi, F.R. Tay, Drug Delivery (Nano)Platforms for Oral and Dental Applications: Tissue Regeneration, Infection Control and Cancer Management, *Adv. Sci*. (2021). doi.org/10.1002/advs.202004014

9- P. Makvandi, M. Ghomi, M. Ashrafizadeh, A. Tafazoli, T. Agarwal, M. Delfi, J. Akhtari, E.N. Zare, V.V.T. Padil, A. Zarrabi, N. Pourreza, W. Miltyk, T.K. Maiti, A review on advances in graphene-derivative/polysaccharide bionanocomposites: Therapeutics, pharmacogenomics and toxicity, *Carbohydr. Polym*. 250 (2020). doi.org/10.1016/j.carbpol.2020.116952

Patents

- Patent application N. 102021000003698 is pending.

Attended congresses/conferences/schools/teaching activities:

- May 13-14, 2019: Spring School in **Transferable Skills** held at the University of Naples Federico II.

- May 2019: Participation in tutoring program in the Chemical Sciences department at the University of Naples Federico II as a laboratory teaching assistant for **General Chemistry Course**.

- June 27, 2019: Participation in congress "**The Task Force on Microbiome Meets the Stakeholder**" held in Naples.

- July 24-26, 2019: Summer School on **Protein Evolution** held at SZN.

- October 3-4, 2019: Participation in **IFIB 2019** Conference and Poster presentation: M. Delfi, S. Leone, and D. Picone: "**New Mutants of Sweet Protein Monellin with Improved Sweetness and Stability**"

- October 28, 2019: Participation in congress "**BiolD&A Biotechnology Identity and application**".

- October 1-2, 2020: Participation in **IFIB 2020** Conference.